ANION RECOGNITION BY HALOGEN BONDING

Master's Thesis

University of Jyväskylä

Department of Chemistry

24.7.2022

Arttu Elias Lehikoinen

ABSTRACT

In the literature review, anion recognition and key concepts of it, predominantly halogen bonding, are introduced. The different aspects of halogen bonding anion receptors, and the objectives for their design are discussed. Lastly, a brief overview of halogen bond mediated anion sensing is given.

In the experimental section, 17 syntheses were performed to create neutral receptor molecules that could bind anions using halogen bonds. Five different primary reagents were used, 3-iodoaniline, 3-bromoaniline, 2-amino-6-bromopyridine, as well as 1,3-diethynylbenzene and isophthaloyl dichloride. No receptors were successfully synthesized but a novel by-product was obtained.

TIIVISTELMÄ

Kirjallisuuskatsauksessa esitellään anionien tunnistus käsitteenä ja siihen liittyviä keskeisiä aiheita, ensisijaisesti halogeenisidos, käydään läpi. Myös halogeenisidosanionireseptorit ja niiden suunnittelun eri näkökulmat esitellään. Lopuksi tähänastinen tutkimus anionien aistimisesta halogeenisidosten avulla käydään lyhyesti läpi.

Kokeellisessa osuudessa suoritettiin 17 synteesiä, joiden tavoitteena oli muodostaa neutraaleja reseptorimolekyylejä, jotka kykenisivät sitomaan anioneita halogeenisidoksilla. Synteeseissä käytettiin viittä eri päälähtöainetta: 3-jodianiliinia, 3-bromianiliinia, 2-amino-6-bromipyridiiniä, sekä 1,3-dietynyylibentseeniä ja isoftaloyylidikloridia. Tavoitereseptoreita ei saatu syntetisoitua, mutta yksi uudenlainen sivutuote löydettiin synteeseistä.

PREFACE

This thesis was written from September 2021 to July 2022 in Jyväskylä, Finland. The supervisors of the thesis were Arto Valkonen and assisting supervisor with experimental work was Lauri Happonen. The experimental work was done in the the Department of Chemistry at the University of Jyväskylä from the 14th of June until the 6th of October 2021.

The subject is limited to anion recognition mediated by halogen bonds, i.e., combinatory binding with other non-covalent interactions, mainly hydrogen bonds, are not included. Literature was acquired through University of Jyväskyläs' network and was acquired from the internet with Google Scholar, University of Jyväskylä library discovery service JykDOK, and Web of Science.

Thanks are given to my thesis supervisor Arto, as well as Lauri. Additional thanks go to Kaisa Helttunen for reviewing this thesis with Arto, to Matti Salmela, and to Milla S.M. Mattila for various problem-solving solutions during the experimental work. I would also like to thank every person who has guided, helped, or assisted me during my studies in any way. You've all given me much over the years and I will cherish every memory for years to come. I would like to say the same to my friends I met at the University of Prince Edward Island. Lastly, I would like to thank Maaria Kangasniemi for constantly motivating me throughout the writing of this thesis, my family for support, and thank anyone for reading.

Arttu Lehikoinen

Jyväskylä, 24th of July 2022

TABLE OF CONTENTS

ABBREVIATIONS AND NOTATIONS

2-2 = synthesis product **2**, second synthesis

3-2 = synthesis product **3**, second synthesis

9-2 = synthesis product **9**, second synthesis

9-3 = synthesis product **9**, third synthesis

AIE = aggregation-induced emission

CuAAC = copper-catalyzed azide-alkyne cycloaddition

CV = cyclic voltammetry

DCM = dichloromethane

DMAP = 4-dimethylaminopyridine

DMF = dimethylformamide

DMNB = 2,3-dimethyl-2,3-dinitrobutane

DPEphos = bis(2-diphenylphosphinophenyl)ether

DPV = differential pulse voltammetry

ED = electron-donating

EtOAc = ethyl acetate

EW = electron-withdrawing

HB = hydrogen bond

Hex = *n*-hexane

LOD = limit of detection

MeCN = methyl cyanide, acetonitrile

MeOH = methyl alcohol, methanol

MIM = mechanically interlocked molecule

MS = mass spectrometry

NDI = naphthalene diimide

NEt_3 = triethylamine

NMR = nuclear magnetic resonance spectroscopy

SWCNT = single-walled carbon nanotube

SWV = square-wave voltammetry

T_3 = triiodothyronine

T_4 = thyroxine

TBAF = tetra-*n*-butylammonium fluoride

TBTA = tris((1-benzyl-4-triazolyl)methyl)amine

THF = tetrahydrofuran

TLC = thin-layer chromatography

TMS = trimethylsilyl

TTF = tetrathiafulvalene

vdW = van der Waals

XB = halogen bond

XRD = X-ray diffraction

1 INTRODUCTION

Anions are plentiful in nature and industry. The selective capture or detection of many anions would possibly bring many benefits. Iodide, chloride, and large polyanions such as DNA, RNA, and ATP are bioactive anions. The misfunction of any brings problems to the human organism. Overuse of nitrate and phosphate in agriculture disrupts aquatic life and causes eutrophication.[1] Perrhenate and pertechnetate are used as radioactive pharmaceuticals.[2,3] Pertechnetate is also a pollutant of nuclear power.[2] Azides, cyanides, and perchlorates are all toxic industrial pollutants that need to be closely regulated and prevented from releasing to the environment to prevent harm.[1]

Anions can be captured and sensed with supramolecular hosts called anion receptors. The field of selectively detecting or binding negatively charged species, i.e. anions, is called anion recognition.[4] Anion receptors have typically bound anions using hydrogen bonds[5] (HBs) but recently, halogen bonding anion receptors have been introduced as a new alternative. Halogen bond (XB) receptors have some advantages compared to hydrogen bonding systems, which include higher binding affinity, better selectivity, intrinsic hydrophobicity, and their ability to bind 'soft' anions strongly.[6,7] Some disadvantages of XBs include challenging synthesis,[8] less universality, i.e., higher selectivity causes some anions to not be bound which, e.g., an analogous, less-selective hydrogen-bond receptor could form HBs with. For cationic receptors additional disadvantages include limited solubility in less polar solvents, and that the presence of counterions can interfere with XB-donors.[9] Despite these disadvantages, halogen bonds can be a potent replacement for hydrogen bonding anion receptors. This thesis specifically focuses on halogen bond driven anion recognition and anion receptors.

There is a variety of objectives and requirements that anion sensors should aim to accomplish for real world applications. The requirements for anion recognition include high selectivity and capability to function in competitive solvent media.[10] Functionality in water is important for anion receptors in potential medical and environmental applications. There are some examples of functional XB anion receptors in water, e.g., halotriazole-based systems in Figure 1.[1]

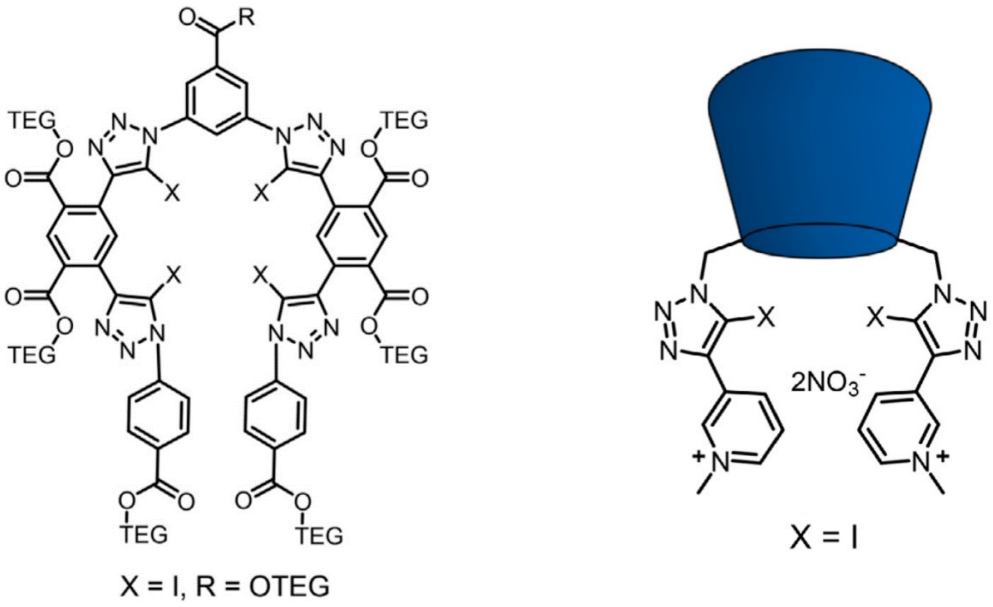

Figure 1. Functional anion receptors in water. Left: halotriazole-based receptor with incredibly high I^- affinity in water with its 2:1 host-guest complex ($\beta_2 = 7.28 \times 10^9\ M^{-2}$).[11] A similar receptor with fluorescent R-groups at the terminal ends of the receptor had a very high affinity for perrhenate ($\beta_2 = 6.66 \times 10^8\ M^{-2}$) and other anions, TEG = triethylene glycol. Right: α-cyclodextrin-based (blue) receptor with pyridinium-halotriazole arms that is selective for perrhenate (ReO_4^-) in water, which is considered analogous to the highly toxic pertechnetate ion ($^{99}TcO_4^-$).[12]
Adapted from *Coord. Chem. Rev.*, **416**, Pancholi, J. and Beer, P. D., Halogen bonding motifs for anion recognition, 213281, 2020, with permission from Elsevier.[1]

In general, an anion receptor with high binding affinity or functionality in water is a great beginning when designing anion recognition systems. There is a variety of problems and aspects to consider when designing anion recognition systems. These questions include, e.g., device integration, ease of use, manufacturing costs, and recycling possibilities. These questions need to be solved before an anion recognition device can be fully-equipped for real-world use. Some proof-of-concept level XB-based anion sensor devices exist which will be discussed in section 6, among anion sensing in general.[13]

In the first sections of this thesis, central concepts of anion recognition, including halogen bonds and the donors and acceptors of XBs in anion recognition, are presented. Next are provided brief overviews of anion receptor design and anion

sensing. Experimental work to create neutral halogen bonding anion receptors was performed as a part of this thesis, the objectives and results of which, along with discussion, are given penultimately. Conclusions from the reviewed literature and experimental work are presented in closing.

2 CONCEPTS

2.1. HALOGEN BONDS

A halogen bond is a non-covalent interaction between a halogen bond donor and an acceptor. A typical XB-donor is a halogen atom bound to an R-group. A typical XB-acceptor is an electron-rich moiety. A halogen bond is represented as R–X· · · Y, where R–X is a covalently bound molecule. X is a halogen atom acting as the donor of the halogen bond (Lewis acid) and Y is a Lewis base as the acceptor of the halogen bond. Typical R–X molecules (XB-donors) include dihalogens, interhalogens, haloarenes and haloheteroarenes.[14]

The strength of a halogen bond is determined by the electron density on the interacting site. The stronger the electron-withdrawing potential of the groups surrounding the donor (halogen), the stronger the bond. This is because of the electropositive region of the donor becomes more pronounced when electron-withdrawing groups are situated around the donor. The strength of the XB is also affected by the electron-richness of the XB-acceptor. The richer the acceptor, the stronger the formed XB.[15]

The strength of a halogen bond varies from 10–200 kJ/mol.[4,16] Typical hydrogen bond strengths range from 0.2 to 40 kJ/mol[17] but some compounds, e.g., HF_2^-, have been calculated to reach HB strengths of 175 kJ/mol.[18,19] Although halogen bonds are quite like hydrogen bonds, they have some differences between each other. Most importantly, the atoms the interactions happen between are different. XBs have halogen atoms acting as Lewis acids, whereas HBs have hydrogen atoms as Lewis acids. Both HBs and XBs grow stronger as linearity of the bond increases, but halogen bond interactions especially prefer near linear conformations. This is mainly due to non-bonding valence electrons that halogens have, and hydrogen does not.[20] The linear conformation of halogen bonds is resultant from the so called σ-hole in the halogen atom entity.

2.2. σ-HOLE

The σ-hole is the resultant electron-poor region of a halogen atom molecular entity that is caused by the halogen atom being covalently bound to a molecule or an atom. When this other entity acts as an electron-withdrawing group to the halogen atom, it causes an electron-deficient region, or the σ-hole, to form on the halogen. This region forms along the C–X axle to the opposite end of the halogen atom (Figure 2). The location of the σ-hole being on the terminal end of the molecule from the covalent bond causes halogen bonds to be highly directional. In general, the closer the binding angle of R–X· · · Y is to 180°, the stronger the halogen bond interaction.[21,22]

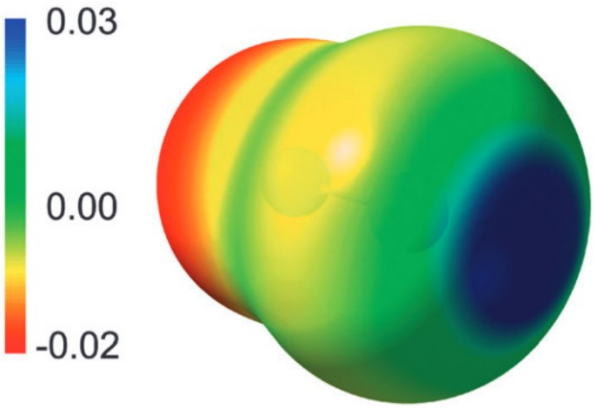

Figure 2. The electron deficient region or σ-hole (blue) of BrF that includes a covalently bound halogen (Br) to some other electron-withdrawing entity (F).[22] Scale in atomic units. Adapted from M. Novák, C. Foroutan-Nejad and R. Marek, *Phys. Chem. Chem. Phys.*, 2015, **17**, 6440, with permission from the Royal Society of Chemistry.

2.3. XB-DONOR MOIETIES

Most XB-donor moieties have the titular atom in them — a halogen. Typical halogen atoms in XB-donors include F, Cl, Br, or I. They can also contain multiple halogens (dihalogens, interhalogens) or have a polyatomic group, e.g., cyano- or isothiocyanate group, that resembles a halogen by its chemical properties (pseudohalogens). Halonium ions have also been documented as XB-donors that form three-center halogen bonds, e.g., $[N \cdots I \cdots N]^+$.[23] Halogens bound to organic molecules, i.e. organohalides, are possible XB-donors, and they are well known.[24 a)] In particular, $C_{sp} - X$ and $C_{sp^2} - X$ hybridized systems are typical. $C_{sp^3} - X$ systems are also

possible by tuning the EW groups of the XB-donor. There are also some cases of halogens bound to heteroatoms, such as *N*-haloimides.[24 b),25]

2.4. XB-ACCEPTOR MOIETIES

There are four main types of XB-acceptor moieties: neutral lone pair(s), anions, pi-electron possessing XB-acceptors and radicals. Neutral lone pair containing acceptors and anions are prominent in crystal engineering. Naturally, in anion recognition acceptors are anions. Radical and pi-electron possessing acceptors are rarer, as the former are quite reactive, and the latter form weaker XBs.[24 c)]

2.4.1. Neutral Lone Pair(s)

Neutral lone pair XB-acceptors are atoms with lone pairs of electrons. The most prominent lone pair possessing XB-acceptors are nitrogen-containing systems. These include mostly sp^3, sp^2, and sp-hybridized nitrogen derivatives. The XB accepting capability of nitrogen is notably inverted compared to their carbon analogues, i.e., $N_{sp} < N_{sp^2} < N_{sp^3}$. Additional group 15 XB-acceptor moieties, such as phosphines and arsines, have also been reported.[24 b),26–28] However, these are rarely used as supramolecular synthons.

Group 16 elements (mainly oxygen, sulfur) are also frequently used as XB-acceptors, but they generally form weaker XBs than their nitrogen-containing analogues.[29] Oxygen compounds, e.g., phenolate, enolates, carboxylates, sulfonates and oxyanions,[15] have all been reported as XB acceptors. Sulfur compounds, e.g., thiols, thioethers, isothiocyanates, and thioketones,[24 c)] are also noteworthy from the group 16 elements as XB-acceptors. Any elements (group 16) or compounds with multiple lone pairs of electrons can act as multidentate XB-acceptors, i.e., form up to one XB per lone pair.

2.4.2. Anions

An anion is a negatively charged atom or molecule. Some examples of anions include halides, such as chloride and iodide, and oxyanions, like perchlorate, sulfate, nitrate. Anions too can accept multiple XBs at once and multiple XBs are often employed in

anion binding, as single XBs tend to be too weak to fully bind anions. Anions can be classified as soft and hard bases according to the HSAB theory. As anions are typically bases, anions themselves can be called hard and soft, the latter to which XBs tend to form strong interactions with. Soft anions are easily polarizable, have large atomic radii, and low nuclear charge. Hard anions are hard to polarize, have high nuclear charges, and are small. Some soft anions include iodide, thiocyanate, and hydride. Hard anions include, e.g., hydroxide, nitrate, and fluoride. An anion as an XB-acceptor is ideal due to the electron-rich nature of anions. Hence, virtually any anion can act as an XB-acceptor if it can donate electron density.[1,7,30]

2.4.3. π-Electron Possessing XB-Acceptors and Radicals

Any molecular system with π-electrons can act as an XB-acceptor, but this wide range of possibilities comes at a cost. The XBs formed by π-acceptors tend to be weak.[24 c)] They are used more seldom because of this tendency but examples of XBs between triple bond π-electrons[31] and aryl ring π-electrons[32] have been reported. Radical molecules, e.g., nitronyl radicals, can also act as XB-acceptors.[33] However, they too are used more seldom, as radical compounds are typically labile.

2.5. SUPRAMOLECULAR HOST-GUEST COMPLEXES

Supramolecular chemistry is the chemistry of non-covalent bonds. The parties of supramolecular non-covalent bonds typically involve a large molecule (host) binding a smaller molecule (guest). The binding between a host and a guest happens at binding sites, which are regions of the host or guest that are capable of non-covalent interactions. The host typically has multiple convergent binding sites, while the guest has corresponding divergent sites, resulting in the two binding together to form a 'host-guest complex' or supramolecule. A host can be capable of binding multiple guests, or a guest can interact with multiple hosts. These complexes are denoted with corresponding ratios, e.g., a host bound to two guests is called a 1:2 host-guest complex. A supramolecular host can be, e.g., a biological molecule, such as an enzyme, or a large synthetic cyclic molecule. A supramolecular guest can be many things, such as mono- or polyatomic ions or small molecules.[34 a)]

The driving forces behind supramolecular chemistry are many and the most important are ion and dipolar interactions (ion-ion, ion-dipole, dipole-dipole), hydrogen bonding, aromatic interactions (cation-π, anion-π, and π-π), van der Waals (vdW) forces, and closed shell interactions. Other significant forces are crystal packing forces as well as solvation and hydrophobic effects.[34 b)] Halogen bonding is considered a closed shell interaction, along with metallophilic and secondary bonding interactions.[34 c)]

2.6. ANION RECEPTORS AND ANION RECOGNITION

An anion receptor is a supramolecular host that can specifically bind anions as guests. A receptor typically binds a range of distinct anions, and can also favour one anion over another, i.e., be more selective to a specific anion. When an anion receptor binds an anion, the formed supramolecule is called the anion complex of the receptor. The binding between an anion and its receptor can happen with a range of non-covalent interactions and multiple distinct interactions can participate in the binding at once, e.g., multiple HBs and XBs. The interactions happen between the binding sites of guests and hosts, which for XB anion recognition are called donors and acceptors (anions). The field of selectively detecting or binding negatively charged species is called anion recognition.[4] Typical XB-donors in anion recognition to date include halotriazole, halotriazolium, haloperfluoroarene, and haloimidazolium moieties (Figure 3).[4] The electron rich nature of anions causes them to be good candidates as the acceptors of halogen bonds.

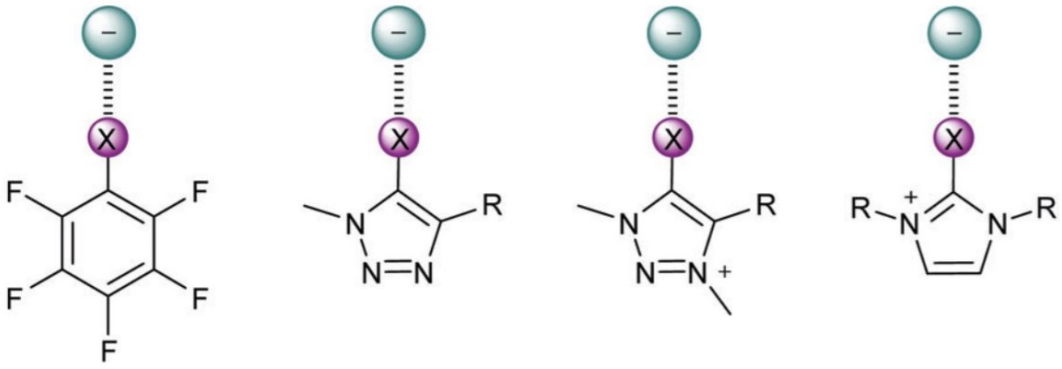

Figure 3. Typical XB-donor moieties in anion receptors. From left to right: haloperfluoroarene, halotriazole, halotriaziolium and haloimidazolium moieties.[4] X = F, Cl, Br, or I. Reproduced from A. Brown and P. D. Beer, *Chem. Commun.*, 2016, **52**, 8645, with permission from the Royal Society of Chemistry.

3 ANION RECEPTOR XB-DONORS

Anion receptor XB-donors typically contain a cyclic R-group bound to a halogen atom. A halogen bond donor typically is neutral or positive in charge. The strength of a halogen bond is dependent on the polarizability of the halogen on the XB-donor. Fluorine is the least polarizable and the heavier the halogen, the more polarizable it is (F < Cl < Br < I). This increased polarizability is demonstrated in Figure 4 that compares molecules containing different halogens.

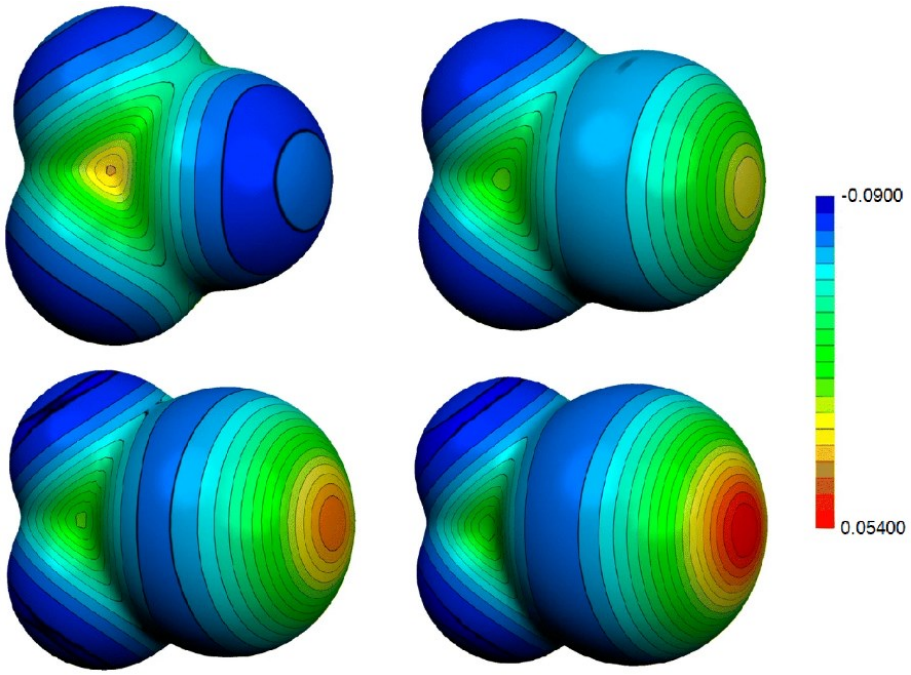

Figure 4. A demonstration of the effect of a single atom exchange in the electron density of a tetrasubstituted methane molecule. From left to right, top to bottom: CF_4, CF_3Cl, CF_3Br, and CF_3I.[21] Adapted by permission from Springer Nature: Springer, *J. Mol. Model,* Halogen bonding: the σ-hole, Clark, T., Hennemann, M., Murray, J.S. *et al.*, Copyright Springer-Verlag 2006.

Fluorine especially requires strong EW-groups to function as an XB-donor,[35] and as such, Cl, Br, and I are more commonly used in anion recognition. Astatine is the heaviest occurring halogen and a very rare element on Earth.[36] However, astatine has been calculated and experimentally proven to be a very good XB-donor.[37,38] In terms of anion recognition, astatine is not yet relevant as there is no published research on the subject.

The strength of a halogen bond can be modified (or tuned) in three different ways.[6,24] By exchanging a single atom in the bond (Figure 4), by changing the sp-character of the atom the halogen is covalently bound to, or by modifying the electron density of the atoms surrounding the halogen bond. The latter is done by changing the electron-donating (ED) qualities surrounding the XB-acceptor moiety, or by modifying the electron-withdrawing (EW) capability of the substituent R the halogen is bound to.[1]

3.1. NEUTRAL XB-DONOR MOIETIES

The most typical neutral XB-donor moieties are haloperfluoroarene and halotriazole moieties (Figure 8 and Figure 5), as well as dihalogens and halogenated heterocyclic compounds (Figure 11, Figure 12). Typically, neutral donor moieties are employed in aprotic solvent media. Multiple moieties are incorporated in an anion receptor to achieve strong anion binding. Neutral XB-donor moieties can bind various anions. Most notably, they prefer halide ions. Some systems, such as the iodotriazole based XB foldamers synthesized by Borissov *et al.*,[39] can also bind oxyanions but most of them bind halides with even greater affinity.

3.1.1. Halotriazole

Halotriazoles (Figure 5) are neutral XB-donors with a 5-membered heteroatomic ring containing 3 nitrogen atoms. The nitrogen atoms act as an EW group to the halogen, strengthening the σ-hole of the XB-donor.

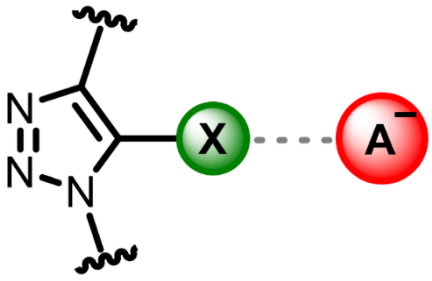

Figure 5. 1,2,3-Halotriazole XB-donor moiety.[1] Adapted from *Coord. Chem. Rev.*, **416**, Pancholi, J. and Beer, P. D., Halogen bonding motifs for anion recognition, 213281, 2020, with permission from Elsevier.

Halotriazoles are popular XB-donors because of their ease of synthesis via ‘click’ reactions. These include a wide range of potential reactions, pertinent of which to halotriazoles is the copper-catalyzed azide-alkyne cycloaddition (CuAAC) reactions (Figure 6). CuAAC reactions are possible with a wide range of functional groups in many reaction conditions. In addition, the syntheses are facile and swift to perform.[40]

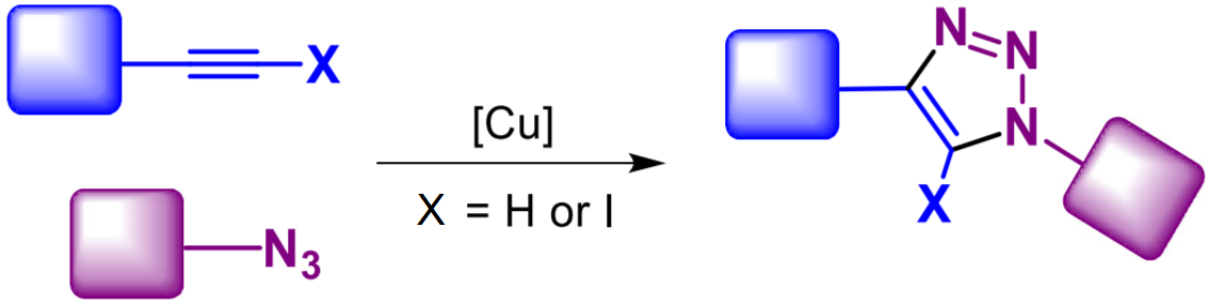

Figure 6. A diagram of a copper-catalyzed azide-alkyne cycloaddition (CuAAC) reaction to form 1,2,3-triazoles.[1] Adapted from *Coord. Chem. Rev.*, **416**, Pancholi, J. and Beer, P. D., Halogen bonding motifs for anion recognition, 213281, 2020, with permission from Elsevier.

An example of a halotriazole-based anion receptor is presented in Figure 7. What makes it noteworthy is that it has a high affinity for chloride in an aqueous solution (2.5 % H_2O in DMSO). Functional XB anion receptors in water are typically cationic in nature as the additional positive charge enhances the anion-binding ability of the receptor. Moreover, other neutral anion receptors typically have some stabilization factors in addition to XBs, e.g., HBs, which the receptor in question does not have. The receptor of Figure 7 has a high affinity to Cl^- which the authors attributed to the high level of preorganization of the macrocycle and to the size-compatibility of the receptor to the chloride anion.[41]

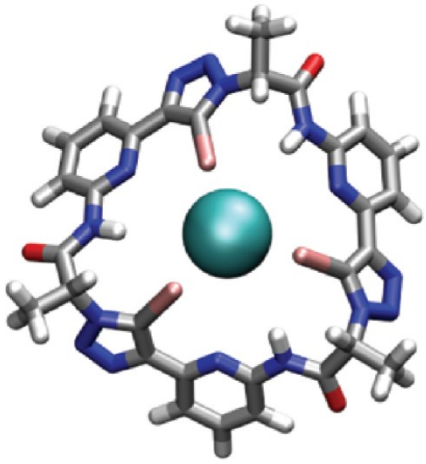

Figure 7. A neutral triazole-based macrocyclic anion receptor complex. It consists of three iodotriazole moieties in a macrocycle, bound via XBs to Cl^-.[41] Adapted from D. Mungalpara, S. Stegmüller and S. Kubik, Chem. Commun., 2017, **53**, 5095, with permission from the Royal Society of Chemistry.

3.1.2. Haloperfluoroarene

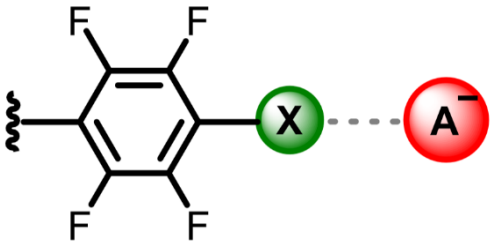

Figure 8. Haloperfluoroarene XB-donor moiety.[1] Adapted from *Coord. Chem. Rev.*, **416**, Pancholi, J. and Beer, P. D., Halogen bonding motifs for anion recognition, 213281, 2020, with permission from Elsevier.

Haloperfluoroarenes (Figure 8) are neutral XB-donors and contain a fluorinated arene ring with at least one other, heavier halogen, e.g., Cl, Br, I. Haloperfluoroarenes have an advantage over other XB-donors, e.g., halotriazoles and haloimidazoliums, as they have multiple positions (i.e., ortho, meta, para) where a halogen can be bound to. This flexibility allows for a wider variety of possible anion receptors, such as mono-, bi-, and tridentate receptors. The increased number of XB-donors can result in multiple XBs to achieve stronger anion recognition. Perfluoroarenes in general can also be used as an

EW-group next to an XB-donor to further enhance the ability of a receptor to bind anions. An example of perfluoroarenes used as an EW-group is presented in Figure 17.

Haloperfluoroarenes were used as one of the first recognized XB-donors to utilize halogen bonding as an anion recognition interaction in solution.[42] The aforementioned complex is presented in Figure 9. Unlike typical anion recognition receptors, the receptor is capable of binding both counterions of a salt, causing the receptor to retain a neutral charge. This can have possible applications for transferring hydrophilic salts through organic membranes.[43] Another example of anion transport utilizing haloperfluoroarenes is the linear XB based scaffold by Jentzsch and Matile.[44] This scaffold uses an "anion hopping" mechanism to transport anions across lipid bilayer membranes.

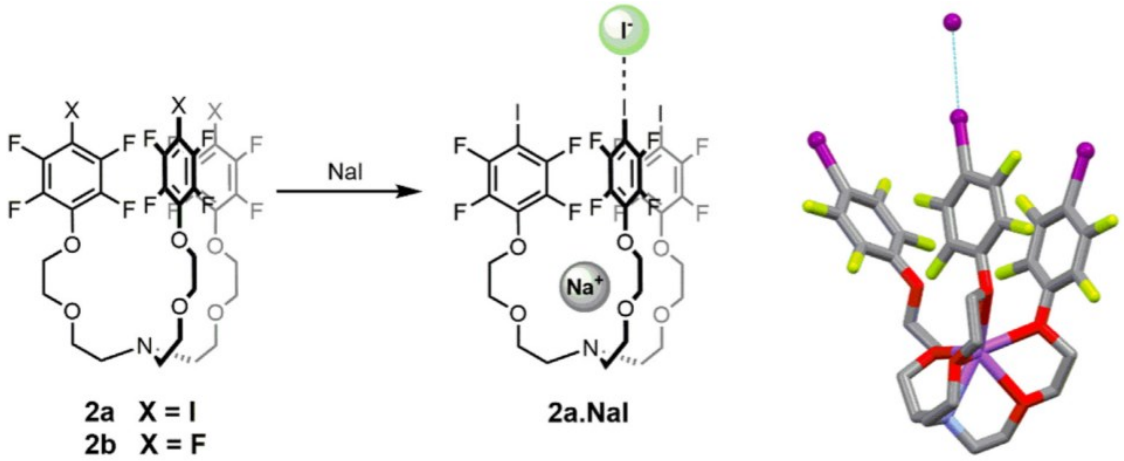

Figure 9. The first XB-based anion recognition receptor in solution, capable of binding ion-pairs (NaI pictured, I^- is XB-bound, Na^+ is cation coordinated).[42] Solid-state structure of the ion pair complex determined by XRD (right). Adapted from *Coord. Chem. Rev.*, **416**, Pancholi, J. and Beer, P. D., Halogen bonding motifs for anion recognition, 213281, 2020, with permission from Elsevier.[1]

3.1.3. Dihalogens

Dihalogens (X_2) are diatomic halogen molecules covalently bound to another atom of the same element, e.g., I_2, Br_2, Cl_2. Dihalogens can form two types of halogen-halogen interactions, type I, and type II. Type I halogen interactions are dispersion-repulsion type vdW interactions resultant from close-packed halogens.[45] Type I interactions are not considered halogen bonds as there is no attractive force and the interaction is

non-linear.[6,46 a)] In type II halogen-halogen interactions the halogen acts as an electrophile akin to a conventional XB and is therefore considered halogen bonding.[6,14] An illustrative graph of the different types of halogen-halogen contacts is presented in Figure 10.

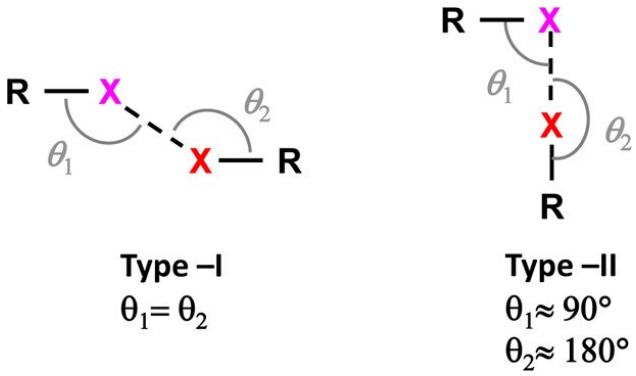

Figure 10. The different halogen-halogen contacts. There are two types of halogen-halogen contacts, type I (left) and type II (right). Type I involves two halogens with identical contact angles. Type II involves a halogen-halogen contact with non-identical contact angles. Only type II is considered a halogen bond.[6]

Dihalogens can have some interesting interplay between the two halogens. E.g., I_2 has two identical iodine atoms, I_A, and I_B. When one iodine, e.g., I_A, forms a halogen bond, depending on the XB I_A has formed, I_B can act either as a second XB-donor, or even as a XB-acceptor. The role of I_B is determined by the strength of the charge transfer in the XB donored by I_A. When the charge transfer is strong, I_B is less likely to act as a XB-donor because it gains more negative charge. In such a case I_B is more likely to act as a XB or HB-acceptor. It is also possible for the charge transfer to be extreme enough to cleave the X_A–X_B bond of a homonuclear dihalogen. In such a case X_B^- is cleaved and, formally, X_A^+ is left halogen bonded to an XB-acceptor. X^+ is known as a halonium ion which are further discussed in section 3.2.4.[46 b)]

3.1.4. Interhalogens

Interhalogens contain two or more halogen atoms covalently bound to each other that are distinct elements, i.e., X_nY_m where X is one halogen, e.g., Br, and Y is another halogen, e.g., Cl. An interhalogen only consists of halogen atoms. An interhalogen with only two atoms can also be called a heteronuclear dihalogen.[46188-190]

Dihalogens follow the same XB strength tendencies as classical XBs, with heteronuclear dihalogens forming the strongest bonds ($F_2 < Cl_2 < Br_2 < I_2 < IBr < ICl$) irrespective of the XB acceptor.[46 d),47] Heteronuclear dihalogens form the strongest XBs because one of the halogens is more electronegative than the other, which then acts as an EW-group for the other halogen, strengthening the formed XB further than any homonuclear dihalogens can.

Although homonuclear dihalogens can have cases where the two halogens act as a XB-donor, diatomic interhalogens do not have the same tendencies. For example, the diatomic interhalogen IBr has a more electronegative atom, Br, and a less electronegative atom, I. The iodine acts as an XB-donor, while Br acts as an EW-group for iodine. As bromine draws more electron density to itself, it is more likely to act solely as an XB-acceptor. In other words, as bromine is more electronegative, the charge transfer in the iodine XB is too strong for bromine to act as a XB-donor.[46 c)]

3.1.5. Other Neutral XB-donors

Tetrathiafulvalene (TTF) derivatives are less common XB-donor moieties. TTF is used in these derivatives as an EW-group to enhance the σ-hole of halogens added to the TTF moiety.[48] A depiction of a TTF molecule and a XB-capable derivative is presented in Figure 11.

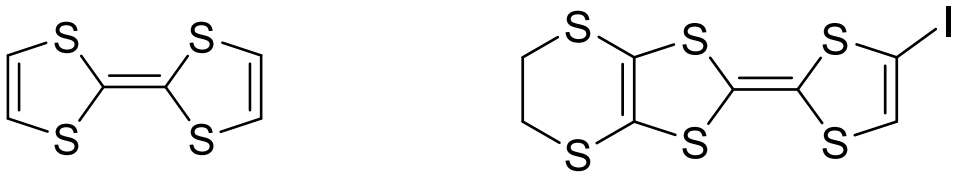

Figure 11. A tetrathiafulvalene molecule (left) and a tetrathiafulvalene derivative (iodo-ethylene-dithio-tetrathiafulvalene, I-EDT-TTF) capable of forming XBs (right).

There are also some XB-donor cases where a halogen atom is bound to a heteroatom (other than a halogen). The most well-known group of halogenated heterocyclic compounds are most likely *N*-haloimides. *N*-haloimides, e.g., *N*-iodosuccinimide (Figure 12), contain a halogen atom covalently bound to a nitrogen in an imide group. The N–X bond is particularly polarized by the two surrounding carbonyl groups, resulting in very short, strong XBs.[25]

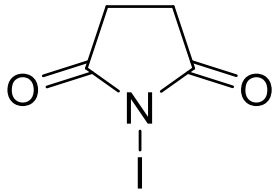

Figure 12. *N*-iodosuccinimide XB-donor moiety.

Biological systems also contain XB-donors, the most common of which are the iodinated thyroid hormones T_3 (triiodothyronine) and T_4 (thyroxine).[6] There have also been studies of the Protein Data Bank which determined that a large portion of structures showed O · · · X interactions. There, chlorine in halogenated nucleotides or drugs was the most common XB-donor, with oxygen being the most common acceptor.[49]

3.2. CATIONIC XB-DONOR MOIETIES

Increased solvent effects in protic solvent media compete with the anion binding capability of XBs. This competition causes stronger XB-donors, such as cationic XB-donors, to be needed. The positive charge helps the anion binding of an XB-donor via charge assistance and by strengthening the polarization of the XB. Cationic moieties are more capable of binding oxyanions than neutral donor moieties. Common cationic XB-donor moieties include halotriazolium, haloimidazolium, and halopyridinium, which are shown in Figure 13. Other notable charged XB-donor moieties include halonium ions and halotetrathiafulvalenium.[15]

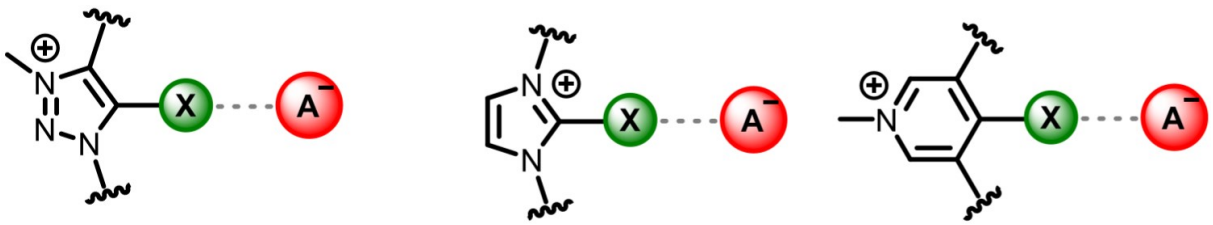

Figure 13. Common cationic XB-donor moieties. From left to right: halotriazolium, haloimidazolium, and halopyridinium.[1] Adapted from *Coord. Chem. Rev.*, **416**, Pancholi, J. and Beer, P. D., Halogen bonding motifs for anion recognition, 213281, 2020, with permission from Elsevier.

3.2.1. Haloimidazolium

Haloimidazolium (Figure 13 middle) is a positively charged halogen substituted variant of imidazole. It contains two nitrogen atoms on both side of the C–X moiety, causing additional polarization of the C–X bond. This extreme proximity of the EW groups and the positive charge of the moiety causes haloimidazolium to typically bind with great affinities that can exceed over other cationic XB-donors, e.g., halotriazolium.[5]

Macrocyclic anion receptors using haloimidazolium XB-donors have been reported.[50] The receptors (Figure 14) bound halide anions with very high affinities (K_a = 6.3 x 10^5 M^{-1} for I^-, K_a = 9.55 x 10^5 M^{-1} for Br^-). Additionally, the receptors became highly fluorescent upon anion binding, enabling them to function as fluorescent sensors. These imidazoliophanes represent some of the first XB-chemosensors to function in aqueous solvent media (9:1 MeOH/H_2O).

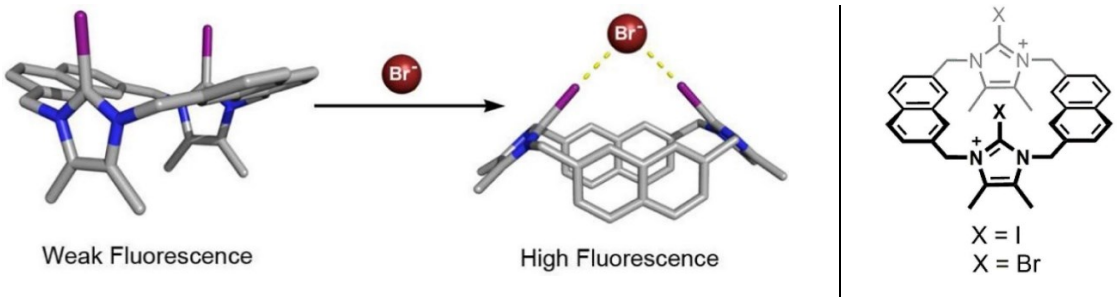

Figure 14. A diagram of the fluorescence change mechanism of a macrocyclic haloimidazoliophane anion recognition receptor (left)[50] and its' structure (right)[1]. Left picture reprinted with permission from *J. Am. Chem. Soc.* 2012, **134**, 28, 11533–11541. Copyright 2012 American Chemical Society. Right picture adapted from *Coord. Chem. Rev.*, **416**, Pancholi, J. and Beer, P. D., Halogen bonding motifs for anion recognition, 213281, 2020, with permission from Elsevier.

3.2.2. Halotriazolium

Halotriazolium (Figure 13 left) is the cationic version of the halotriazole moiety. The added positive charge enhances the EW capabilities of the triazole ring, resulting in a more pronounced, electron-poor σ-hole and thus, stronger XBs. Triazolium XB-donors have been found to be more effective than their triazole counterparts.[7]

Halotriazolium can exist as 1,2,3- and 1,2-4-constitutional isomers, and according to Tepper *et al.*,[7] 1,2,4-triazolium C–X bonds are more polarized than 1,2,3-triazolium equivalents. This increased polarization happens because of the added proximity of nitrogen atoms to the C–X bond. However, due to excessive polarization, no XBs are possible with 1,2,4-triazolium donors as the C–X bonds cleave in two when brought to the proximity of XB-acceptors.

Another promising functioning anion receptor in aqueous solutions (9:1 MeCN: H_2O) is the pyrrole-based receptor reported by Lim and Beer.[51] This acyclic cleft-type triazolium receptor (Figure 15) is capable of selectively binding SO_4^{2-} and $H_2PO_4^-$ with relatively high association constants. Sulfate host-guest complexes reached association constants K_a of 7700 ± 200 M^{-1} for 1:1 and 9900 ± 200 M^{-1} for 2:1, and for dihydrogen phosphate the highest association constant was for the 1:1 complex with a K_a of 3460 ± 60 M^{-1}.

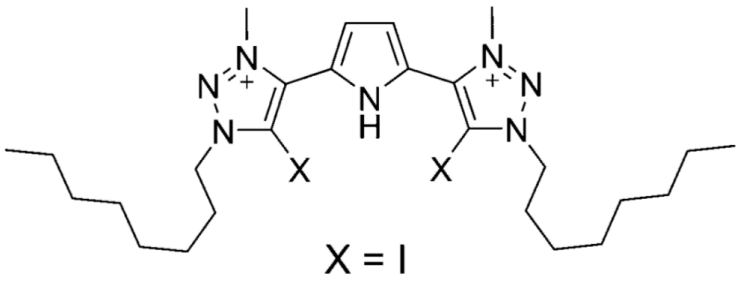

Figure 15. Pyrrole-based iodotriazolium anion receptor capable of selectively recognising and sensing SO_4^{2-} and $H_2PO_4^-$ in aqueous solutions.[51] Reproduced from J. Y. C. Lim and P. D. Beer, *New J. Chem.*, 2018, **42**, 10472, with permission from the Centre National de la Recherche Scientifique (CNRS) and the Royal Society of Chemistry.

3.2.3. Halopyridinium

Halopyridinium (Figure 13 right) is another less typical cationic XB-donor. Most often it contains an *N*-methylated pyridine, *N*-methylpyridinium, bound to a halogen. One example of pyridinium as a XB-donor is shown in Figure 16. The cleft-type receptor binds ReO_4^- with two XBs in 3:2 chloroform-d3/acetone-d6. An analogous receptor with *N*-octylpyridinium groups bound ReO_4^- with a high binding constant K_1 of 8990 M^{-1}.[52]

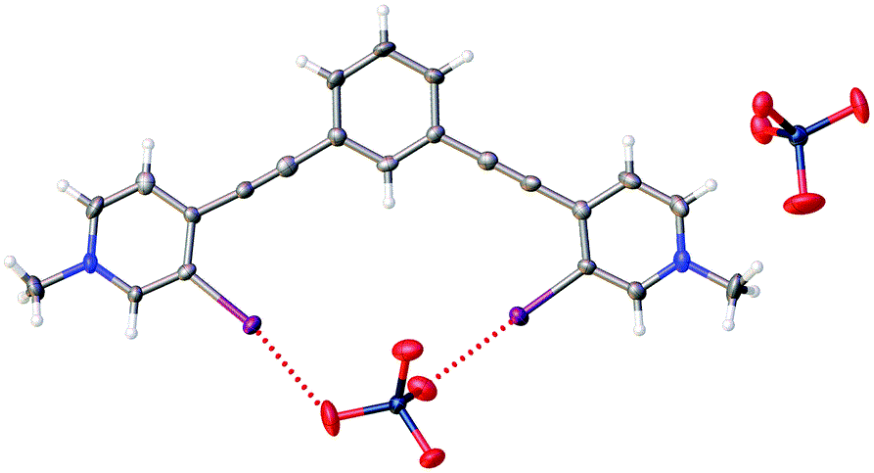

Figure 16. Bidentate iodopyridinium-based ReO_4^- receptor.[52] Adapted from C. J. Massena, A. M. S. Riel, G. F. Neuhaus, D. A. Decato and O. B. Berryman, Chem. Commun., 2015, **51**, 1417 with permission from the Royal Society of Chemistry.

Pyridinium differs from other XB-donor moieties in that it is more commonly used as a cationic electron-deficient group for other XB-donors, enhancing their ability to bind anions (Figure 17). The cationic pyridinium as a spacer group, combined with electron-deficient perfluoroaryl groups next to a XB-donor, triazole, forms a very potent anion receptor that forms halogen bonds to I^- with very high affinity.[8]

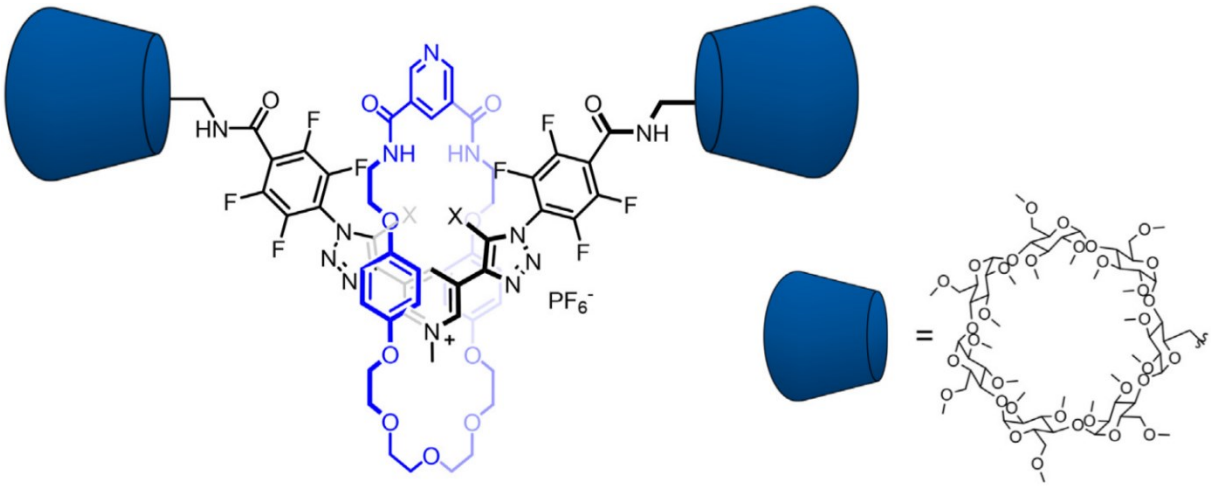

Figure 17. A [2]rotaxane anion receptor with β-cyclodextrin (blue cone) capped ends.[8] The receptor incorporates iodotriazole XB-donors with perfluoroarenes surrounding them, along with a pyridinium spacer group in between them. The receptor is capable of binding I^- with an association constant of $>10^5$ in 1:1 D_2O/acetone d6. X = I. Adapted from *Coord. Chem. Rev.*, **416**, Pancholi, J. and Beer, P. D., Halogen bonding motifs for anion recognition, 213281, 2020, with permission from Elsevier.[1]

Another example of pyridinium as an electron-deficient group is shown in Figure 1, where two pyridinium moieties are used as terminal ends to a receptor. This makes the receptor cationic, strengthening it to be selective to perrhenate in water.

3.2.4. Other Cationic Systems

Halonium ions can form three-center halogen bonds that consist of a formally positively charged halogen, and two Lewis bases. The arrangement is linear like other halogen bonds and can be depicted as $[D \cdots X \cdots D_1]^+$ (D and D_1 = Lewis base/electron-donor; X = halogen).[23] A simple depiction of a classical XB and a three-centered XB is presented in Figure 18.

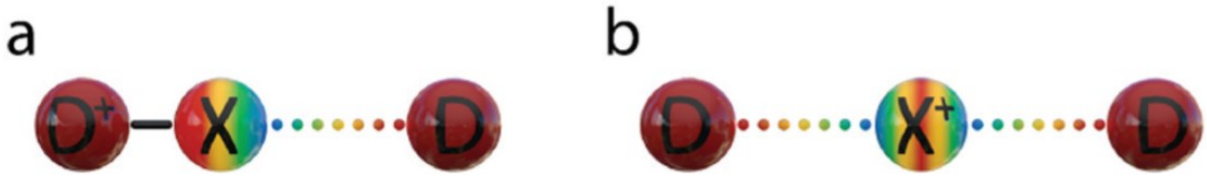

Figure 18. A depiction of a classical (or two-centered) XB (a) and a three-centered XB (b).[23] The halogen of (a) is covalently bound to an atom (D^+), it is neutral or negative in charge, and it has an electron-poor region (blue) on the right side (σ-hole). The electron-donor (D) donates electron density to the σ-hole of the halogen, forming a halogen bond.
On the right (b), a positively charged halogen, X^+, has two electron-poor regions (blue) caused by an empty p-orbital. The regions can accept electron density from a Lewis base (D). Two electron-donors each contribute a lone pair of electrons, which redistributes the charge of the halogen, and form a four-electron, three-center $[D \cdots X \cdots D]^+$ system.

The three-center XBs of halonium ions do not contain a covalent bond, unlike regular XBs. They are bound by XBs that exist between the Lewis bases and the empty p-orbital of the central halogen.[23] Three-center XBs have only recently been introduced as supramolecular synthons and as such, there is limited research on the subject. They have been reported to form supramolecular capsules, cages, and helices[23] but so far, no anion receptors using three-center halogen bonds have been reported.

Halotetrathiafulvalenium is a radical cation of TTF. It has mainly been used as a synthon in supramolecular networks as a cationic XB-donor[15] and anion receptors utilizing TTF^+ are rare. A recent example of a redox-active TTF^+ sensor[53] (Figure 29) is further discussed in section 6.3.1.

4 ANIONS AS XB-ACCEPTORS

Anions are electron-rich XB-acceptors. Some of the most common anions used as XB-acceptor moieties include perchlorate, carboxylate, and *N*-oxide anions, which all are considered oxygen-containing anions, or oxyanions.[24,49] Another common category of anions used in anion recognition are halides. Oxyanions and halides are also some of the most common anions in biology. The capability to bind them with anion receptors could be quite significant as it could open avenues for new applications in biochemistry and medicine.[1,6,54,55]

4.1. OXYANIONS

The most prominent ions in organic chemistry are oxyanions. Oxyanions are negatively charged molecular anions that have an oxygen atom and some other element(s) in them. Oxyanions can be divided into multiple categories, e.g., organic, and inorganic oxyanions, as well as monomeric or polyoxyanions.[15]

Typical organic oxyanions include phenolates, enolates, carboxylates, and sulfonates. Typical inorganic oxyanions include perchlorates, nitrates, sulfates, and phosphates, the former of which is the most common inorganic oxyanion bound to halocarbons. Monomeric oxyanions include a single central atom, to which one to four oxygen atoms are bound. The most prominent monomeric oxyanions are the tetrahedral oxyanions, which include four oxygen atoms, e.g., perchlorate (ClO_4^-), phosphate (PO_4^{3-}), sulfate (SO_4^{2-}).[15] Polyoxyanions are large molecules, chains or networks that consist of multiple monomeric oxyanions.

Oxyanions are strongly solvated in aqueous media as they easily form HBs with water molecules. This causes oxyanions to be especially problematic to bind in scenarios that would correspond with real-world applications.[51] An example of an anion receptor capable of selectively binding hydrogen pyrophosphate ($HP_2O_7^{3-}$), an oxyanion, is presented in Figure 19.[56] The doubly cationic receptor achieves selective strong halogen bonding of $HP_2O_7^{3-}$ (K_a = 9838 ± 500 M^{-1} in 9:1 CD_3CN/methanol d4) while addition of HSO_4^-, NO_3^-, F^-, Br^-, I^-, AcO^-, ClO_4^-, PF_6^-, $C_6H_5CO_2^-$, $H_2PO_4^-$, and SO_4^{2-} did not induce any spectral changes.[56] Additionally, the receptor incorporates pyrene fluorescent markers at its terminal ends that enable functionality as a fluorescent chemosensor.

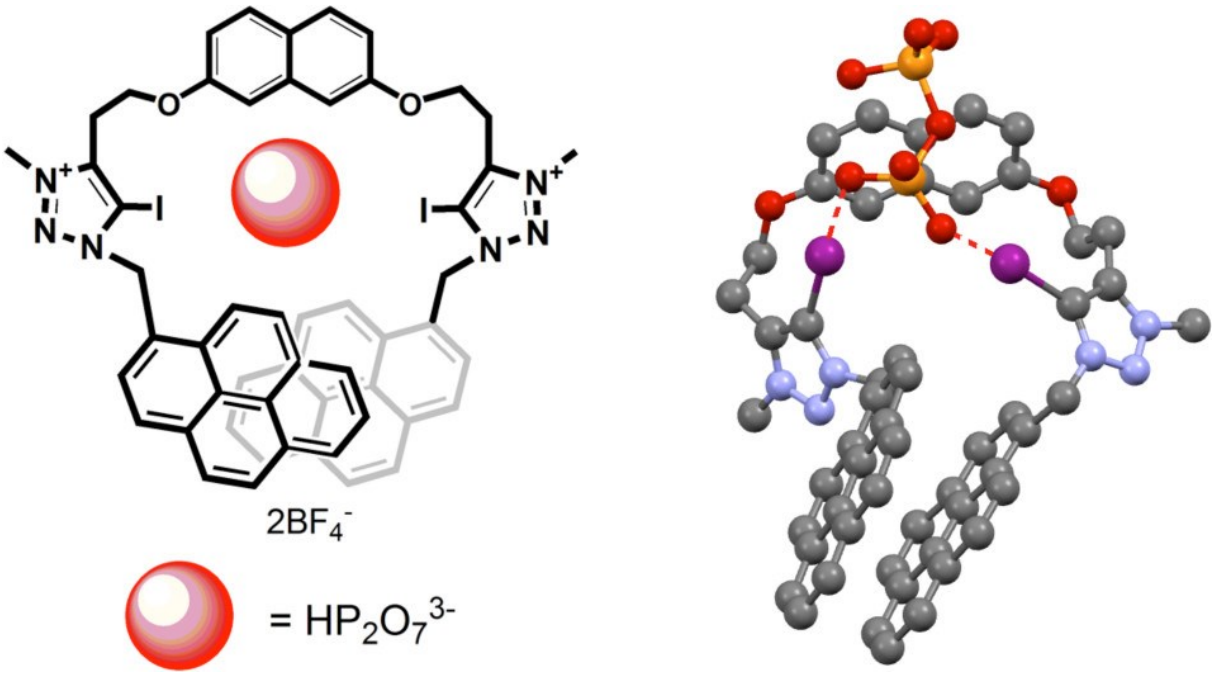

Figure 19. Iodotriazolium based receptor capable of selective fluorescent sensing of the hydrogen pyrophosphate anion. A rare example of an all XB-based oxyanion selective receptor.[56] Reprinted with permission from *J. Org. Chem.* 2014, 79, 6959−6969. Copyright 2014 American Chemical Society.

4.2. HALIDES

Halides are common anions as XB-acceptors.[16] They consist of a halogen atom with a negative charge, e.g., F^-, Cl^-, Br^-, I^- and At^-. The most common halides as XB-acceptors are chloride (Cl^-), bromide (Br^-), and iodide (I^-). Halides can act as multidentate acceptors. In general, they are bound with two or three XBs. Halides such as chloride[55] are important anions in human biology and therefore, their control with anion receptors, e.g., to transport anions across cell membranes,[57] could be quite significant.

Fluoride[16] (F^-) and astatide (At^-) are less common in XB anion receptors. Fluoride is a very small ion with low polarizability, which makes it difficult to bind with XBs. Astatine is not very abundant on Earth due to its short half-life (~8.1 hours for ^{210}At), and it is mostly the result of nuclear decay of heavier elements.[36] As such, there is little research of astatide (At^-) as an XB-acceptor, as of yet.

4.3. POLYHALOGENS

Polyhalogens are an odd species of molecules that contain neutral, negative, and even positive molecules comprised of halogens, bound together by halogen bonds.[58] Polyhalogen anions, or polyhalides, are negatively charged molecules that can act either as a XB-donor, or a XB-acceptor. I.e., a polyhalide can form type I and type II halogen interactions. A simple polyhalide, tribromide, and the halogen interactions it can form are depicted in Figure 20.

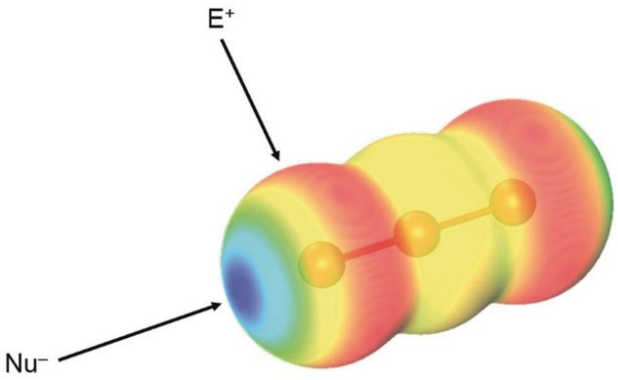

Figure 20. Electrostatic potentials of tribromide $[Br_3]^-$.[58] Tribromide can interact with an electrophile (E^+) with a type I interaction, and a nucleophile Nu^- with a type II interaction, i.e., a halogen bond. Red = electron-rich region, blue = σ-hole, i.e., electron-poor region.

The triatomic structure $[X_3]^-$ can be used to build large polyhalides with two other building blocks, X^- and X_2.[59,60] These polyhalides, e.g., I_7^{3-}, can be stabilized in supramolecular structures and further studied.[60] In terms of anion recognition, polyhalides are rather unstable without these stabilization structures to be utilized in anion recognition.

Neutral polyhalogens always consist of either two or more halogen elements, e.g., I_2, BrCl, I_2Cl_6, IF_7.[59] The diatomic polyhalogens can participate in XBs, like described in sections 3.1.3 and 3.1.4. The larger neutral polyhalogens are centered around a more electropositive central atom, e.g., Br in BrF_3, which can also act as an XB-donor.[61] However as XB-acceptors, there is limited research on neutral polyhalogens. Polyhalogen cations are more reactive than polyhalogen anions and as such, literature

is sparse.[59] Some examples, e.g., $[Br_3]^+$,[62] exist but literature on whether they can be utilized in halogen bonding anion receptors, is so far unreported.

4.4. OTHER ACCEPTORS

Pseudohalogens are polyatomic halogen-like molecules that can act as both XB-acceptors and donors, and they resemble dihalogens or interhalogens in their chemistry. There is a wide range of pseudohalogens, and they can be categorized in three: symmetric and non-symmetric pseudohalogens, and pseudohalogen anions. Symmetric pseudohalogens include, e.g., cyanogen $(CN)_2$ and thiocyanogen $(SCN)_2$. Non-symmetric pseudohalogens include cyanogen halides, e.g., BrCN, ClCN, ICN. Pseudohalogen anions are monoanionic compounds, they are sometimes called pseudohalides, and include, e.g., SCN^-, CN^-, N_3^-.[59]

Pseudohalogens are much like interhalogens as they too have an increasingly pronounced σ-hole when compared to homonuclear dihalogens. Only, pseudohalogens can go a step further in halogen polarization, as they can have even more electropositive σ-holes than comparable diatomic interhalogens. The increased polarization of a pseudohalogen can be utilized to build polypseudohalides or utilized as a XB-acceptor. A comparative graph of the pseudohalogen σ-hole to other dihalogens is presented in Figure 21.[59]

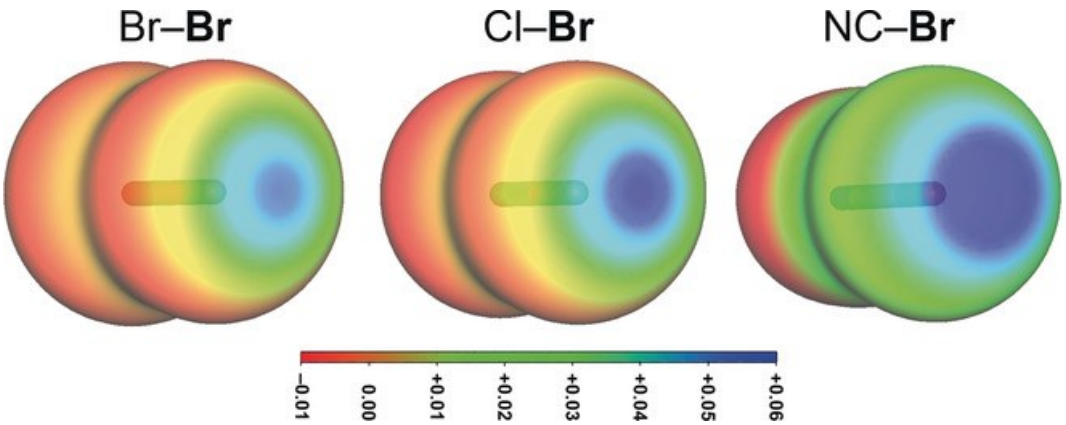

Figure 21. Comparison of electrostatic potentials of bromine compounds.[59] As the electron-withdrawing character of the moiety bromine is bound to grows (Br < Cl < CN), the more pronounced the σ-hole on the bromine is. The σ-hole on dibromine (left) is less pronounced than bromine chloride (middle), which in turn has a less pronounced σ-hole than cyanogen bromide (right).

Thiocyanate (SCN^-) is a particularly interesting pseudohalide as it has two potential halogen bond acceptors at its ends, the sulfur, and the nitrogen atom. Both have lone pairs of electrons that can accept halogen bonds and they can be utilized to form up to five halogen-pseudohalogen interactions, like in Figure 22.

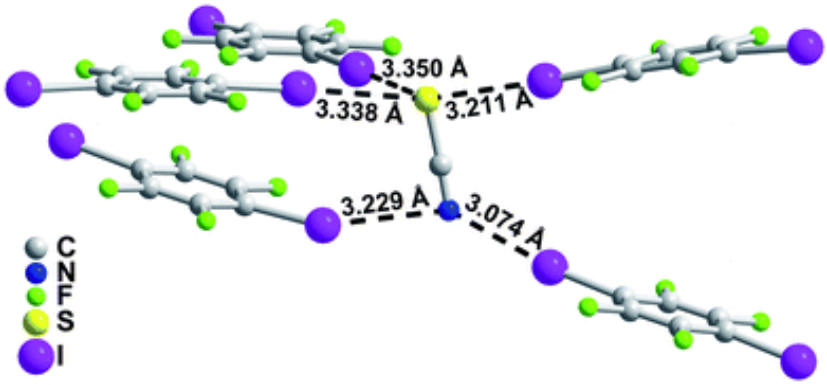

Figure 22. Thiocyanate pseudohalide network formed with *p*–$C_6F_4I_2$.[63] Thiocyanate forms five halogen-pseudohalogen interactions with tetrafluorodiiodobenzene molecules. The sulfur atom of thiocyanate engages in three interactions, while nitrogen engages in two. Tetraethylammonium (Et_4N^+) counter cations have been omitted for clarity.

Cauliez *et al.*[63] stated that the five interactions in Figure 22 are indeed all halogen bonds and that five are possible because of one of three mesomeric forms of the SCN^- anion, $S^- - C^+ = N^-$ (Figure 23 C). Both nitrogen and sulfur have negative charges, enabling them both to accept XBs with an additional electron pair.

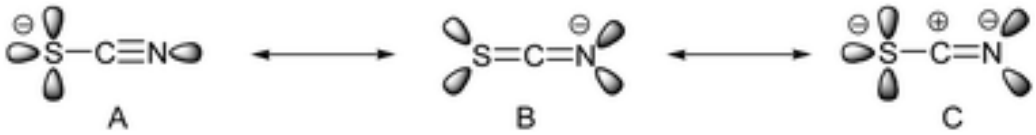

Figure 23. Mesomeric forms of thiocyanate.[63] Form C is the one contributing to the conformation of thiocyanate in Figure 22. Reproduced from P. Cauliez, V. Polo, T. Roisnel, R. Llusar and M. Fourmigué, *CrystEngComm*, 2010, **12**, 558, with permission from the Royal Society of Chemistry.

Additionally noteworthy from Figure 22 are the binding angles of sulfur. Nitrogen accepts the XBs at bent, non-linear I · · · N ≡ C angles (145–170°), while sulfur accepts XBs at acute I · · · S–C angles (<90°). It is easy to dismiss the sulfur XBs as type I halogen-halogen interactions, when in actuality, confirmed by Cauliez *et al.*,[63] it is an intrinsic ability of sulfur to accept XBs at approximately 90° I · · · S–C angles. According to their calculations, the electron density of S on SCN^- has a second small σ-hole on the backside of the S–C bond. This causes the optimal binding angle of S to a halogen to be near 90° and I · · · S distance lengthening, which they experimentally observed.[63]

There are some naturally occurring XBs in biological systems. T_3 and T_4 interact with transthyretin and thyroid hormone receptors with XBs.[6] A study of the protein databank determined that there were 778 cases of short contact interactions that involved halogens. A majority of these were C–X · · · O interactions in in protein backbones between carbonyl oxygens and halogens of small molecules (e.g., halogenated nucleotides or drugs).[6,49,64] Data from biological short contact halogen systems[6,65 a)] was used to interpret that Br and I generally prefer R–X · · · Y angles closer to 150–180°. Cl systems are more flexible with R–X · · · Y angles varying from 85–180°, with a slight majority presence at 145–150°. Chlorine systems with small R–X· · · Y angles (much less than the ideal 150° for XBs)[66] likely are either type I halogen interactions with electrophiles (Figure 20) or other interactions and are not actual halogen bonds.

5 ANION RECEPTORS

Anion receptors are supramolecular hosts capable of binding anionic guests with various non-covalent interactions. Typical anion receptors utilize HBs to bind anions.[5] XB-based anion receptors are new and XBs in general tend to compete with HBs when in competitive solvent media. Typical anion receptors are also cationic in nature. Cationic XB-donors bind anions more strongly than neutral donors,[7,67] but the counter ions (anions) of the cationic receptors have considerable effects on the binding strength of XBs that are not yet fully understood.[68] Cationic charge can also be used to control the binding stoichiometry of an anion receptor complex, i.e., whether, e.g., 2:1 or 1:1 complexes are formed can be controlled with the amount of cationic XB-donors in the receptor.[69]

Host-guest binding happens in solution and the solvent has a large impact on the binding. As the concentration of the solvent is much higher than either the guest or the host, the likelihood of it competing with the guest molecules is very high. This competition is guided by polarity, hydrophobicity and the strength of the possible bonds created between the host and the guest. Guest binding to a host is often quantitated with a binding constant (K_a). The binding constant K_a is unfortunately relative to the solvent medium and the effect of solvents are difficult to estimate.[56] However, it can still be used as an approximation of binding strength.

As a solute is being solvated, solvent molecules arrange themselves around a solute molecule according to their dipoles. This creates solvation complexes. Both the receptor and the target anion can be enveloped in a solvent complex.[34 d)] Anions in general are strongly solvated in protic solvent media, which creates increased difficulties. As such, the introduction of solvated guests to a solvated receptor can be difficult.

Macrocyclic receptors bind anions with greater affinities than acyclic receptors. Mechanically interlocked molecules (MIMs) typically bind with greater affinities to anions than non-interlocked molecules. MIMs have several advantages over other receptors. They typically have a hydrophobic center with multiple binding sites. This center can assist in desolvation of the guest, which is particularly valuable in competitive solvent media, e.g., water. MIMs also have a large molecular scaffold around their central binding core which can be modified to, e.g., improve solubility by

adding suitable groups, indicate binding of anions with optical or fluorescent reporter groups.[1]

5.1. DESIGNING ANION RECEPTORS

There are a variety of different aspects to consider when designing anion receptors. These include appropriate binding sites, solubility compatibility, size compatibility of the receptor to the target anion, geometry of the receptor, charge balance between the receptor and the guest etc. These should be considered after the necessary moieties have been determined for the binding of guests.

Anion receptors have a range of different moieties, but most can be categorized as either a spacing group, as part of the XB-donor and its EW-groups, and R-groups. Spacing groups are incorporated for various reasons e.g., to increase the guest cavity of a receptor, adjust the binding angles of the receptor, or space out different moieties. According to the calculations of Nepal and Scheiner,[5] it is difficult to predict the binding strength of an anion receptor based on geometric parameters, such as the size of the spacer group or the bite angle of the receptor.

As introduced in section 3, XB-donors can incorporate a range of different EW-groups as a part of them to increase XB strength, e.g., perfluoroarenes, pyridinium, nitrogen or oxygen-containing groups. R-groups can be used to adjust receptor properties, e.g., adjust receptor solubility in target medium,[11] assist in receptor synthesis, function as a luminescent marker to indicate anion binding,[1] or assist in desolvation of a guest anion.[1] R-groups can bring a lot of flexibility to a receptor, and they can be adjusted along the synthesis route of a receptor to assist in different ways as needed. Figure 24 shows an example of cleft-type anion receptor design.

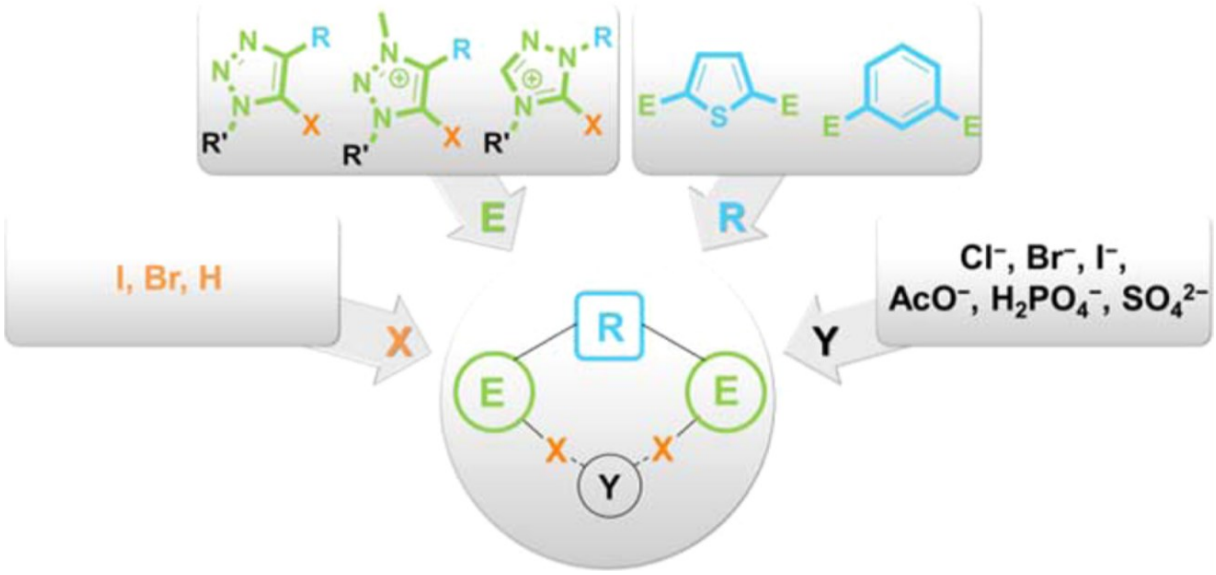

Figure 24. Example scheme of a cleft-type anion receptor design.[7] Different spacer groups (R) are used to connect XB-donor groups (E), where donor atoms (X) bind to an anion (Y). Changing one parameter (R, E, X, Y) can change whether the receptor binds an anion at all. EW groups (R') can be used to adjust different properties of the receptor, such as solubility or C–X polarization. Reprinted with permission from *J. Org. Chem.* 2015, **80**, 3139–3150. Copyright 2015 American Chemical Society.

Tepper *et al.*[7] investigated cleft-type anion receptors and their properties. These included the effect of halogen polarization, the spacer group between the XB-donor groups and the influence of the bound anion. They found several conclusions from their experiments, such as that the central spacer group plays a critical role in anion binding. The spacer group changes the bond angle of the receptor to the anion, and it was deduced that the thienyl spacer group receptors had small binding affinities to small anions. Using DFT calculations it was estimated that the thienyl receptors only bound to the anions using a single halogen bond. The phenyl spacer group receptors were found to prefer bidentate XBs to the studied anions with high affinities (K_a = 3400 M^{-1} with sulfate in DMSO-d6).

5.2. SPACER GROUPS

The most typical spacer groups are benzene, pyridine, dimethylnaphthalene, thiophene or carbazole.[1,5,15] All spacer groups contribute to the physical and chemical properties of a receptor, e.g., size, solubility, rigidity, and preorganization. Some spacers, like benzene,[5] can also participate in the binding of an anion, e.g., with HBs.

Scheiner and Nepal[5] compared 4 different spacers with imidazolium and triazolium moieties, as well as different binding atoms (H, Br, I). They compared the binding ability of each receptor to fluoride, chloride, bromide, and iodide through computational means. It was found that the spacer group does affect halide binding although it is difficult to predict. Benzene and naphthalene were found to enhance binding strength the most, although it was unclear why. Benzene was suspected to contribute to HBs in some complexes. Naphthalene was found to cause the largest binding angles of all spacers, although this alone did not seem to matter much to the binding strength of halides. Thiophene and carbazole were found to be poorer spacer groups regarding binding strength. As the contribution of a spacer group is difficult to predict, experimentation with different spacers should be performed when optimizing novel anion receptors.

5.3. BINDING UNITS

Binding units, i.e., XB-donors should be optimized according to various parameters, most important of which are the target anion and the target solvent medium. The more strongly the target anion is solvated in the solvent medium, the harder it is for an anion receptor to effectively bind anions. Neutral XB-donors are typically employed in aprotic solvent media or in mechanically restricted systems (macrocycles, MIMs etc.). Cationic XB-donors should especially be used in protic solvents where increased binding strength is required.[1]

The target anion may not interact with every XB-donor moiety and may pose anion-specific steric requirements. In general, iodine in a charged XB-donor moiety is the most effective at forming XBs. However, iodine has a rather large atomic radius and as XBs are sensitive to steric hindrances,[6] bromine might be more suited for smaller binding cavities of receptors.

5.4. MECHANICALLY INTERLOCKED MOLECULES

In general, mechanically restricted molecules are more effective at forming XBs due to a reduced degree of freedom, i.e., a receptor can exist in fewer possible conformations that would not be optimal for the binding of a guest. Mechanically interlocked molecules (MIMs) are the most restricted receptors in their degree of freedom, typically making them the best possible binders of guests.[1] If possible, anion receptors should be designed to be mechanically restricted to achieve maximal binding affinity.

Figure 7 shows an example of the benefits of mechanical restriction. The receptor by Mungalpara *et al.*[41] is able to achieve strong chloride binding with a neutral, all-XB based receptor in aqueous media.

6 ANION SENSING

6.1. OVERVIEW OF ANION SENSING AND GUIDING PRINCIPLES

An anion sensor is a molecular system capable of detecting the presence of anions and is capable of reporting detection. There are a few different ways to detect the hosts binding anions and it is always dependent on the host-guest complex under study. Some detection methods include colorimetric and luminescent sensors, redox-active sensors, capacitive and chemiresistive sensors.[13] The methods rely on either the intrinsic properties of the receptor, or a covalent reporter-group bound to the anion receptor that changes the output of information, e.g., fluorescence, when a guest is bound. A general overview of anion sensor functionality is presented in Figure 25.

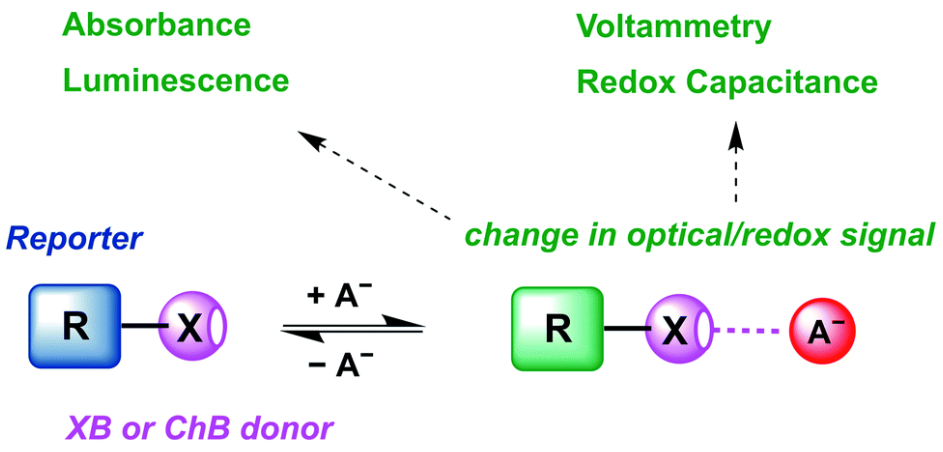

Without Dedicated Reporter:

Capacitance

Potentiometry

Chemiresistance

Figure 25. An overview of XB-based anion sensor functionality.[13]

Anion sensors in general can be assessed in three vital aspects that determine the effectiveness of the sensor. They are sensitivity, selectivity, and functionality in aqueous media.[13] Sensitivity determines the limit of detection (LOD) of a sensor, i.e., in what range of guest concentration the sensor can function. LOD can be determined with the formula

$$\mathrm{LOD} = 3 \cdot \frac{\mathrm{SD}}{\mathrm{S}},$$

where LOD is the limit of detection, SD is standard deviation of the background noise or reference sample, and S is the slope of the calibration curve (sensitivity). If LOD is calculated as such, it can be improved by either reducing SD or increasing the slope of the calibration curve. The latter can be done by enhancing the binding affinity of the sensor. The former is dependent on the measurement method. An ideal sensor has a low LOD and is thus sensitive to even small concentrations of anions. LOD can be reported as concentration values, e.g., molar concentration. Typical ranges are in mM to µM.[13]

Selectivity is dependent on the sensor used. A sensor does not need to be selective to just one anion as multiple sensors can be employed to gather a collective set of data

on the anionic composition of an analyte. In general, a high level of selectivity results in more accurate measurement data and is thus beneficial. A sensor can also benefit from toleration of small amounts of other anions as this gives a sensor flexibility to perform with a wider range of analytes without the need for additional sample preparation.[13]

Functionality in aqueous media is also vital for real-world applications of anion sensors. Sample transfer between solvent media is very arduous and not always possible. Hence, a sensors functionality in, or tolerability of water creates a whole range of applications that would not be there otherwise. Parallel to in-water functionality, another vital viewpoint is device integration. An anion recognition system should be designed to be integrated into some type of device. This can be done by anchoring the anion host system to condensed matter, such as gels, electrodes, or nanoparticles. Anchoring can be achieved with the incorporation of anchor groups, e.g., disulfide,[2] to the anion receptor system.[13]

6.2. OPTICAL SENSORS

Colorimetric sensors are molecular systems that undergo a color change upon guest binding. This change is required to be drastic enough for the naked eye. A classic, visible colorimetric change is the color change iodine goes through upon solvation. The solution is purple in non-polar solvents and turns brown in polar solvents.[70] This can be used to detect the presence of molecular iodine (I_2) and the state of the solvent. This, however, is not a very useful colorimetric sensor as the color change from violet to brown can be hard to detect if only smaller amounts of polar solvents are present, or vice versa.

A more useful colorimetric sensor would, e.g., turn on or off in the presence of a target molecule, as the color change from colorless to colorful is easier to detect. The change in color can be detected via UV/Vis spectroscopy.[71] A strong response (strong color change) caused by anions makes a colorimetric anion sensor even more sensitive as even low concentrations of anions cause detectable changes. An example of a colorimetric sensor is the rotaxane system synthesized by Barendt *et al.*[71] (Figure 26).

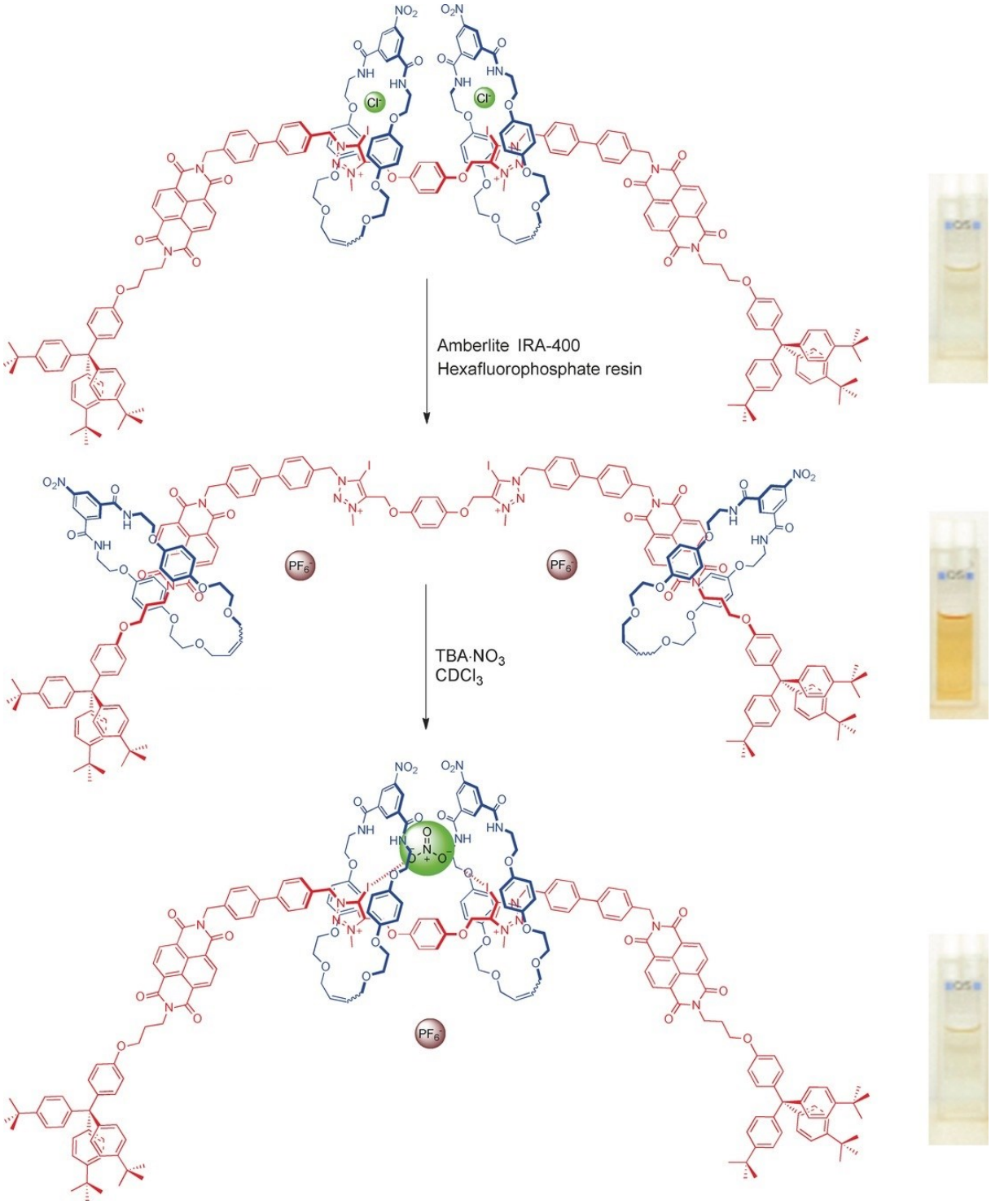

Figure 26. Colorimetric [3]rotaxane anion sensor complexes and the colors of their $CHCl_3$ solutions. Upon binding with Cl^- and NO_3^-, the solution turns from the guest-free orange state (middle) to colorless (top and bottom). The macrocycles of the rotaxane travel from the neutral position of the naphthalene diimide (NDI) recognition sites, or stations, to the triazolium stations in the middle upon guest binding.[71]

The sensor of Figure 26 is selective to nitrate over some other oxyanions and chloride. According to Barendt *et al.*,[71] this is exceptional in interlocked XB anion receptors as HB capable interlocked systems have so far had stronger association constants to anions than XB systems. The sensors of Figure 26 showed reduced response in increasing amounts of methanol added in chloroform solutions, up to 1:1 $CDCl_3$/MeOH, i.e., they were not reported to be functional in aqueous systems.

Like colorimetric sensors, luminescent sensors can be monitored using UV/Vis spectroscopy. Upon anion binding, luminescent sensors typically emit visible or UV light which can be captured with detectors. Luminescent XB sensors can be generally categorized by their structure or their mechanism of function. These include, e.g., organic sensors, metal center sensors or aggregation-induced emission sensors.[13] An example of a simple organic fluorescent anion sensor is shown in Figure 14. Metal atoms used as luminescent reporter groups is also possible. They can be incorporated into many kinds of receptors, e.g., cleft-type receptors, or MIMs. Typical metals used include rhenium, iridium, and ruthenium.[13]

Aggregation-induced emission (AIE) is a term used to describe phenomena where a molecular system, with the introduction of some other molecule or solvent, forms into aggregates and shows an increase in emission intensity.[72] Typical formed aggregates are nanoparticles. In anion recognition, AIE can occur upon guest binding, like the sensor of Figure 27. The tetrakis(iodotriazole) XB anion receptor forms large aggregates of host-guest complexes upon guest binding that show significantly increased fluorescence compared to non-aggregated receptors. AIE responses were not observed for the HB analogue nor non-fluorinated phenyl substituents, i.e., weaker XB-donor moieties, highlighting the importance of strong XBs.[73]

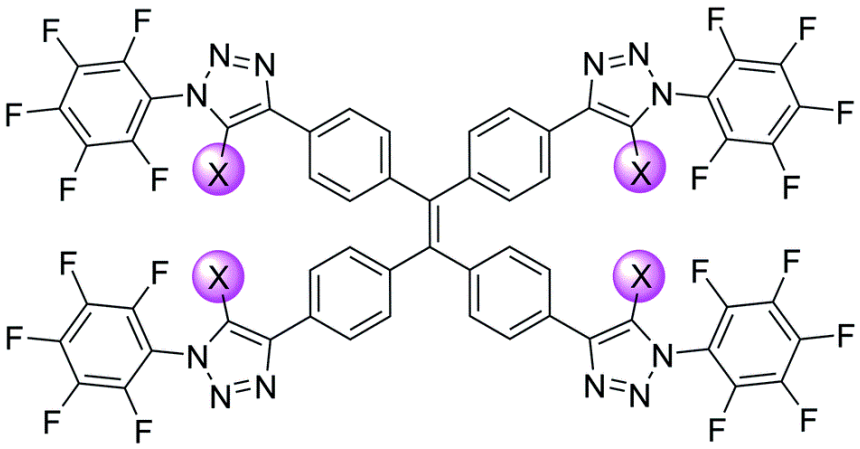

Figure 27. AIE responsive fluorescent anion sensor (X = I).[73] The receptor forms ~100 nm nanoparticles and exhibits increased emission intensity upon binding anions. Picture from Hein and Beer.[13]

6.3. ELECTROCHEMICAL SENSORS

Electrochemical sensors are easy-to-use, low-cost, and a well-known method for sensing various molecules and ions. Especially regarding ion sensors, they are widely used but they can lack selectivity, sensitivity, and they are not best suited for anions. There are electrochemical XB-mediated redox-active sensors, capacitive sensors, and potentiometric sensors.

6.3.1. Redox-active Sensors

Redox-active anion sensors measure the change in potential (V) between the reduced and the oxidated state of the host-guest complex in solution. This change in potential is measured with voltammetric techniques, e.g., cyclic voltammetry (CV), square-wave voltammetry (SWV), and differential pulse voltammetry (DPV).[13,74] Typically, the receptor is redox-active instead of the guest. The measured phenomenon is the change of potential between a reduced receptor and an oxidated host-guest complex. The binding of an anion stabilizes a higher oxidation state of the receptor, i.e., a cationic receptor. The cationic receptor then acts as an enhanced XB-donor, binding an anion more strongly, resulting in stronger XBs when compared to the neutral receptor. An illustration of the change in potential of a redox-active anion sensor is shown in Figure 28.

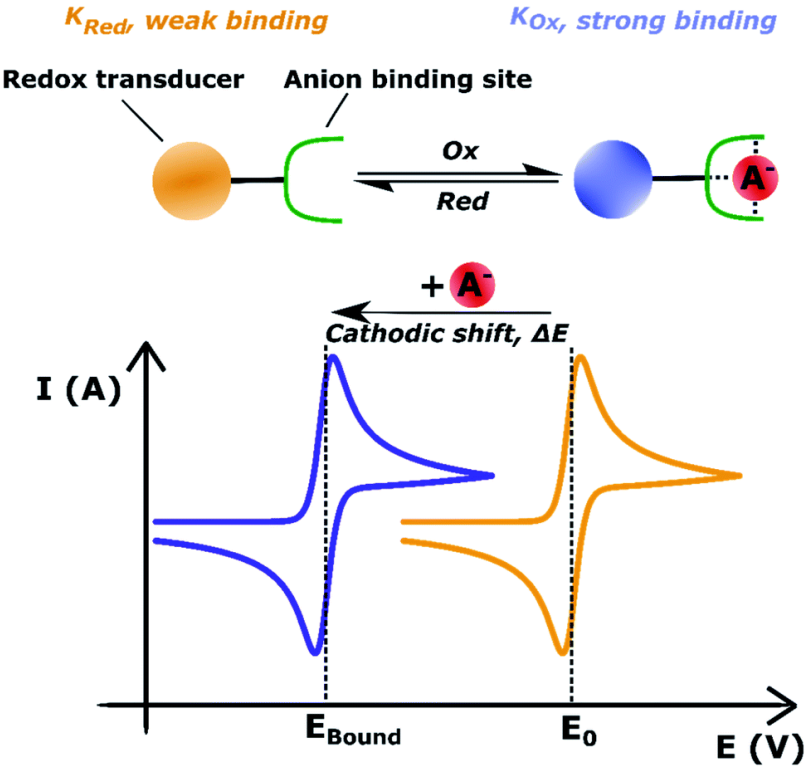

Figure 28. The working principle of a voltammetric redox-active anion sensor.[13] A change of voltage is observed between a reduced anion receptor (E_0, orange) and an oxidated receptor (E_{Bound}, blue). The binding of an anion stabilizes the higher oxidation state of the receptor and is seen as a change in voltage (ΔE). Hence, the change in voltage is directly proportional to the ratio between the binding constants (K) of the oxidation states ($\Delta E \propto \frac{K_{Ox}}{K_{Red}}$).

A common redox-active moiety incorporated into anion receptors is ferrocene[1,13,74] but recently, iodo-TTFs have been used as doubly cationic moieties to investigate XBs. Schöllhorn, Fave and co-workers[53,75] presented iodo-TTF as a redox-active receptor, and used TTF-based sensors to determine that electrolyte anions, e.g., BF_4^-, PF_6^-, NO_3^-, can affect the sensing capabilities of voltammetric anion sensors. This finding could be utilized to adjust the strength of XBs of redox-active anion sensors, which can be used to selectively detect XBs in solution with sensitivity. In Figure 29, the different oxidation states of the TTF-sensor can be discerned, which can be controlled electrochemically. This tendency was used to trigger and sense the formation of XBs, even in a protic medium (5 % water in DMF).[53]

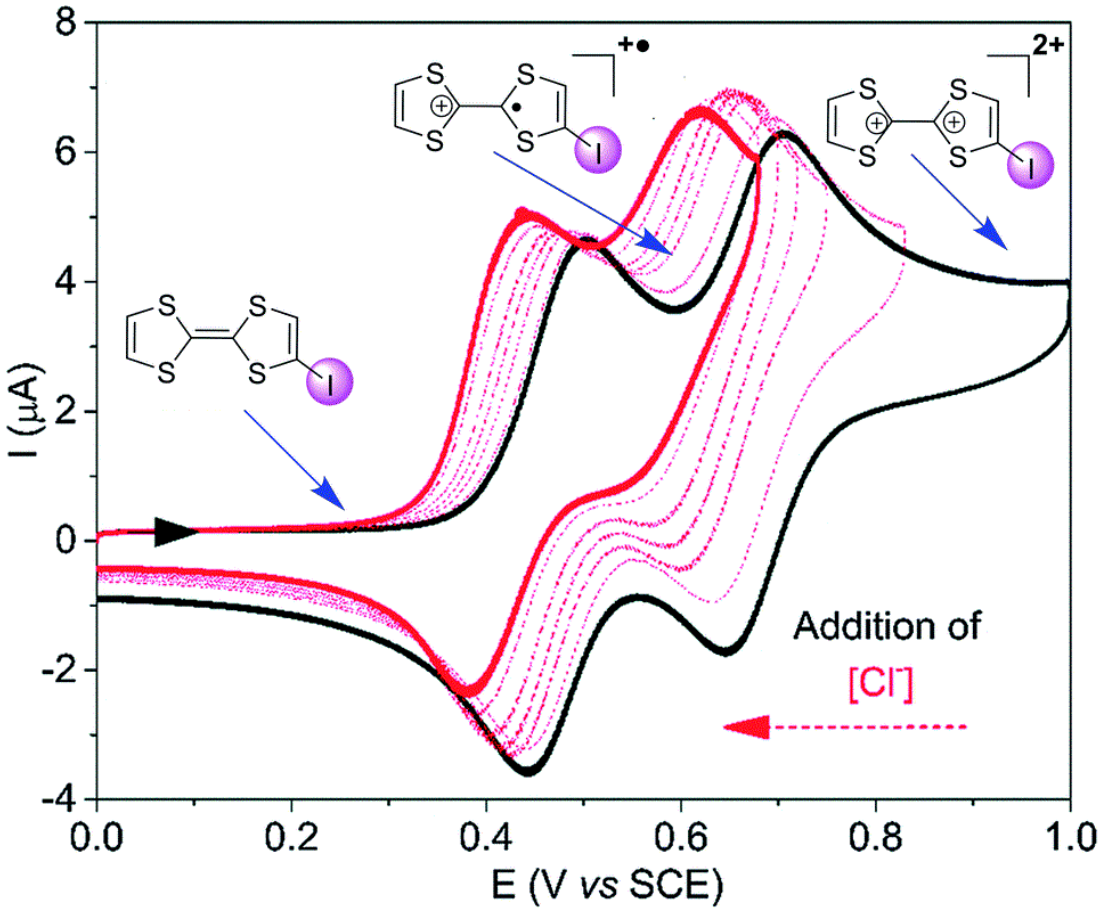

Figure 29. The CV potentials of reduced (left) and oxidated states of iodo-TTFs (middle and right) in DMF.[53] Increasing amounts of Cl^- (up to 50 mM) causes catodic shifts of the potentials (red), compared to a guest-free receptor (black). Picture from Hein and Beer.[13]

In contrast to in-solution receptors, it is also possible to anchor receptors on conductive surfaces, such as electrodes. Compared to diffused in-solution receptors, anchoring is advantageous to circumvent poor receptor solubility and reusability. Additionally, surface-confined receptors are capable of sensing under solvent flow, they have increased responsivity, and they can be easier to incorporate to a device.[74] Sensing with surface-confined receptors can also be called interfacial sensing.

One example of interfacial sensing is self-assembled monolayers (SAMs) (Figure 30 left). Self-assembled monolayers are, in short, single self-assembled layers of molecules anchored on surfaces, typically electrodes or other conducting surfaces. SAM molecules are anchored from one or more moieties to the surface. They can be interlinked, like a polymer chain, and they have a reporter group(s) or binding units at

their non-surface-bound ends. The groups of Beer and Davis[76] incorporated a ferrocene-based XB-receptor to a gold electrode. CV measurements showed the system to be highly responsive, which lead to the creation of a proof-of-principle device, a flow cell (Figure 30 middle). This device was used to measure the response of HSO_4^{2-} over 4.5 hours, which showed the device did in fact function as intended, i.e., as a continuously measuring flow cell.

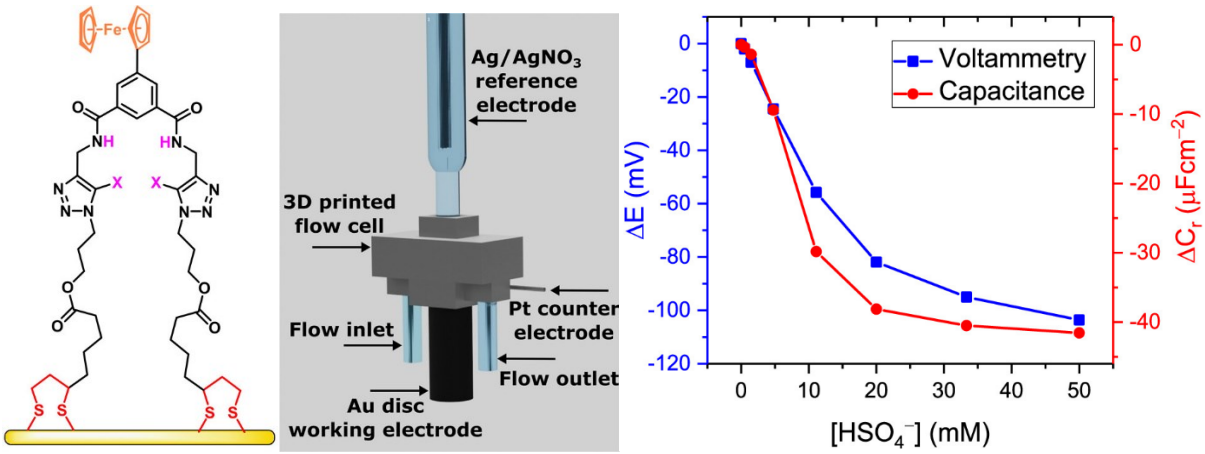

Figure 30. Structure of a SAM-forming receptor (left) (X = I), proof-of-principle device (middle), and a comparison of CV and redox capacitance measurements.[77] Adapted with permission from *J. Am. Chem. Soc.* 2021, 143, 45, 19199–19206. Copyright 2021 American Chemical Society.

In a further study, the device of Figure 30 was used again as a capacitive sensor to measure faradaic capacitance, as redox capacitance is very sensitive to local polarity changes.[77] Compared to voltammetry (Figure 30 right), redox capacitance was determined to be superior compared to CV with better temporal resolution, tunable performance, and direct data readout without further analysis. Capacitive sensors are further discussed in section 6.3.2.

6.3.2. Capacitive Sensors

Capacitive anion sensors change their capacitance when bound to a guest, which can then be detected from the conductive surface they are anchored to. The benefit of capacitive sensors, e.g., compared to redox-active sensors, is they require no redox transducers. Redox transducers are anion-binding enhancers that amplify signals.

Solutions are doped with excess of transducers, thus the lack of them in a sample solution enables facile analysis with more flexibility.[2]

The halotriazole-based neutral anion receptors introduced in section 2 (Figure 1 left) were converted to a SAM to measure capacitance on a gold electrode (Figure 31). The receptor was shown to function in an aqueous phase as a capacitive XB anion sensor, selective to ReO_4^-, I^-, and SCN^-. According to Hein *et al.,*[2] this was the first example of XB-based non-faradaic capacitive anion sensing. Importantly, the same approach could be further utilized to detect any anion with appropriate anion sensors.

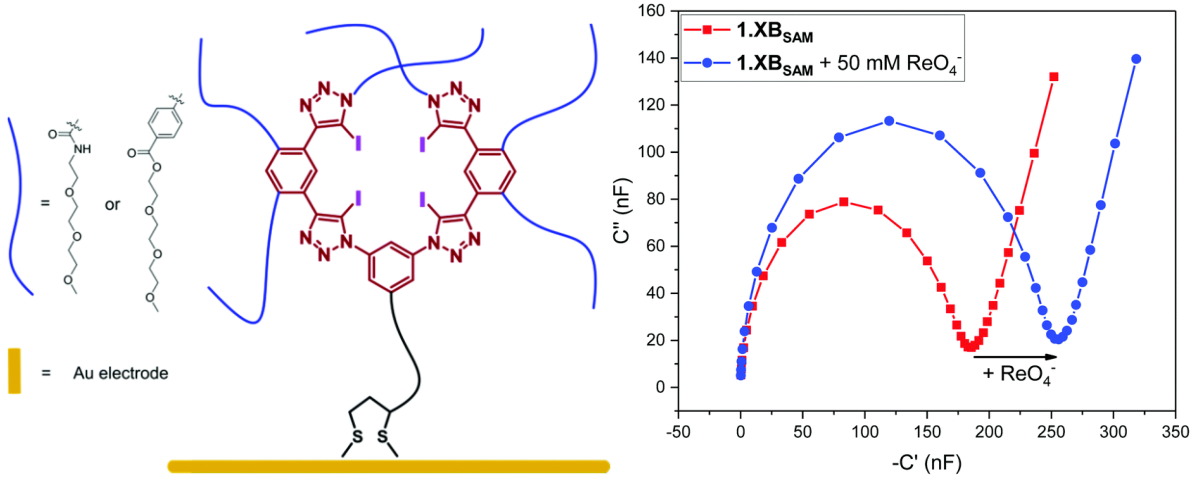

Figure 31. A SAM anion receptor (left), and the Nyquist plots of the receptor with and without 50 mM of ReO_4^- (right).[2] Disulfide (black) acts as an anchor to a gold electrode (yellow), while hydrophilic polyethylene glycol groups (blue) surrounding the binding cavity (purple, iodine) increase water solubility. Reproduced from R. Hein, A. Borissov, M. D. Smith, P. D. Beer and J. J. Davis, *Chem. Commun.*, 2019, **55**, 4849, with permission from the Royal Society of Chemistry.

6.3.3. Potentiometric Sensors

As a proof-of-concept example for XB-based potentiometric sensors, Lim, Goh and co-workers[78] synthesized a halogen bonding ionophore that can be used in an ion selective electrode for potentiometric anion sensing. The ionophore (Figure 32) showed selectivity towards I^-, with a LOD ≈ 1.25 μM, and had anti-Hofmeister series preference for I^- over SCN^-. As the first XB-based potentiometric sensor, the ionophore serves as a basis for future research.

Figure 32. XB-based ionophore selective to I^-.[78] Adapted with permission from *Anal. Chem.* 2021, 93, 46, 15543–15549. Copyright 2021 American Chemical Society.

6.4. CHEMIRESISTORS

Chemiresistors are sensors that measure a change of conductivity from suspended material between two electrodes. The conductivity change is induced by the presence of an analyte, which can be a gaseous molecule or an ion in solution. Halogen bonding has been used in chemiresistive gas sensors as enhancers to detect pyridine, cyclohexanone, and 2,3-dimethyl-2,3-dinitrobutane (DMNB).[79,80] The sensors used single-walled carbon nanotubes (SWCNT) non-covalently functionalized with non-fluorinated or fluorinated *p*-dihalobenzene, or 3-halodurene (3-halo-1,2,4,5-tetramethylbenzene). The arenes were introduced to the SWCNTs by "ball milling", i.e., mechanical abrasion together. This composite of SWCNTs and arenes was then introduced between two gold electrodes, to which the gaseous analytes were introduced. DMNB was introduced from acetonitrile.

Iododurene and diiodobenzene showed stronger responses to pyridine concentrations as low as 1 ppm, when compared to much higher concentrations of interferents (>1000 ppm).[79] This successful selective detection was attributed to the swelling of the sensor matrix by recognition-induction caused by XBs formed between the haloarenes and pyridine.[79] Iodoarenes were found to have the strongest responses,[79,80] which is indicative of XBs and the donor ability of halogen atoms (I > Br > Cl). Haloarene functionalized SWCNTs were demonstrated to have stronger detection responses to cyclohexanone and DMNB than non-functionalized SWCNTs.[80]

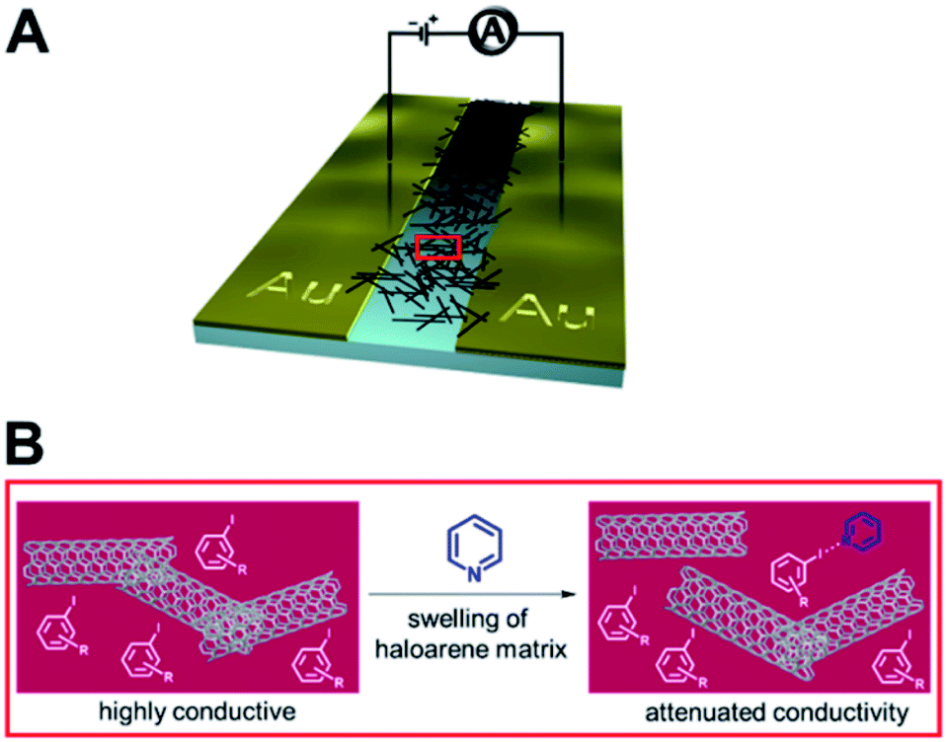

Figure 33. A schematic of a pyridine-selective chemiresistor, and the proposed sensing mechanism.[79] A) A diagram of the chemiresistor. SWCNTs functionalized with haloarenes suspended between two gold electrodes. B) Swelling of the sensing matrix, induced by XBs formed with pyridine. The conductivity of the system decreases as the matrix swells, which is then detected. Reprinted with permission *ACS Sens.* 2016, 1, 2, 115–119. Copyright 2016 American Chemical Society.

6.5. OTHER SENSING METHODS

Visual detection can be done in other ways than colorimetric measurements. A visual breakdown of a gel is moderately easy to see and can be used as an anion sensing method when the breakdown happens due to the introduction of anions.

Liu *et al.*[81] synthesized an organogelator capable of selective visual anion sensing (Figure 34). The iodoperfluoroarene-based dendritic gelator forms large fibrous networks with itself, which can trap solvents and thus form gels. The gels can be broken down with the introduction of Cl^- to the gel. This was attributed to the formation of XBs which disrupt the π-π stacking interactions, breaking the structure of the fibril network. Other anions were tested, and only other halides were found to induce breakdown with higher concentrations than Cl^- (2.0 eq. for Br^-, 5.0 eq. for I^-).

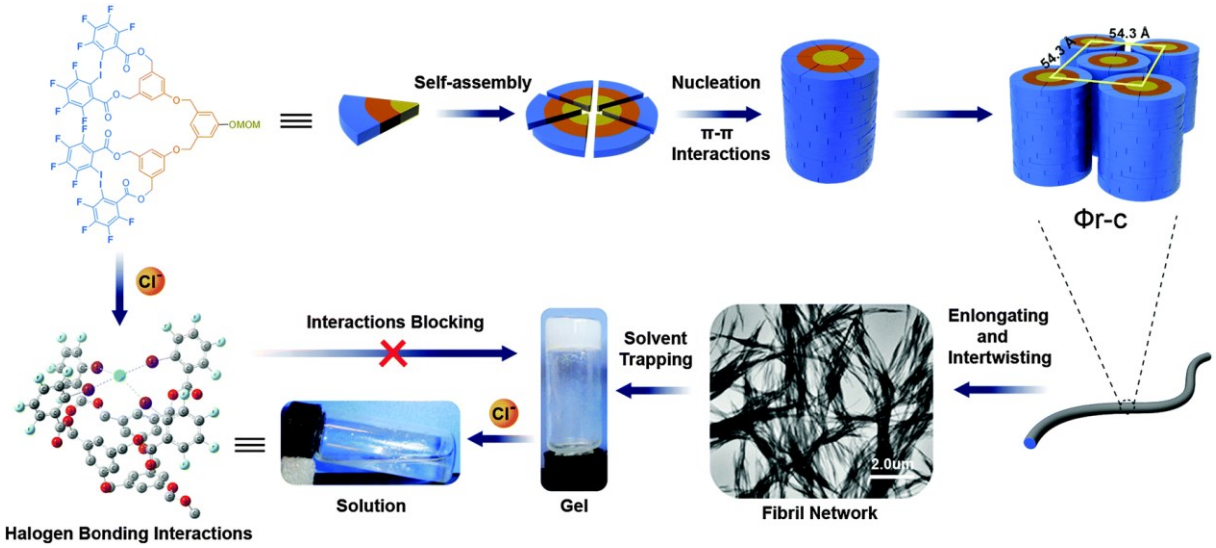

Figure 34. A diagram of visual anion sensing interactions by an organogelator.[81] The gelator (top left) can form fibril networks (bottom right) with itself with π-π interactions. These networks can trap solvents to create gels (white, bottom middle photograph), which can be broken down with the introduction of Cl^- to the gel.

Reproduced from Z. Liu, Y. Sun, Y. Feng, H. Chen, Y. He and Q. Fan, *Chem. Commun.*, 2016, **52**, 2269, with permission from the Royal Society of Chemistry.

EXPERIMENTAL SECTION

7 OBJECTIVES

The goal of the laboratory work was to create receptor molecules that could form halogen bonds to anions and selectively recognize them. These receptors included a tridentate macrocyclical XB receptor[41,82] and two cleft-type bidentate XB receptors (Table 1).[83–85] Five different reagents were used as a basis for these molecules, 3-bromoaniline, 3-iodoaniline, 2-amino-6-bromopyridine as well as 1,3-diethynylbenzene and isophthaloyl dichloride.

The syntheses performed were performed under Ar, mostly in room temperature. A typical synthesis would follow a structure of reaction, filtration, evaporation of solvents and the left-over product would be purified via column chromatography. Synthesis products were characterized using NMR, MS and XRD measurements.

All attempted reactions did not proceed as desired, and it was hard to control the self-reaction of click-ready molecules. The iodination reactions of terminal hydrogen of ethynyls resulted in an unresolved mixture of compounds. Thus, the goals of the experimental work were not achieved.

This experimental work was performed in the Department of Chemistry at the University of Jyväskylä, under the supervision of Arto Valkonen and Lauri Happonen, as part of a Master's thesis (KEMS9550) from the 14th of June until the 6th of October 2021.

Table 1. Simplified synthesis schemes* of target receptors[41,82–85]

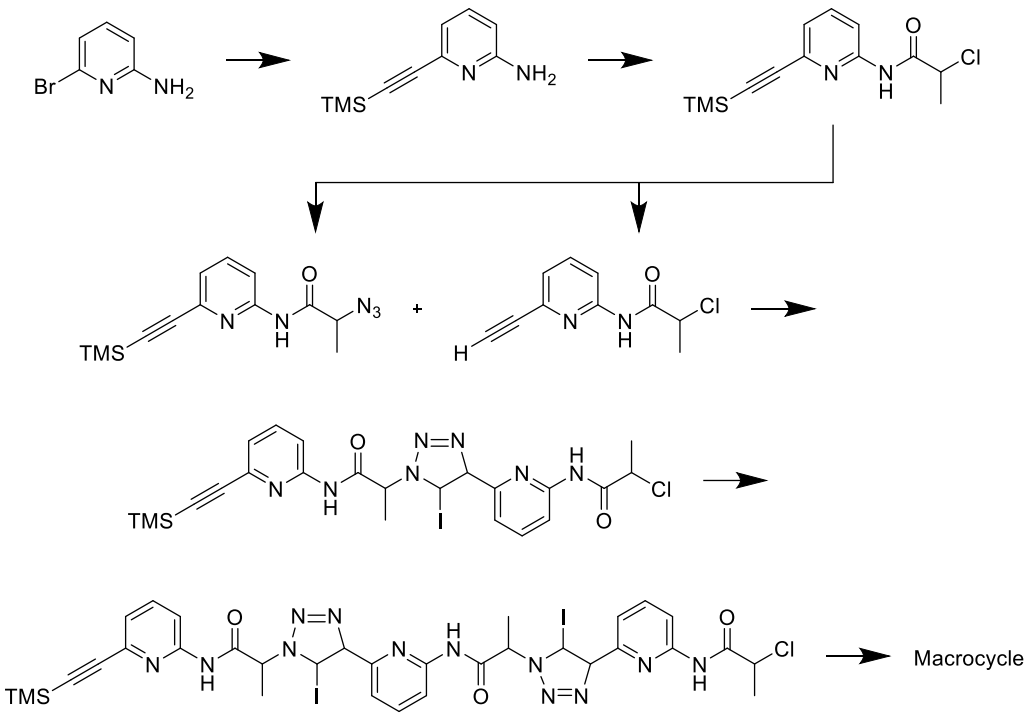

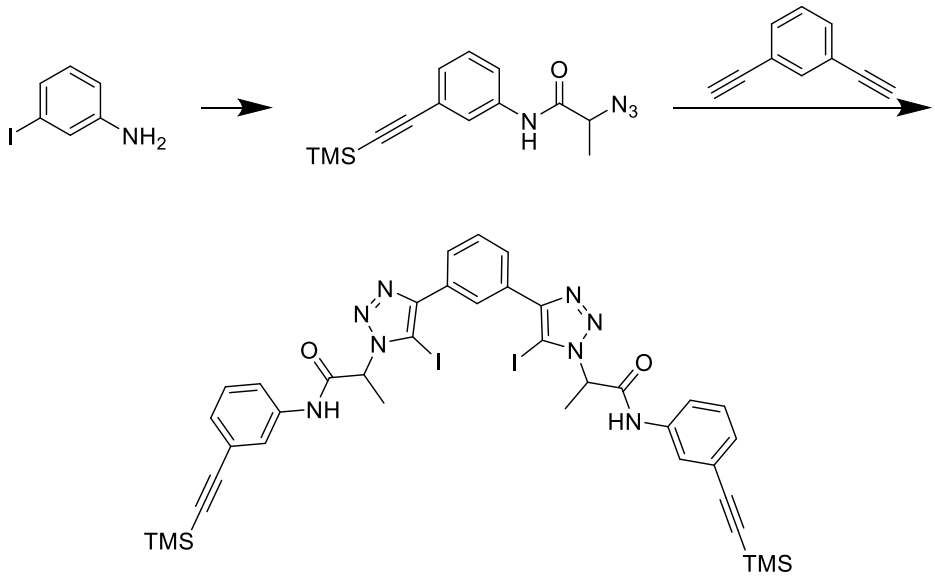

*Reaction conditions have been omitted for clarity. Conditions are detailed in section 11.

8 MATERIALS AND METHODS

All syntheses were performed under Ar. In all syntheses solvent was evaporated from samples with a rotary evaporator using a 40–80 °C heated bath. TLC was performed with silica gel 60 F254 silica gel as a solid phase. Column chromatography was performed with silica gel 60 with a grain size of 0.040-0.063 nm. The width of the column used was 3.2 cm unless otherwise specified. Lengths of the columns used are reported individually in each synthesis. A Tetra APS150 aquarium pump was used as a source of constant uniform pressure with each column to shorten retention times.

NMR measurements were performed at 30 °C with a Bruker Avance III HD Nanobay 300 MHz NMR spectrometer or a Bruker Avance III 500 MHz NMR spectrometer. Single-crystal XRD measurements were performed with a Rigaku SuperNova single-source diffractometer equipped with an Eos CCD detector and using mirror-monochromated Mo-Kα (λ = 0.71073 Å) radiation. MS measurements were performed with a Micromass LCT ESI-TOF mass spectrometer. Methanol was used as the eluent with a flow rate of 5 µL/min. Other measurement parameters include capillary voltage range of 2800–3000 V, sample core voltage 10 V, extraction core voltage 5 V, desolvation temperature 120 °C, and a source temperature of 80 °C.

A list of solvents used in this thesis is presented in Table 2, along with their suppliers, and their degree of purity. An analogous table for reagents used is presented in Table 3.

Table 2. A list of used solvents, their suppliers, and their degree of purity

Solvent	Supplier	Purity (%)
DCM	VWR	100.0*
DCM (dry)	Fischer Sci	-
DMF	VWR	99.9
EtOAc	VWR	99.9
Hex	Honeywell Riedel-de-Haën	>97
MeCN	VWR	>99.95
MeOH	-	-
NEt_3	VWR	99
THF	-	-
THF (dry)	Merck	≥99.9
THF (dry)	Sigma Aldrich	≥99.9

*Contains 0,002% of 2-methyl-2-butene for stability.

Table 3. A list of used reagents, their suppliers, and their degree of purity

Reagent	Supplier	Purity (%)
2-Amino-6-bromopyridine	ABCR GmbH	97
3-Bromoaniline	Sigma-Aldrich	98
2-Chloropropionyl chloride	TCI	>95.0
Copper(I) iodide	ABCR GmbH	99.999
Copper(I) iodide	Sigma-Aldrich	99.999
Copper perchlorate hexahydrate	Gfs Chemicals	-
1,3-Diethynylbenzene	TCI	>96.0
DMAP	Sigma	-
DPEphos	VWR	99
3-Ethynylaniline	TCI	>98.0
Ethynyltrimethylsilane	TCI	>98.0
Iodine	Sigma-Aldrich	-
3-Iodoaniline	TCI	>99.0
Isophthaloyl dichloride	TCI	>99.0
Morpholine	Merck	>95.0
$(Ph_3P)_2PdCl_2$*	TCI	>98.0
Pyridine	VWR	99.8
Sodium azide	Aldrich	≥99.0
Sodium iodide	Alfa Aesar	>99.5
TBAF	ABCR	97
TBTA	TCI	>97.0

*Bis(triphenylphosphine)palladium(II) dichloride

9 RESULTS AND DISCUSSION

Seventeen syntheses were performed with yields varying from 0 to 103 % (Table 4). In general, the syntheses performed were seldom completed as expected and many contained additional challenges. Of the starting reagents, 3-bromoaniline was a poor reactant for the addition of TMS-ethynyl moieties (Table 4, product **1**, bromoaniline) with a twice-confirmed yield of 0 %. The analogous 3-iodoaniline, however, accepted TMS-ethynyl in the same conditions as 3-bromoaniline failed in with a yield of 95 % (Table 4, product **1,** 3-iodoaniline). Compared to literature[82] the iodoaniline reaction was performed with comparable yields (95 % vs 97 %), only with slight impurities found in the mixture.

When comparing the addition of TMS-ethynyl to 2-amino-6-bromopyridine (Table 4, product **2**) and 3-iodoaniline (Table 4, product **1**, iodoaniline), iodoaniline performed much better than the bromopyridine (95 % vs 32 %). This can be due to the presence of iodine. Either the reaction proceeds with higher yields, or product **1** is much better separated from its reagents than product **2**. It is also possible that the synthesis and purification for the iodoaniline derivative were performed with greater care than the bromopyridine synthesis. When comparing 3-bromoaniline (Table 4, product **1**, bromoaniline) and 2-amino-6-bromopyridine (Table 4, product **2**), the pyridine moiety (Table 5, products **1** and **2**) possibly has some positive effect on synthesis yield (0 % vs 32 %) as the syntheses were performed in succession. Products **2** and **2**-2 had lesser yields (Table 4) than the reactions performed in literature[82] with identical reagents (32 and 52 % compared to 97 %). It is possible that the column chromatography performed did not separate products from reagents as efficiently as possible.

Products **3**, **3**-2, and **8** had their amine groups substituted with 2-chloropropanamide (Table 5) with lesser yields (Table 4) than in literature[82] (35, 61 and 29 % compared to 83 %). It is possible the chlorine moieties of the reagents used had detrimental effects on column chromatography, or reaction completion rate. Yield improved from **3** to **3**-2, likely due to only one column chromatography purification performed in the synthesis of **3**-2, compared to **3**. When comparing the synthesis of **8** to **3**-2, it is possible that the pyridine moiety of product **3**-2 (Table 5) has some positive effect on product

separation from reagents during column chromatography. Products **3**-2 and **8** had a similar column with the same eluent, with differing yields (61 % vs 29 %).

Azidation reactions (Table 4, products **4**, **9**-2, and **9**-3) were found to have been very successful, if the reaction was performed in sufficiently high temperature (50–60 °C) for long enough (1 to 4 h). Product **9** had a yield of 0 %, likely due to a lower temperature (40–50 °C) and a short reaction time (1 h). Yields jumped from product **9**-2 to **9**-3 (36 to 96 %). This is most likely due to no column chromatography performed for **9**-3 combined with an extended reaction time (4 h compared to 1 h with **9**-2). Compared to literature,[82] both **4** and **9**-3 had higher yields but without column chromatography performed. Column chromatography was performed only with **9**-2 with significantly lower yield compared to literature (36 vs 90 %). This drop in yield could be resultant from the lack of a pyridine moiety in **9**-2 (Table 5), which is present in literature. The lack of pyridine might affect the separation of product from reagents in a column chromatograph, or the reaction completion rate.

The removal of the TMS-moiety was found to be successful with product **5** (Table 4) with a moderate yield of 56 %. This compared to literature[82] is lower (56 vs 86 %). The lower yield might be resultant from the lack of a mesylate moiety in product **5**, where instead is a chlorine atom (Table 5, product **5**). This difference might affect column chromatography or reaction rate adversely.

The ‘click’-reactions between azides and other compounds were found to be challenging and yielded little to no product (Table 4, products **6** and **10**). The performed ‘click’-reactions were thus found to be unsuccessful. According to Hein and Fokin[86], the presence of oxygen in a CuAAC reaction can lead to oxidative byproducts which were likely obtained in the synthesis of product **6**. The synthesis of product **10** likely resulted in only these oxidative byproducts. Degassing of solvents or the introduction of ascorbate, in combination with the used catalyst copper(II)perchlorate, would remove dissolved oxygen from the reaction medium. It would also enable the reaction to be conducted in water, or perhaps other aqueous solutions. This might solve the issue of poor solubility of products in nonpolar solvents. Both literature equivalents of compound **6**[41] and compound **10**[83] had much higher yields (82 and 93 % vs 13 and 0 %). The difference is likely due to the presence of oxygen in the synthesis of compounds **6** and **10**. Additional purification for product **6** would have reduced the

sample to a few milligrams at best, thus further purification or reactions were not attempted.

Isophthaloyl dichloride was found to be a challenging reagent that yielded mixtures of products (Table 4 and Table 5, product **11** and **12**). These mixtures had poor solubility and were difficult to purify or perform measurements on. Product **11** had an impossibly high yield of 103 %. In the beginning of product **12**, an insoluble substance from product **11** was observed, which was likely a part of the extra 3 % yield, and possibly more. Compared to literature,[84] the product **11** was not washed with 1 M HCl as the product precipitated. Perhaps a part of the impossible yield would have dissolved with the HCl wash. In addition, it is possible product **11** was partially wet as the product was not dried under reduced pressure. The introduction of product **11** to a vacuum would have likely dried the mixture further but this was not done due to time constraints. Compared to literature,[84] product **11** had a higher but impossible yield. This was likely a combination the insoluble compound observed in the following synthesis, and the possible presence of unevaporated solvents.

Product **12** had a very poor yield of a few milligrams (Table 4). This was likely due to the column chromatography performed as compound **12** had very poor solubility in the eluent of choice (2:1 Hex/EtOAc). In literature,[85] products were purified with a flash chromatograph in ethyl acetate with a 90 % yield. As product **12** had very poor solubility in nonpolar solvents, it is likely flash chromatography in ethyl acetate would not have had very different results. Purification through other methods, e.g., recrystallization, would perhaps have yielded more product. However, other methods were not pursued due to time constraints.

Table 4. The yields of syntheses performed compared to literature, and their types

Synthesis product	Reaction type	Yield (%)	Yield in literature (%)
1 (from 3-bromoaniline)	Substitution	0	97
1 (from 3-iodoaniline**)**	Substitution	95	97
2	Substitution	32	97*
2-2	Substitution	52	97*
3	Substitution	35	83
3-2	Substitution	61	83
4	Azidation	∼100†	90
5	Substitution	56	86
6	Click	∼13°	82
Byproduct **7**	Substitution	-	-
8	Substitution	29	83
9	Azidation	0	90
9-2	Azidation	36	90
9-3	Azidation	96	90
10	Click	0	93
11	Substitution	103	90
12	Substitution	~0	90

*Reaction performed with identical, reagents compared to literature. I.e., all syntheses, other than product **2** and **2**-2, were performed with similar, but nonidentical reagents compared to literature.

†Estimation.

°Product is a mixture of indiscernible compounds.

Table 5. Structural formulas of attempted synthesis products

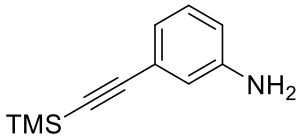 **1**	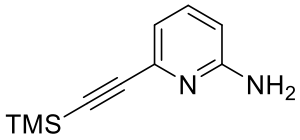 **2**
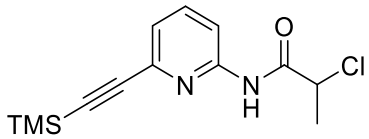 **3**	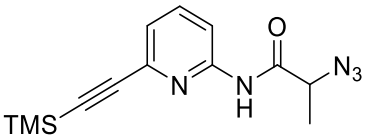 **4**
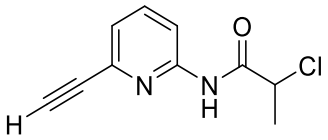 **5**	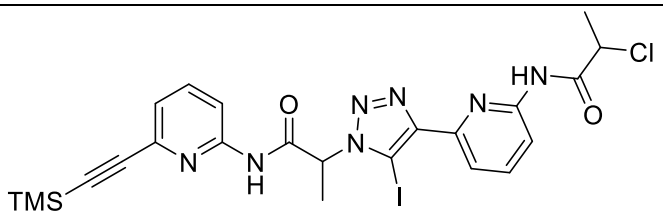 **6**
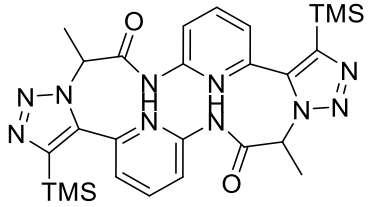 **7**	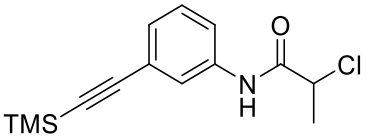 **8**
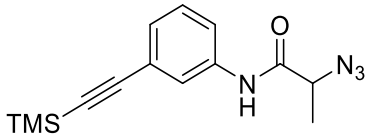 **9**	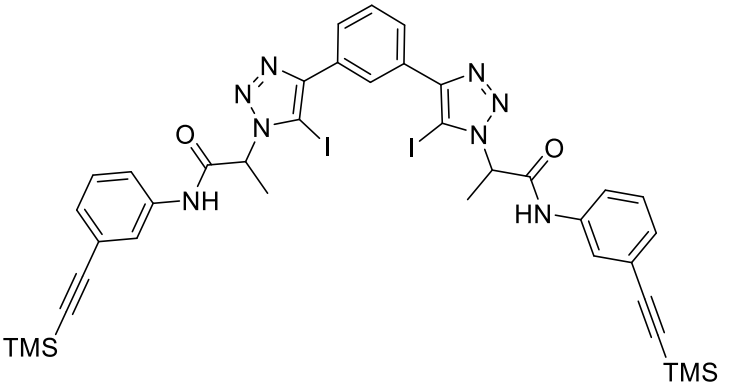 **10**
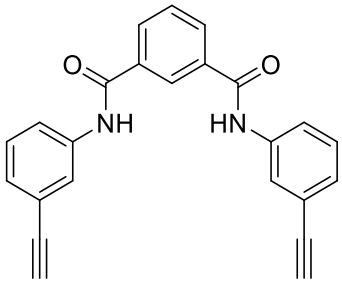 **11**	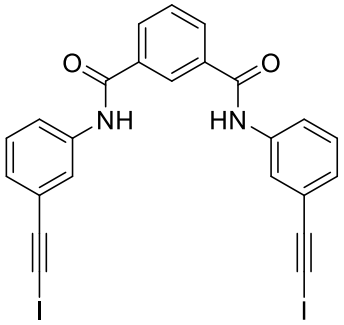 **12**

The purification of products with column chromatography was found to be challenging as the separation of product from reactant proved difficult. Most columns resulted in a large mixture of reactant and product with only a small amount of mostly pure product. Purification with other methods such as an automated flash chromatograph might yield more product with each purification. The solubility of products also proved to be poor. The larger the molecule, the more likely it would only be soluble in DMF and DMSO. This created additional challenges for product purification and measurements.

Most synthesis products were difficult to recrystallize, but two crystal structures were obtained from XRD measurements. These structures include the macrocyclic by-product **7** (Figure 35) and product **8** (Figure 36). It would perhaps be possible to create an analogous macrocycle to **7** where the TMS-moieties would be iodine atoms from the beginning of the synthesis. This replacement could result in a macrocycle capable of halogen bonding.

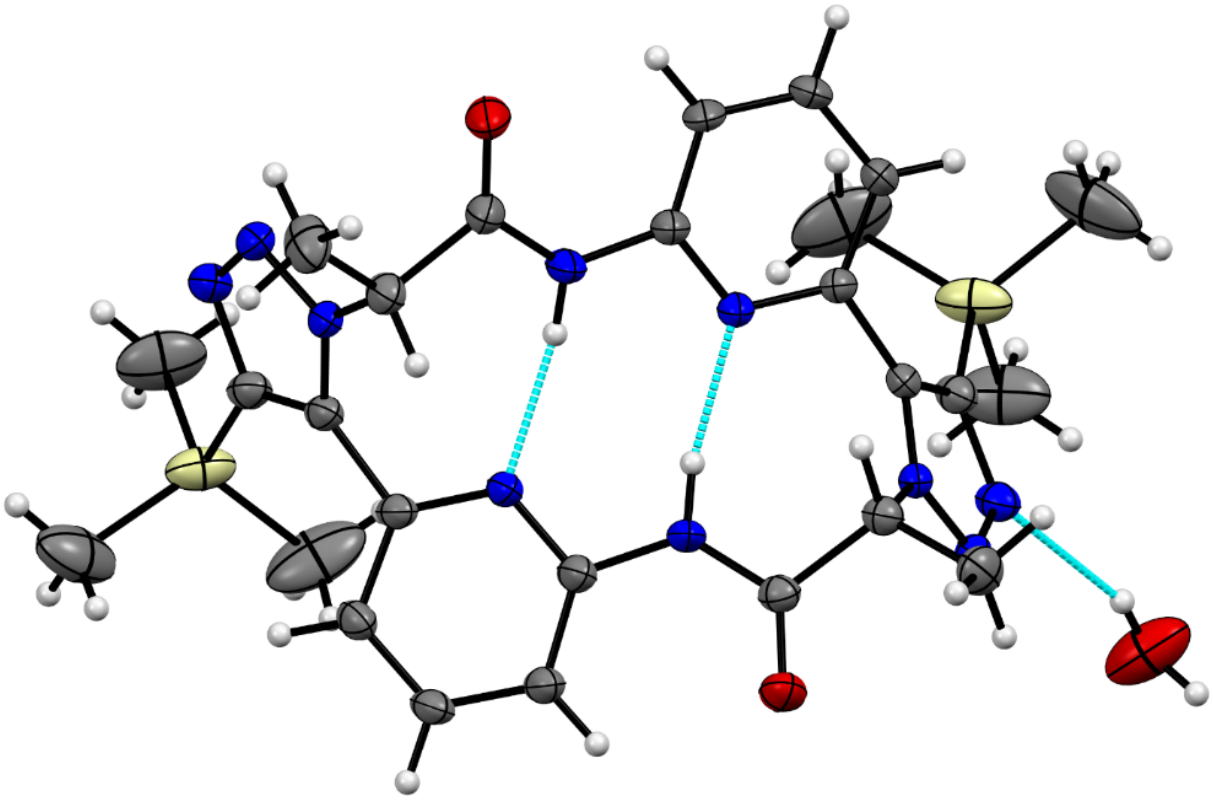

Figure 35. The crystal structure of by-product **7** from XRD measurements, which reveal the structure is a hydrate. The dotted cyan lines represent hydrogen bonds. Color code: grey = carbon, white = hydrogen, red = oxygen, blue = nitrogen, pale yellow = silicon.

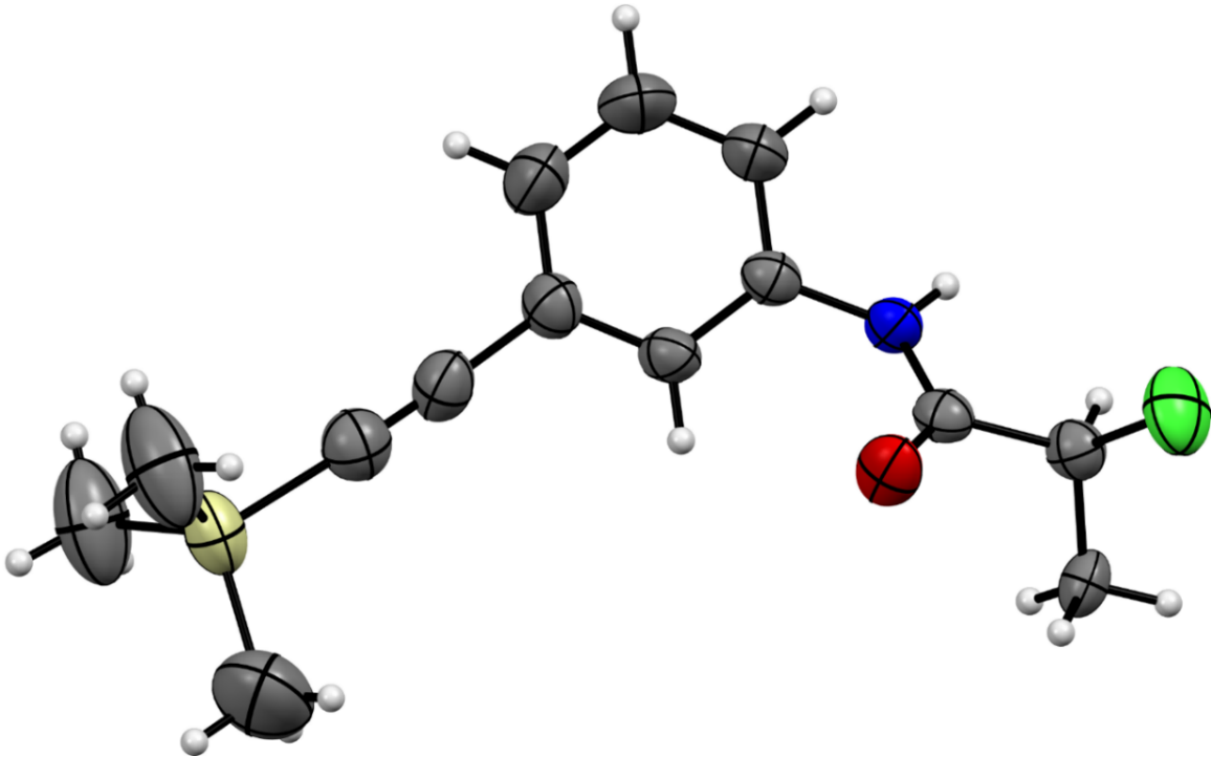

Figure 36. The crystal structure of **8** from XRD measurements. Color code: grey = carbon, white = hydrogen, red = oxygen, blue = nitrogen, pale yellow = silicon, green = chlorine.

MS-measurements were found to produce very inconsistent results as only one measurement (product **6**) yielded discernible fragments. This could be the result of the products having poor solubility, combined with the fact that samples contained mixtures of products. The addition of specific groups, e.g., hydrophobic hydrocarbons or HB-capable oxygen-rich groups, to the products could increase interactions with certain solvents and thus improve solubility. However, this could decrease reactivity and/or create possibilities for unwanted reactions.

Overall, no system capable of halogen bonding was synthesized. The incorporation of iodine into larger molecules (Table 5, products **6**, **10** and **12**) was found to have been difficult and yielded little to no product. As no halogen bonding was created, no anion receptors of interest were synthesized. Additional time would perhaps have yielded more results.

10 CONCLUSIONS

Anion recognition by halogen bonding is difficult but possible with the right building blocks. Halogen bonding offers a more selective, typically stronger anion binding option to anion recognition compared to hydrogen bonding. The most common XB-donors are halotriazole, halotriazolium, haloperfluoroarene, and haloimidazolium. The most common XB-donor atoms are iodine, bromine, and chlorine, in decreasing donor ability. The most potent donors are cationic iodine donors, e.g., iodoimidazolium and iodotriazolium. Halonium ions also form strong XBs, but a halonium-ion based anion receptor, or their incorporation into anion sensors has not been reported.

Oxyanions in particular are a challenging anionic species to bind with XB-receptors but should be focused as they are ample in nature and industry. They can cause a range of problems without regulation and capture, and control of them even help with medical research and disease.

In general, cationic receptors achieve the highest binding affinities. Neutral receptors can be employed in anion recognition, particularly when they are incorporated with multiple EW-groups into multidentate MIMs. There are some proof-of-concept level XB anion sensors that should inspire further research that will result in usable anion sensors in real-world applications.

The performed experimental work demonstrated that even facile ‘click’ reactions (CuAAC) do not succeed with all reagents and conditions and that oxygen should likely be eliminated from the reaction medium. Three different neutral receptors were targeted, one macrocycle and two cleft-type receptors. The macrocyclic and one of the cleft-type receptors were attempted to be synthesized with ‘click’ reactions (Figure 42 and Figure 47) between an azide and an alkyne moiety. Both the reaction between product **4** and product **5**, as well as the reaction between product **9** and 1,3-diethynylbenzene were found to be unsuccessful. Hence, ‘click’ reactions were deemed unsuccessful.

The third receptor was attempted to be synthesized with substitution reactions (Figure 48 and Figure 49). The potential receptor, product **12**, was obtained as an insoluble powder that was subjected to column chromatography and yielded little to no product.

The chosen receptor reactions (Figure 42, Figure 47, Figure 49) resulted in small amounts of products with poor solubility. However, most intermediate products (products **1**, **2**, **3**, **4**, **5**, **8**, **9**) were successfully synthesized. As the molecular weight of products increased, product solubility decreased even further. Poor solubility resulted in various problems. Column chromatography of reaction products proved to be challenging, as well as measurements of products (NMR, MS). Only one product, product **8**, crystallized (Figure 36).

A by-product **7** (Figure 35) was also synthesized and crystallized. This by-product proved to be a macrocycle with two intramolecular hydrogen bonds. The molecule has some potential to be capable of halogen bonding if the TMS-moieties of the macrocycle can be exchanged to halogen atoms.

Future research based on the experimental work performed in this thesis should focus on the by-product, specifically its recreation and further derivation. Additional goals of future research are experimentation of different starting reagents of the syntheses. For example, the chlorine moiety of the chosen reagents or the spacer groups of the targeted receptors could be exchanged. Experimental synthesis takes time and receptors should be relentlessly designed and synthesized until desirable results are achieved. As there is an incredible number of variations possible for different XB-donors, EW groups and R-groups, receptor design and syntheses should be performed systematically with perseverance.

11 EXPERIMENTAL PROCEDURES

11.1. 3-BROMOANILINE DERIVATIVES

11.1.1. 3-((Trimethylsilyl)ethynyl)aniline

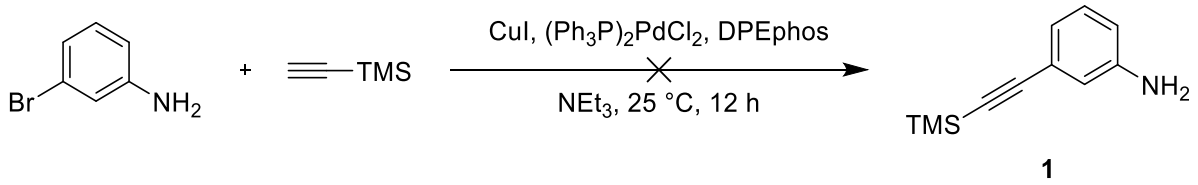

Figure 37. Reaction scheme of the synthesis for compound **1**.[82]

Copper(I) iodide (164 mg, 861 µmol, 10 mol%), $(Ph_3P)_2PdCl_2$ (240 mg, 342 µmol, 4 mol%) and DPEphos (185 mg, 344 µmol, 4 mol%) were suspended in 30 ml of distilled NEt_3 under Ar. To this solution, 3-bromoaniline (0.95 ml, 8.72 mmol) was added to form a light brown solution. After 30 minutes, ethynyltrimethylsilane (1.3 ml, 9.38 mmol) was added dropwise to produce a dark drown solution. The reaction was left in room temperature overnight after which a small amount of dark colored crystals had formed around the reaction flask. The solvent was evaporated, and the dark mixture was separated with column chromatography (EtOAc/Hex, 4:1 with 1 % DCM). Fractions of the column chromatography were analyzed with TLC and NMR measurements, and the reaction was found to have not produced any amount of **1**.

A second synthesis was performed as above but with a different eluent in the column chromatography (Hex/EtOAc, 2:1). This reaction was also found to have not produced any amount of **1**. The reaction scheme of the attempted syntheses is presented in figure 37.

11.2. 2-AMINO-6-BROMOPYRIDINE DERIVATIVES

11.2.1. 6-((Trimethylsilyl)ethynyl)pyridin-2-amine

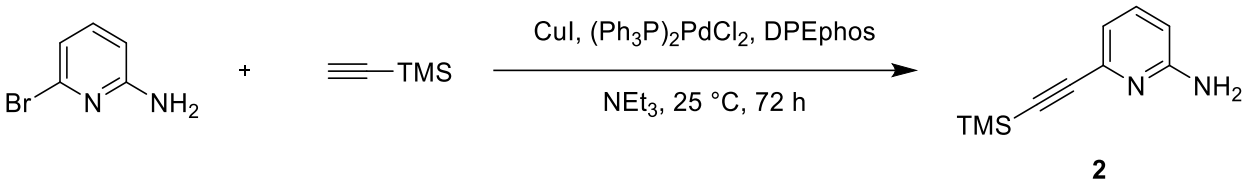

2

Figure 38. Reaction scheme of the synthesis for compound **2**.[82]

Copper(I) iodide (165 mg, 870 µmol, 10 mol%), $(Ph_3P)_2PdCl_2$ (240 mg, 345 µmol, 4 mol%), DPEphos (186 mg, 345 µmol, 4 mol%) and 2-amino-6-bromopyridine (1.5 g, 8.67 mmol) were suspended in 30 ml of distilled NEt_3 under Ar. After 30 minutes to this orange solution, ethynyltrimethylsilane (1.3 ml, 9.38 mmol) was added dropwise to produce a dark green solution. The reaction was left in room temperature over a weekend. Solvent was evaporated and the resulting dark brown solid was purified with column chromatography (Hex/EtOAc 2:1, l = 25 cm) to give a brown solid with off-white spots (619 mg, 38 %). The reaction scheme of the synthesis is presented in figure 38. The measured spectra of **2** are presented in Appendix 3 and Appendix 4.

The ^{1}H and the ^{13}C NMR spectrums both show the presence of some unknown compound. A HSQC spectrum (Appendix 5) was measured to solve the peaks that correspond with compound **2**. It is likely the unknown compound was 2-amino-6-bromopyridine, but comparative spectrums were not measured due to time constraints.

R_f = 0.39 (Hex/EtOAc 2:1); ^{1}H NMR (300 MHz, DMSO-d6): δ = 7.33 (aryl, t, 1 H), 6.64-6.60 (aryl, m, 1 H), 6.44 (aryl, d, 1 H), 6.07 (NH_2, s, 2 H), 0.21 (TMS-CH_3, s, 9 H); ^{13}C NMR (125 MHz, DMSO-d6): δ = 159.6, 137.3, 115.6, 114.0, 108.8, 105.4, 91.4, -0.2.

A second synthesis was performed as above with the exception that solids were filtered out of the reaction mixture before the evaporation of the solvent. This resulted in 864 mg (52 %) of **2**. The measured ^{1}H NMR spectrum of the second synthesis product (**2**-2) is presented in Appendix 6. The same unknown compound was present as in the NMR spectrums of product **2**.

R_f = 0.34 (Hex/EtOAc 2:1); ^{1}H NMR (300 MHz, DMSO-d6): 7.36-7.31 (aryl, m, 1 H), 6.64-6.60 (aryl, m, 1 H), 6.45-6.42 (aryl, m, 1 H), 6.07 (NH_2, s, 2 H), 0.21 (TMS-CH_3, s, 9 H).

11.2.2. 2-Chloro-*N*-(6-((trimethylsilyl)ethynyl)pyridin-2-yl)propanamide

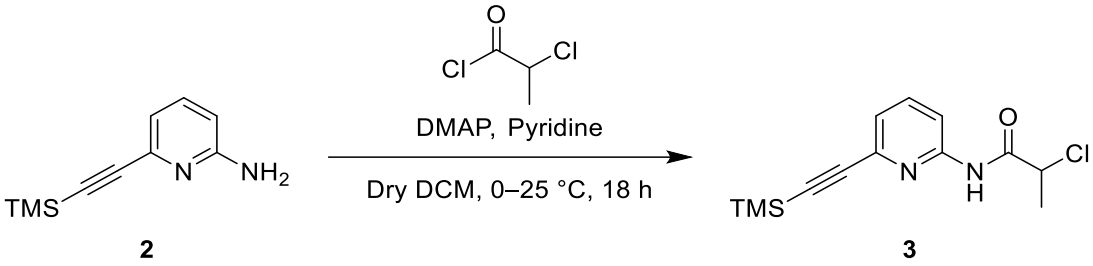

Figure 39. Reaction scheme of the synthesis for compound **3**.[82]

Pyridine (0.48 ml, 5.93 mmol), 6-((trimethylsilyl)ethynyl)pyridin-2-amine **2** (619 mg, 3.25 mmol) and 4-dimethylaminopyridine (3.75 mg, 31 µmol) were mixed in 15 ml of dry DCM and cooled to 0 °C in an ice bath. To this chilled solution, 2-chloropropionyl chloride (0.61 ml, 6.30 mmol) in 3 ml of dry DCM was added dropwise at 0 °C. The solution was left overnight to warm to room temperature while stirring. After this, the solution was washed with 20 ml of aqueous K_2CO_3 (10 %) and 20 ml of water. Solvents were evaporated from the organic layer and the resulting brown oil was subjected to column chromatography (Hex/EtOAc 2:1, l = 20 cm). The liquid fractions were shown to be a largely a mixture of the reactants and products with NMR. The mixture fractions were thus repurified with column chromatography (Hex/EtOAc 5:1, l = 32 cm). In total, 317 mg of 2-chloro-*N*-(6-((trimethylsilyl)ethynyl)pyridin-2-yl)propanamide **3** was obtained (35%). The reaction scheme of the synthesis is presented in figure 39. The measured ^{1}H NMR spectrum of **3** is presented in Appendix 7.

R_f = 0.77 (Hex/EtOAc 2:1); R_f = 0.50 (Hex/EtOAc 5:1); ^{1}H NMR (300 MHz, $CDCl_3$): δ = 8.86 (NH, s, 1 H), 8.19-8.16 (aryl, m, 1 H), 7.69 (aryl, t, 1 H), 7.27-7.25 (aryl, m, 1 H), 4.50 (CHCl, q, 1 H), 1.80 (CCH_3, d, 3 H), 0.28 (TMS-CH_3, s, 9 H).

A second synthesis was performed as above with 864 mg of **2** to give 773 mg (61 %) of **3**. The reaction mixture was only subjected to column chromatography once (Hex/EtOAc 2:1, l = 33 cm). The measured spectra of the second synthesis product (**3**-2) are presented in Appendix 8 and Appendix 9.

The 20.82 ppm peak in the ^{13}C NMR spectrum of **3**-2 is overlayed with the 20.68 ppm peak of the residual ethyl acetate.

R_f = 0.66 (Hex/EtOAc 2:1); ^1H NMR (300 MHz, DMSO-d6): 11.08 (NH, s, 1 H), 8.09-8.06 (aryl, m, 1 H), 7.83 (aryl, t, 1 H), 7.31-7.28 (aryl, m, 1 H), 4.78 (CHCl, q, 1 H), 1.60 (methyl, d, 3 H); 0.24 (TMS-CH_3, s, 9 H); ^{13}C NMR (125 MHz, DMSO-d6): 168.3, 151.7, 140.1, 139.3, 123.1, 113.9, 103.5, 94.1, 54.3, 20.8, -0.4.

11.2.3. 2-Azido-*N*-(6-((trimethylsilyl)ethynyl)pyridin-2-yl)propanamide

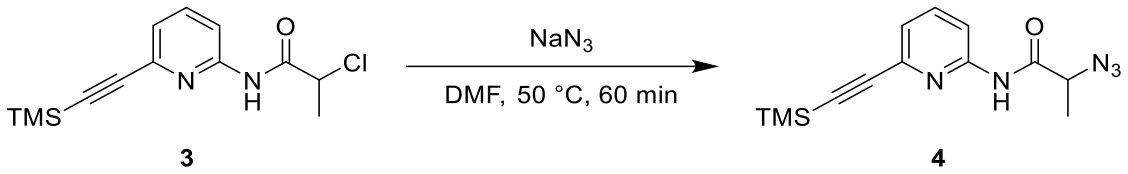

Figure 40. Reaction scheme of the synthesis for compound **4**.[82]

Safety note: sodium azide is highly toxic and an explosion hazard with heavy metals.[87] Increased safety precautions were taken, such as proper ventilation was ensured, additional safety equipment was worn, and metal surfaces were covered. Potential traces of sodium azide were neutralized with water and were collected for disposal.

Sodium azide (88 mg, 1.35 mmol) and 2-chloro-N-(6-((trimethylsilyl)ethynyl)pyridin-2-yl)propanamide **3** (317 mg, 1.13 mmol) were dissolved in 3 ml of DMF. The solution was heated at 50 °C for 60 minutes (the hotplate used had temperature fluctuations, from 40 °C up to 60 °C at times) after which 10 ml of EtOAc was added. The diluted solution was washed twice with 10 ml of H_2O, after which solvents were evaporated from the solution. The brown solid was measured with NMR and was determined to be of 2-azido-*N*-(6-((trimethylsilyl)ethynyl)pyridin-2-yl)propanamide **4** (324 mg) with no traces of **3**. The reaction scheme of the synthesis is presented in figure 40. The measured spectra of **4** are presented in Appendix 10 and Appendix 11.

^1H NMR (500 MHz, DMSO-d6): δ = 10.98 (NH, s, 1 H), 8.08 (aryl, d, 1 H), 7.82 (aryl, t, 1 H), 7.29 (aryl, d, 1 H), 4.10 (C_2ClC-H, q, 1 H), 1.44 (CCH_3, d, 3 H), 0.23 (TMS-CH_3, s, 9 H); ^{13}C NMR (125 MHz, DMSO-d6): 151.6, 140.1, 139.3, 123.1, 114.1, 103.5, 94.2, 57.2, 16.6, 1.8, -0.4.

11.2.4. 2-Chloro-*N*-(6-ethynylpyridin-2-yl)propanamide

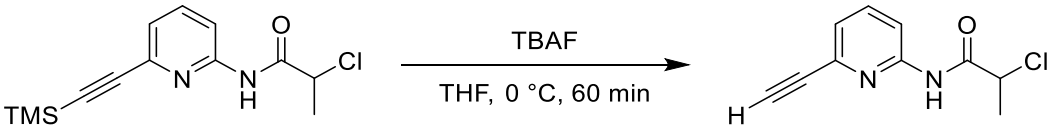

3 **5**

Figure 41. Reaction scheme of the synthesis for compound **5**.[82]

To a cooled solution (0 °C) of 2-chloro-N-(6-((trimethylsilyl)ethynyl)pyridin-2-yl)propanamide **3** (0.77 g, 2.75 mmol) in 10 ml THF, tetra-*n*-butylammonium fluoride (1.02 g, 3.89 mmol) in 10 ml THF was added dropwise. The mixture was stirred for 1 h, after which 20 ml of EtOAc was added. The resulting pale-yellow solution was washed with 40 ml of H_2O, which produced a large, murky water phase and a small organic phase. The water layer was washed twice with 20 ml of EtOAc (2 x 20 ml), which turned the phase clear and see-through. The organic layers were combined, and solvents were evaporated. The resulting brown product was subjected to column chromatography (Hex/EtOAc 2:1) to give 324 mg (56 %) of 2-chloro-*N*-(6-ethynylpyridin-2-yl)propanamide **5**. The reaction scheme of the synthesis is presented in figure 41. The measured spectra of the **5** are presented in Appendix 12 and Appendix 13.

R_f = 0.60 (Hex/EtOAc 2:1); ^{1}H NMR (300 MHz, Acetone-d6): 9.65 (NH, s, 1 H) 8.20 (aryl, d, 1 H), 7.83 (aryl, t, 1 H), 7.31 (aryl, d, 1 H), 4.87 (CHCl, q, 1 H), 3.74 (C≡CH, s, 1 H), 1.73 (CCH_3, d, 3 H); ^{13}C NMR (125 MHz, Acetone-d6): 169.1, 152.7, 141.5, 139.7, 124.4, 114.7, 83.2, 78.7, 55.4, 21.4.

11.2.5. 2-Chloro-*N*-(6-(5-iodo-1-(1-oxo-1-((6-((trimethylsilyl)ethynyl)pyridin-2-yl)amino)propan-2-yl)-1*H*-1,2,3-triazol-4-yl)pyridin-2-yl)propanamide

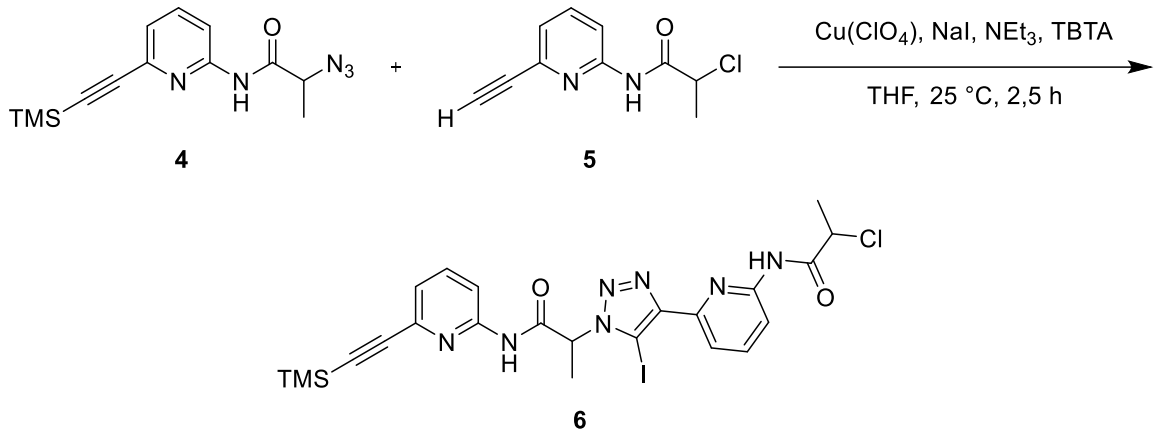

Figure 42. Reaction scheme of the synthesis for compound **6**.[41]

Copper(II) perchlorate hexahydrate (886 mg, 5.44 mmol), NaI (692 mg, 4.62 mmol) and TBTA (62 mg, 117 µmol) were suspended in 30 ml of dry THF. To this brown solution, triethylamine (157 µL, 1.13 mmol) was added which clouded the solution. Dissolved in a small amount of dry THF, 2-chloro-*N*-(6-ethynylpyridin-2-yl)propanamide **5** (440 mg, 2.11 mmol) was added and the mixture was stirred for 20 minutes. Dissolved in 5 ml of dry THF and a few drops of DCM, 2-azido-*N*-(6-((trimethylsilyl)ethynyl)pyridin-2-yl)propanamide **4** (324 mg, 1.13 mmol) was added as a milky-white cloudy solution, which turned the reaction mixture murky and a mustard-yellow color. The mixture was stirred for 2.5 h, after which 100 ml of water and a 1:1 mixture of aqueous NH_4Cl (25 %) and aqueous NH_3 (25 %) was added. This turned the mixture dark green with blue spots. The mixture was washed twice with 100 ml of EtOAc (2 x 100 ml) and the second wash was left overnight to separate in a separatory funnel. During the night, a part of the mixture had escaped the funnel and an estimated 20 ml of the second 100 ml EtOAc wash was lost. The leftover organic layers were combined and washed thrice with 50 ml of water (3 x 50 ml), after which they were dried over $MgSO_4$. Solvents were evaporated and the leftover mixture was purified with column chromatography (d = 4.5 cm, l = 15 cm, Hex/EtOAc 3:1, after which the column was purged with EtOAc). The product was transferred to a smaller vial with THF and was left to evaporate for a few weeks, producing light brown crystals (93 mg, 13,3 %). An R_f value could not be determined as the product showed 4 different lines on the TLC sheet. The reaction

scheme of the synthesis is presented in figure 42. The measured MS spectrum of **6** is presented in Appendix 14.

ESI-TOF MS (ES+): [**6** + Na]$^+$ *m/z* = 644.0529, calcd. *m/z* for $C_{23}H_{25}ClIN_7O_2Si$ + Na^+ = 644.04699.

The ^1H and ^{13}C NMR spectrums showed the sample to be a mixture of various indiscernible compounds.

The combined liquid fraction from the EtOAc purge was crystallized in room temperature from EtOAc over a few weeks, as small light brown crystals. The reaction was found to have formed a by-product, which was measured with XRD, NMR and MS measurements. The by-product likely contained two 2-azido-*N*-(6-((trimethylsilyl)ethynyl)pyridin-2-yl)propanamide molecules that formed a small macrocycle. A simplified structure of the macrocycle is presented in Figure 43, the crystal structure from XRD measurements is presented in Figure 35 and the measured ^1H NMR spectrum of the by-product **7** is presented in Appendix 15.

^1H NMR (300 MHz, DMSO-d6): 11.88 (NH, s, 1 H), 8.05 (aryl, t, 2 H), 7.85 (aryl, d, 2 H), 7.40 (aryl, d, 2 H), 5.74 (CH, d, 2 H), 1.88 (CH_3, d, 6 H), 0.24 (TMS-CH_3, s, 9 H).

The MS measurements showed no discernible m/z fragments of interest.

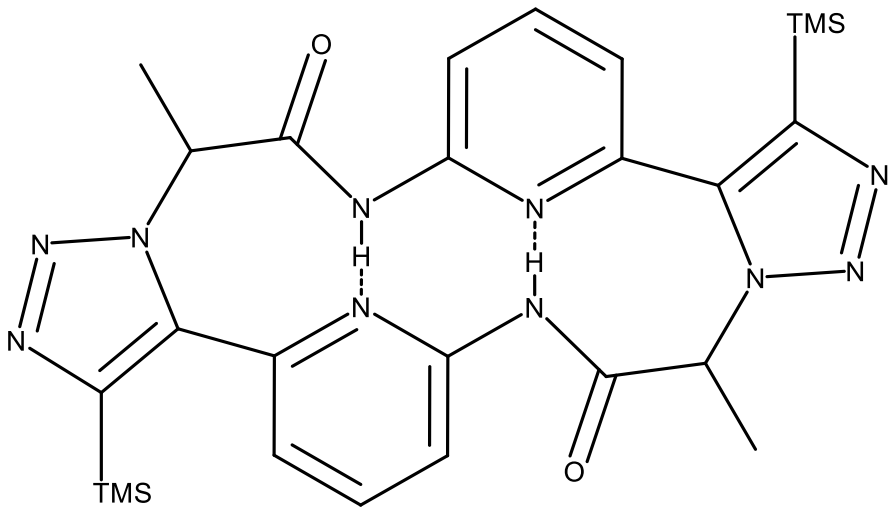

Figure 43. A macrocyclic by-product **7** formed from two 2-azido-*N*-(6-((trimethylsilyl)ethynyl)pyridin-2-yl)propanamide (product **4**) molecules.

11.3. 3-IODOANILINE DERIVATIVES

11.3.1. 3-((Trimethylsilyl)ethynyl)aniline

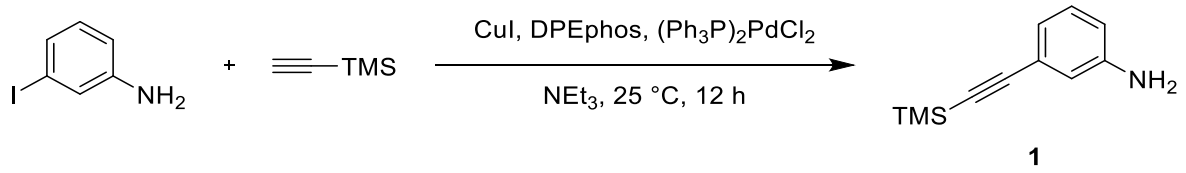

1

Figure 44. An alternative reaction scheme of the synthesis for compound **1**.[82]

Copper(I) iodide (172 mg, 903 µmol, 10 mol%), $(Ph_3P)_2PdCl_2$ (249 mg, 354 µmol, 4 mol%), DPEphos (186 mg, 345 µmol, 4 mol%) and 3-iodoaniline (1.05 ml, 8.70 mmol) were suspended in 25 ml of distilled NEt_3 under Ar. After 30 minutes to this mixture, ethynyltrimethylsilane (1.3 ml, 9.38 mmol) was added dropwise to produce visible precipitate in the flask. The reaction was left in room temperature overnight and was found to have formed even more precipitate in the flask. These were filtered out of the mixture with cotton, after which solvent was evaporated. The resulting dark brown solid was suspended in Hex/EtOAc 2:1 overnight and undissolved solids were filtered out with paper. Out of the filtered oil, crystals began to form, which were also filtered out. The crystals were measured with XRD and found to contain triethylammoniumiodide. The crystals were thus discarded.

The leftover solution was subjected to column chromatography (Hex/EtOAc 2:1, l = 35 cm) to give a brown solid (1.568 g, 95 %). The reaction scheme of the synthesis is presented in figure 44. The measured spectra of **1** are presented in Appendix 1 and Appendix 2.

The product was found to have contained slight impurities with NMR, but it was assessed to have been sufficiently pure to be used for the next synthesis. For example, in the ^{13}C NMR spectrum some impurity can be clearly seen at 1.80 ppm. It was concluded to be of no significance as no possible by-product could contain a carbon atom that would produce such a low shift.

R_f = 0.60 (Hex/EtOAc 2:1); ^1H NMR (300 MHz, DMSO-d6): 6.99 (aryl, t, 1 H), 6.64 (aryl, s, 1 H), 6.57 (aryl, m, 2 H), 5.17 (NH_2, s, 2 H), 0.20 (TMS-CH_3, s, 9 H); ^{13}C NMR (125 MHz, DMSO-d6): 148.4, 129.1, 122.4, 119.1, 116.7, 114.9, 106.3, 92.3, -0.1.

11.3.2. 2-Chloro-*N*-(3-((trimethylsilyl)ethynyl)phenyl)propanamide

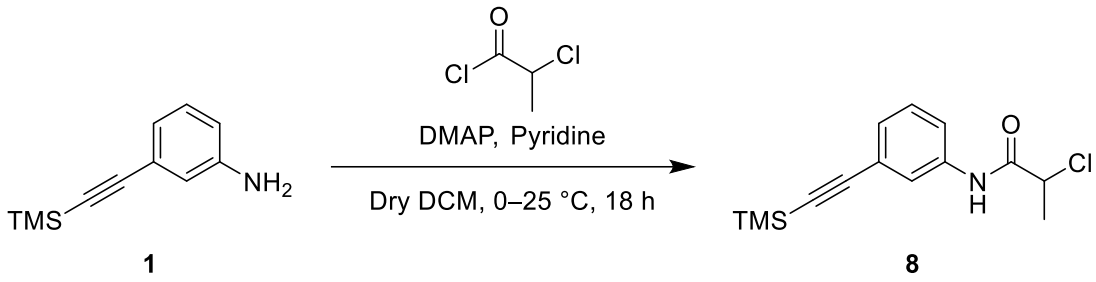

Figure 45. Reaction scheme of the synthesis for compound **8**.[82]

Pyridine (0.95 ml, 11.75 mmol), 3-((trimethylsilyl)ethynyl)aniline **1** (1.57 g, 8.28 mmol) and 4-dimethylaminopyridine (8.07 mg, 66 µmol) were mixed in 15 ml of dry DCM and cooled to 0 °C in an ice bath. To this chilled solution, 2-chloropropionyl chloride (1.21 ml, 12.5 mmol) in 3 ml of dry DCM was added dropwise at 0 °C. The solution was left overnight to warm to room temperature while stirring. After this, the solution was washed with 20 ml of aqueous K_2CO_3 (10 %) and 20 ml of water. Solvents were evaporated from the organic layer and the resulting dark brown oil was subjected to column chromatography (Hex/EtOAc 2:1, l = 35 cm) to give 668 mg (29 %) of pure 2-chloro-*N*-(3-((trimethylsilyl)ethynyl)phenyl)propanamide **8** and 1.232 g of mixed, impure product.

Estimating from the measured ^{1}H NMR spectrums, the percentage of impurities varied from 6–20 % within the samples. This totals to approximately 164 mg of the 1.232 g. Thus, an estimate 1.068 g of product was within the impure fractions (~46 %).

The impure product was transferred to a smaller vial with THF and was left to evaporate for some weeks, producing a light brown crystal solid. These crystals were measured with XRD to give a crystal structure presented in figure 36. The measured spectra of **8** are presented in Appendix 16 and Appendix 17. The reaction scheme of the synthesis is presented in figure 45.

R_f = 0.65 (Hex/EtOAc 2:1); ^{1}H NMR (300 MHz, DMSO-d6): 10.38 (NH, s, 1 H), 7.80 (aryl, t, 1 H), 7.55-7.51 (aryl, m, 1 H), 7.34 (aryl, t, 1 H), 7.17 (aryl, m, 1 H, J = 7.74, 1.28 Hz), 4.65 (CHCl, q, 1 H), 1.61 (CCH_3, d, 3 H), 0.23 (TMS-CH_3, s, 9 H); ^{13}C NMR (125 MHz,

DMSO-d6): 167.6, 138.6, 129.4, 126.9, 122.6, 122.3, 120.1, 104.9, 94.2, 54.7, 20.9, -0.2.

11.3.3. 2-Azido-*N*-(3-((trimethylsilyl)ethynyl)phenyl)propanamide

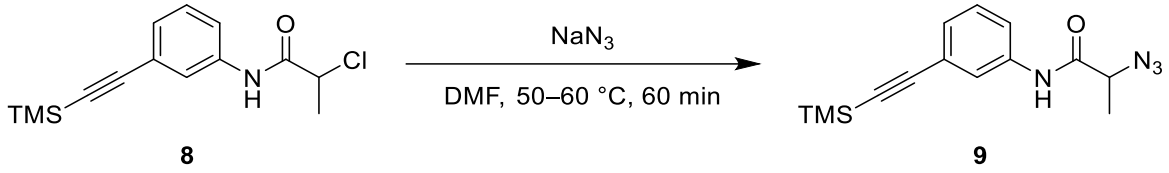

8 **9**

Figure 46. Reaction scheme of the synthesis for compound **9**.[82]

Safety note: sodium azide is highly toxic and an explosion hazard with heavy metals.[87] Increased safety precautions were taken, such as proper ventilation was ensured, additional safety equipment was worn, and metal surfaces were covered. Potential traces of sodium azide were neutralized with water and were collected for disposal.

Sodium azide (199 mg, 3.06 mmol) and 2-chloro-*N*-(3-((trimethylsilyl)ethynyl)phenyl)propanamide **8** (668 mg, 2.39 mmol) were dissolved in 5 ml of DMF. The solution was heated at 50 °C for 60 minutes with the temperature fluctuating between 50–60 °C due to the hotplate used. After the hour the solution had turned cloudy, and 10 ml of EtOAc was added which caused some precipitate to form in the flask. The diluted solution with the precipitate was washed thrice with 10 ml of H_2O (3 x 20 ml). The precipitate dissolved during the washes. After this, solvents were evaporated from the organic layer. The crude product was subjected to column chromatography (Hex/EtOAc 4:1) which yielded an off-white solid (246 mg, 36 %) of **9**.

A mixture of the unreacted 2-chloro-*N*-(3-((trimethylsilyl)ethynyl)phenyl)propanamide **8** and a small amount of **9** was also collected (239 mg of **8** and **9**). The reaction scheme of the synthesis is presented in figure 46. The measured spectra of **9**-2 are presented in Appendix 18 and Appendix 19.

R_f = 0.47 (Hex/EtOAc 4:1); ^{1}H NMR (300 MHz, DMSO-d6): 10.23 (NH, s, 1 H), 7.81 (aryl, t, 1 H), 7.54-7.51 (aryl, m, 1 H), 7.34 (aryl, t, 1 H), 7.17 (aryl, dt, 1 H, J = 7.69, 1.25 Hz), 4.03 (CHCl, q, 1 H), 1.45 (CCH_3, d, 3 H), 0.23 (TMS-CH_3, s, 9 H); ^{13}C NMR (125 MHz,

DMSO-d6): 169.2, 138.5, 129.3, 126.9, 122.6, 122.4, 120.2, 104.9, 94.2, 57.5, 16.6, -0.2.

This synthesis was performed an additional two times. The first time, the synthesis was performed with 668 mg of **8** between 40–50 °C for 1 hour and was found to have formed no amount of **9**.

The second additional synthesis was performed as above with the 239 mg collected mixture of **8** and **9**. The reaction stoichiometry was calculated with the assumption of the mixture to be only **8**. The synthesis was done in 3 ml of DMF at 50–60 °C for 3.5 hours. The diluted mixture was also washed only twice with 10 ml of H_2O (2 x 20 ml). The crude product was measured with NMR and was found to have been mostly from **9** (235 mg, 96 %) with trace amounts of solvents. The measured spectra of **9**-3 are presented in Appendix 20 and Appendix 21. The quartet at 4.03 ppm in the ^{1}H NMR spectrum (Appendix 20) is overlayed with the quartet from the residual ethyl acetate in the sample, increasing the integral by 1.

^{1}H NMR (300 MHz, DMSO-d6): 10.23 (NH, s, 1 H), 7.81 (aryl, t, 1 H), 7.54-7.51 (aryl, m, 1 H), 7.33 (aryl, t, 1 H), 7.18-7.16 (aryl, m, 1 H), 4.03 (CHCl, q, 1 H), 1.45 (CCH_3, d, 3 H), 0.23 (TMS-CH_3, s, 9 H); ^{13}C NMR (125 MHz, DMSO-d6): 169.2, 138.5, 129.3, 126.9, 122.6, 122.4, 120.2, 104.9, 94.2, 57.5, 16.7, -0.2.

11.4. 1,3-DIETHYNYLBENZENE DERIVATIVES

11.4.1. 2,2'-(1,3-Phenylenebis(5-iodo-1*H*-1,2,3-triazole-4,1-diyl))bis(*N*-(3-((trimethylsilyl)ethynyl)phenyl)propanamide)

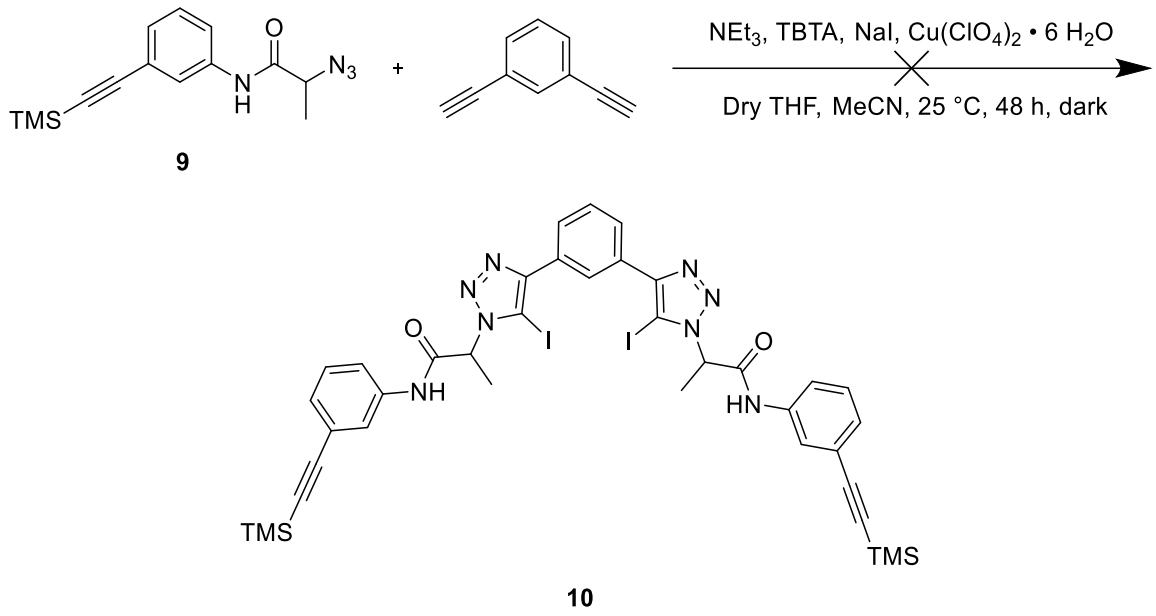

Figure 47. Reaction scheme of the synthesis for compound **10**.[83]

Sodium iodide (1.01 g, 6.73 mmol) was dissolved in 20 ml of dry THF and stirred vigorously for 20 minutes. To this solution, copper perchlorate hexahydrate (1.259 g, 3.40 mmol) was added with 5 ml of dry THF, and the mixture was stirred for 5 more minutes. After this, 2-azido-*N*-(3-((trimethylsilyl)ethynyl)phenyl)propanamide (481 mg, 1.68 mmol), TBTA (22 mg, 41 µmol), triethylamine (234 µL, 2.36 mmol) and 1,3-diethynylbenzene (106 µL, 797 µmol) were added successively with a total of 25 ml MeCN among them. The reaction was covered in foil to block out light from entering the mixture and the mixture was left in the dark under vigorous stirring while the reaction was monitored with TLC every 24 h. After 48 h, the mixture had turned to a maple syrup-like color and diluted with 100 ml of $CHCl_3$. The mixture was washed twice with 30 ml of 10 % aqueous NH_3 (2 x 30 ml), after which the combined aqueous layers were washed twice with 20 ml of $CHCl_3$. The organic layers were combined and washed with 50 ml of brine and dried over $MgSO_4$, after which solvents were evaporated to produce a porous layer of brown, foam-like solid. The solid was purified with column chromatography (3 % MeOH/DCM) to produce 70 mg (4.4 %) of solid.

The reaction scheme of the synthesis is presented in figure 47. MS, ^{1}H and ^{13}C NMR spectrums were measured but the samples were found to be a mixture of indiscernible compounds.

11.5. ISOPHTHALOYL DICHLORIDE DERIVATIVES

11.5.1. *N*^{1},*N*^{3}-Bis(3-ethynylphenyl)isophthalamide

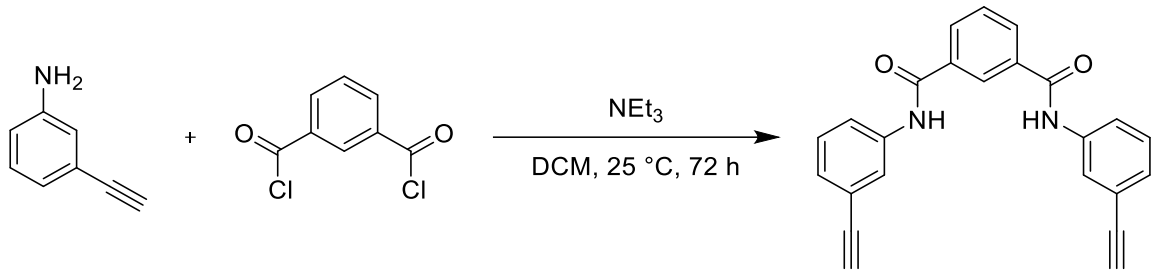

11

Figure 48. Reaction scheme of the synthesis for compound **11**.[84]

Isophthaloyl dichloride (602 mg, 2.97 mmol) was dissolved in 10 ml of dry DCM. To this solution, triethylamine (905 µL, 6.49 mmol) was added to produce a slightly yellow solution. After this, 3-ethynylaniline (1 ml, 8.88 mmol) was added in 10 ml of dry DCM and the solution turned brown. The mixture was stirred for 72 h, after which it was diluted with 20 ml of dry DCM. The diluted solution was washed with 10 ml of 1 M NaOH, which caused the product to precipitate out of the solution. The precipitate was filtered out and dried on a petri dish over 24 h to produce an off-white porous, brittle solid (1.109 g, 103 %). This solid was found to contain some insoluble compound in the following synthesis, which can also be seen from the impossibly high yield. The reaction scheme of the synthesis is presented in figure 48. The measured spectra of **11** are presented in Appendix 22 and Appendix 23.

There are only 12 discernible peaks in the measured ^{13}C NMR, when the structure of **11** has 13 unique carbon atoms. The measured spectrum also had some phase correction issues and the sample used had a low concentration. The missing peak is likely from an aromatic carbon that, because of the measurement issues, has blended with another chemical shift. A new measurement with a higher concentration sample might yield a higher quality spectrum that would have 13 peaks.

^{1}H NMR (500 MHz, DMSO-d6): 10.54 (NH, s, 2 H), 8.55 (central aryl, s, 1 H), 8.16-8.14 (aryl, m, 2 H), 7.98 (terminal aryl, s, 2 H), 7.85-7.83 (aryl, m, 2 H), 7.71 (central aryl, t, 1 H), 7.39 (aryl, t, 2 H), 7.24-7.22 (aryl, m, 2 H), 4.19 (C≡CH, s, 2 H); ^{13}C NMR (125 MHz, DMSO-d6): 165.2, 139.3, 134.9, 130.9, 129.2, 128.7, 127.0, 123.2, 122.0, 120.9, 83.4, 80.6.

The MS measurements showed no discernible m/z fragments of interest.

11.5.2. *N*^{1},*N*^{3}-Bis(3-(iodoethynyl)phenyl)isophthalamide

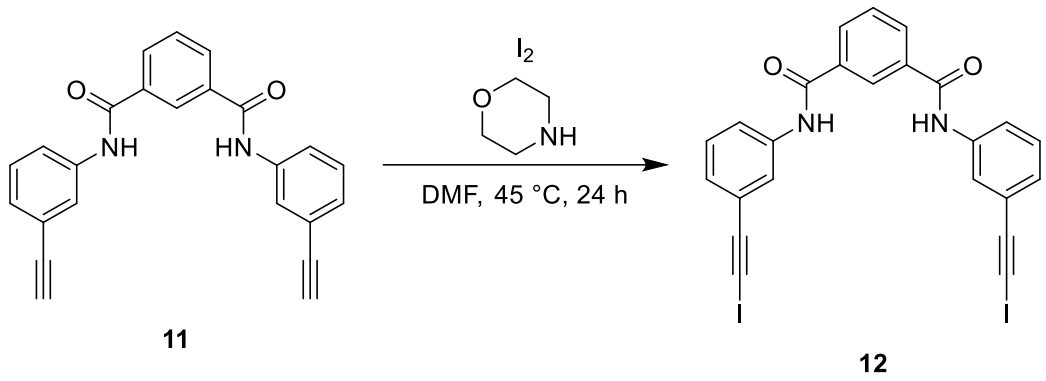

Figure 49. Reaction scheme of the synthesis for compound **12**.[85]

Iodine (844 mg, 3.33 mmol) was dissolved in 3 ml of dried DMF. To this solution, morpholine (0.785 ml, 9.07 mmol) was added with 3 ml of dried DMF and the mixture was stirred for 30 minutes. After this, *N*^{1},*N*^{3}-bis(3-(iodoethynyl)phenyl)isophthalamide **11** (550 mg, 1.51 mmol) was added in 7.5 ml of dried DMF and the mixture was stirred at 45 °C for 24 h. The potential leftover insoluble material was then filtered out and washed twice with 20 ml of EtOAc (2 x 20 ml). The combined organic layers were then washed with saturated aqueous solutions of NH_4Cl (20 ml) and NH_3 (20 ml), followed by 20 ml of H_2O. The washed solution was dried over $MgSO_4$, and solvents were evaporated to give a brown-red powder.

The powder was subjected to column chromatography (Hex/EtOAc 2:1). The powder was found to be insoluble in all solvents (besides DMSO and DMF) and was inserted to the column as a solid. A few milligrams of product were obtained, all of which was spent on the NMR and MS measurements. The reaction scheme of the synthesis is

presented in figure 49. The measured spectra of **12** are presented in Appendix 24 and Appendix 25.

When comparing the ^{1}H NMR spectrum of **12** to the ^{1}H NMR spectrum of **11**, it can be seen from the 4.19 ppm C≡CH shift that approximately 20 % of **11** is still present in the sample of **12**.

It can also be seen in the ^{1}H NMR spectrum that there are approximately 16 protons in the spectrum. Product **12** should only contain 14 protons, so the presence of some other compound, possibly **11**, in the sample is evident. Without further measurements, it is impossible to say which chemical shift in the ^{1}H NMR spectrum belongs to **12**.

R_f = 0.45 (Hex/EtOAc 2:1); ^{1}H NMR (300 MHz, DMSO-d6): 10.53 (NH, s, 2 H), 8.56 (central aryl, s, 1 H), 8.18-8.15 (aryl, m, 2 H), 7.81-7.79 (m, 4 H), 7.71 (t, 1 H), 7.63 (s, 2 H), 7.41 (t, 2 H), 7.05 (d, 2 H); ^{13}C NMR (125 MHz, DMSO-d6): 165.1, 144.0, 139.1, 135.0, 130.8, 128.9, 128.7, 127.0, 123.3, 120.3, 119.5, 96.8, 84.7.

The MS measurements showed no discernible m/z fragments of interest.

REFERENCES

1. Pancholi, J. and Beer, P. D., Halogen bonding motifs for anion recognition, *Coord. Chem. Rev.*, **2020**, *416*, 213281.

2. Hein, R.; Borissov, A.; Smith, M. D.; Beer, P. D. and Davis, J. J., A halogen-bonding foldamer molecular film for selective reagentless anion sensing in water, *Chem. Commun.*, **2019**, *55*, 4849–4852.

3. Volkert, W. A. and Hoffman, T. J., Therapeutic Radiopharmaceuticals, *Chem. Rev.*, **1999**, *99*, 2269–2292.

4. Brown, A. and Beer, P. D., Halogen bonding anion recognition, *Chem. Commun.*, **2016**, *52*, 8645–8658.

5. Nepal, B. and Scheiner, S., Building a Better Halide Receptor: Optimum Choice of Spacer, Binding Unit, and Halosubstitution, *ChemPhysChem*, **2016**, *17*, 836–844.

6. Cavallo, G.; Metrangolo, P.; Milani, R.; Pilati, T.; Priimagi, A.; Resnati, G. and Terraneo, G., The Halogen Bond, *Chem. Rev.*, **2016**, *116*, 2478–2601.

7. Tepper, R.; Schulze, B.; Jäger, M.; Friebe, C.; Scharf, D. H.; Görls, H. and Schubert, U. S., Anion Receptors Based on Halogen Bonding with Halo-1,2,3-triazoliums, *J. Org. Chem.*, **2015**, *80*, 3139–3150.

8. Bunchuay, T.; Docker, A.; Martinez-Martinez, A. J. and Beer, P. D., A Potent Halogen-Bonding Donor Motif for Anion Recognition and Anion Template Mechanical Bond Synthesis, *Angew. Chem. Int. Ed.*, **2019**, *58*, 13823–13827.

9. Bulfield, D. and Huber, S. M., Halogen Bonding in Organic Synthesis and Organocatalysis, *Chem. Eur. J.*, **2016**, *22*, 14434–14450.

10. Sarwar, M. G.; Dragisic, B.; Sagoo, S. and Taylor, M. S., A Tridentate Halogen-Bonding Receptor for Tight Binding of Halide Anions, *Angew. Chem. Int. Ed.*, **2010**, *49*, 1674–1677.

11. Borissov, A.; Marques, I.; Lim, J. Y. C.; Félix, V.; Smith, M. D. and Beer, P. D., Anion Recognition in Water by Charge-Neutral Halogen and Chalcogen Bonding Foldamer Receptors, *J. Am. Chem. Soc.*, **2019**, *141*, 4119–4129.

12. Cornes, S. P.; Sambrook, M. R. and Beer, P. D., Selective perrhenate recognition in pure water by halogen bonding and hydrogen bonding alpha-cyclodextrin based receptors, *Chem. Commun.*, **2017**, *53*, 3866–3869.

13. Hein, R. and Beer, P. D., Halogen bonding and chalcogen bonding mediated sensing, *Chem. Sci.*, **2022**.

14. Desiraju, G. R.; Ho, P. S.; Kloo, L.; Legon, A. C.; Marquardt, R.; Metrangolo, P.; Politzer, P.; Resnati, G. and Rissanen, K., Definition of the halogen bond (IUPAC Recommendations 2013), *Pure Appl. Chem.*, **2013**, *85*, 1711–1713.

15. Cavallo, G.; Metrangolo, P.; Pilati, T.; Resnati, G.; Sansotera, M. and Terraneo, G., Halogen bonding: A general route in anion recognition and coordination, *Chem. Soc. Rev.*, **2010**, *39*, 3772–3783.

16. Metrangolo, P.; Meyer, F.; Pilati, T.; Resnati, G. and Terraneo, G., Halogen Bonding in Supramolecular Chemistry, *Angew. Chem. Int. Ed.*, **2008**, *47*, 6114–6127.

17. Steiner, T., The Hydrogen Bond in the Solid State, *Angew. Chem. Int. Ed.*, **2002**, *41*, 48–76.

18. Li, W.; Kiran, M. S. R. N.; Manson, J. L.; Schlueter, J. A.; Thirumurugan, A.; Ramamurty, U. and Cheetham, A. K., Mechanical properties of a metal–organic framework containing hydrogen-bonded bifluoride linkers, *Chem. Commun.*, **2013**, *49*, 4471–4473.

19. Martín Pendás, A.; Blanco, M. A. and Francisco, E., The nature of the hydrogen bond: A synthesis from the interacting quantum atoms picture, *J. Chem. Phys.*, **2006**, *125*, 184112.

20. Shields, Z. P.; Murray, J. S. and Politzer, P., Directional tendencies of halogen and hydrogen bonds, *Int. J. Quantum Chem.*, **2010**, *110*, 2823–2832.

21. Clark, T.; Hennemann, M.; Murray, J. S. and Politzer, P., Halogen bonding: The σ-hole: Proceedings of 'Modeling interactions in biomolecules II', Prague, September 5th-9th, 2005, *J. Mol. Model.*, **2007**, *13*, 291–296.

22. Novák, M.; Foroutan-Nejad, C. and Marek, R., Asymmetric bifurcated halogen bonds, *Phys. Chem. Chem. Phys.*, **2015**, *17*, 6440–6450.

23. Turunen, L. and Erdélyi, M., Halogen bonds of halonium ions, *Chem. Soc. Rev.*, **2020**, *49*, 2688–2700.

24. Lascialfari, L.; Resnati, G. and Metrangolo, P., Halogen-Bonded Cocrystals. In: Atwood, J. L. (ed.), *Comprehensive Supramolecular Chemistry II*, 2nd edition, Elsevier, 2017, p. a) 53 b) 55 c) 57.

25. Raatikainen, K. and Rissanen, K., Interaction between amines and N-haloimides: a new motif for unprecedentedly short Br···N and I···N halogen bonds, *CrystEngComm*, **2011**, *13*, 6972–6977.

26. Barnes, N. A.; Flower, K. R.; Fyyaz, S. A.; Godfrey, S. M.; McGown, A. T.; Miles, P. J.; Pritchard, R. G. and Warren, J. E., Can the solid state structures of the dihalogen adducts R_3EX_2 (E = P, As; R = alkyl, aryl; X = Br, I) with the molecular spoke geometry be considered good mimics of the gold(i) systems [(R_3E)AuX] (E = As, P; R = alkyl, aryl; X = Cl, Br, I)?, *CrystEngComm*, **2010**, *12*, 784–794.

27. Xu, Y.; Huang, J.; Gabidullin, B. and Bryce, D. L., A rare example of a phosphine as a halogen bond acceptor, *Chem. Commun.*, **2018**, *54*, 11041–11043.

28. Lisac, K.; Topić, F.; Arhangelskis, M.; Cepić, S.; Julien, P. A.; Nickels, C. W.; Morris, A. J.; Friščić, T. and Cinčić, D., Halogen-bonded cocrystallization with phosphorus, arsenic and antimony acceptors, *Nat. Commun.*, **2019**, *10*, 61.

29. Cinčić, D.; Friščić, T. and Jones, W., Isostructural Materials Achieved by Using Structurally Equivalent Donors and Acceptors in Halogen-Bonded Cocrystals, *Chem. Eur. J.*, **2008**, *14*, 747–753.

30. Ho, T.-L., Hard soft acids bases (HSAB) principle and organic chemistry, *Chem. Rev.*, **1975**, *75*, 1–20.

31. Baldrighi, M.; Bartesaghi, D.; Cavallo, G.; Chierotti, M. R.; Gobetto, R.; Metrangolo, P.; Pilati, T.; Resnati, G. and Terraneo, G., Polymorphs and co-crystals of haloprogin: an antifungal agent, *CrystEngComm*, **2014**, *16*, 5897–5904.

32. Shen, Q. J.; Pang, X.; Zhao, X. R.; Gao, H. Y.; Sun, H.-L. and Jin, W. J., Phosphorescent cocrystals constructed by 1,4-diiodotetrafluorobenzene and polyaromatic hydrocarbons based on C–I···π halogen bonding and other

assisting weak interactions, *CrystEngComm*, **2012**, *14*, 5027–5034.

33. Hosokoshi, Y.; Tamura, M.; Nozawa, K.; Suzuki, S.; Kinoshita, M.; Sawa, H. and Kato, R., Magnetic properties and crystal structures of 2-hydro and 2-halo nitronyl nitroxide radical crystals, *Synth. Met.*, **1995**, *71*, 1795–1796.

34. Steed, J. W. and Atwood, J. L., Concepts. In: *Supramolecular Chemistry*, 2nd edition, John Wiley & Sons, Ltd, 2009, p. a) 2-4 b) 27-41, 45 c) 36 d) 39-41.

35. Metrangolo, P.; Murray, J. S.; Pilati, T.; Politzer, P.; Resnati, G. and Terraneo, G., The fluorine atom as a halogen bond donor, viz. a positive site, *CrystEngComm*, **2011**, *13*, 6593–6596.

36. Wilbur, D. S., Enigmatic astatine, *Nat. Chem.*, **2013**, *5*, 246.

37. Liu, L.; Rahali, S.; Maurice, R.; Gomez Pech, C.; Montavon, G.; Le Questel, J.-Y.; Graton, J.; Champion, J. and Galland, N., An expanded halogen bonding scale using astatine, *Chem. Sci.*, **2021**, *12*, 10855–10861.

38. Guo, N.; Maurice, R.; Teze, D.; Graton, J.; Champion, J.; Montavon, G. and Galland, N., Experimental and computational evidence of halogen bonds involving astatine, *Nat. Chem.*, **2018**, *10*, 428–434.

39. Borissov, A.; Lim, J. Y. C.; Brown, A.; Christensen, K. E.; Thompson, A. L.; Smith, M. D. and Beer, P. D., Neutral iodotriazole foldamers as tetradentate halogen bonding anion receptors†, *Chem. Commun.*, **2017**, *53*, 2483–2486.

40. Meldal, M. and Tornøe, C. W., Cu-Catalyzed Azide−Alkyne Cycloaddition, *Chem. Rev.*, **2008**, *108*, 2952–3015.

41. Mungalpara, D.; Stegmüller, S. and Kubik, S., A neutral halogen bonding macrocyclic anion receptor based on a pseudocyclopeptide with three 5-iodo-1,2,3-triazole subunits, *Chem. Commun.*, **2017**, *53*, 5095–5098.

42. Mele, A.; Metrangolo, P.; Neukirch, H.; Pilati, T. and Resnati, G., A Halogen-Bonding-Based Heteroditopic Receptor for Alkali Metal Halides, *J. Am. Chem. Soc.*, **2005**, *127*, 14972–14973.

43. Mahoney, J. M.; Nawaratna, G. U.; Beatty, A. M.; Duggan, P. J. and Smith, B. D., Transport of Alkali Halides through a Liquid Organic Membrane Containing a

Ditopic Salt-Binding Receptor, *Inorg. Chem.*, **2004**, *43*, 5902–5907.

44. Vargas Jentzsch, A. and Matile, S., Transmembrane Halogen-Bonding Cascades, *J. Am. Chem. Soc.*, **2013**, *135*, 5302–5303.

45. Wang, H.; Wang, W. and Jin, W. J., σ-Hole Bond vs π-Hole Bond: A Comparison Based on Halogen Bond, *Chem. Rev.*, **2016**, *116*, 5072–5104.

46. Haukka, M.; Hirva, P. and Rissanen, K., Dihalogens as Halogen Bond Donors. In: *Non-covalent Interactions in the Synthesis and Design of New Compounds*, John Wiley & Sons, Ltd, 2016, p. a) 187-188 b) 190 c) 188-190 d) 188.

47. Ouvrard, C.; Le Questel, J.-Y.; Berthelot, M. and Laurence, C., Halogen-bond geometry: a crystallographic database investigation of dihalogen complexes, *Acta Crystallogr. B*, **2003**, *59*, 512–526.

48. Imakubo, T.; Sawa, H. and Kato, R., Novel radical cation salts of organic π-donors containing iodine atom(s): the first application of strong intermolecular-I···X-(X = CN, halogen atom) interaction to molecular conductors, *Synth. Met.*, **1995**, *73*, 117–122.

49. Pascal, A.; A., H. F.; Eric, W. and Shing, H. P., Halogen bonds in biological molecules, *Proc. Natl. Acad. Sci. U.S.A.*, **2004**, *101*, 16789–16794.

50. Zapata, F.; Caballero, A.; White, N. G.; Claridge, T. D. W.; Costa, P. J.; Félix, V. and Beer, P. D., Fluorescent Charge-Assisted Halogen-Bonding Macrocyclic Halo-Imidazolium Receptors for Anion Recognition and Sensing in Aqueous Media, *J. Am. Chem. Soc.*, **2012**, *134*, 11533–11541.

51. Lim, J. Y. C. and Beer, P. D., A pyrrole-containing cleft-type halogen bonding receptor for oxoanion recognition and sensing in aqueous solvent media, *New J. Chem.*, **2018**, *42*, 10472–10475.

52. Massena, C. J.; Riel, A. M. S.; Neuhaus, G. F.; Decato, D. A. and Berryman, O. B., Solution and solid-phase halogen and C–H hydrogen bonding to perrhenate, *Chem. Commun.*, **2015**, *51*, 1417–1420.

53. Oliveira, R.; Groni, S.; Fave, C.; Branca, M.; Mavré, F.; Lorcy, D.; Fourmigué, M. and Schöllhorn, B., Electrochemical activation of a tetrathiafulvalene halogen bond donor in solution, *Phys. Chem. Chem. Phys.*, **2016**, *18*, 15867–15873.

54. DELANGE, F., The Disorders Induced by Iodine Deficiency, *Thyroid*, **1994**, *4*, 107–128.

55. P., A. M.; J., G. R.; Simon, T.; W., S. D.; Sucharita, P.; C., M. R.; E., S. A. and J., W. M., Demonstration That CFTR Is a Chloride Channel by Alteration of Its Anion Selectivity, *Science*, **1991**, *253*, 202–205.

56. Zapata, F.; Caballero, A.; Molina, P.; Alkorta, I. and Elguero, J., Open Bis(triazolium) Structural Motifs as a Benchmark To Study Combined Hydrogen- and Halogen-Bonding Interactions in Oxoanion Recognition Processes, *J. Org. Chem.*, **2014**, *79*, 6959–6969.

57. Gilday, L. C.; Robinson, S. W.; Barendt, T. A.; Langton, M. J.; Mullaney, B. R. and Beer, P. D., Halogen Bonding in Supramolecular Chemistry, *Chem. Rev.*, **2015**, *115*, 7118–7195.

58. Sonnenberg, K.; Mann, L.; Redeker, F. A.; Schmidt, B. and Riedel, S., Polyhalogen and Polyinterhalogen Anions from Fluorine to Iodine, *Angew. Chem. Int. Ed.*, **2020**, *59*, 5464–5493.

59. Schmidt, B.; Schröder, B.; Sonnenberg, K.; Steinhauer, S. and Riedel, S., From Polyhalides to Polypseudohalides: Chemistry Based on Cyanogen Bromide, *Angew. Chem. Int. Ed.*, **2019**, *58*, 10340–10344.

60. Savastano, M., Words in supramolecular chemistry: the ineffable advances of polyiodide chemistry, *Dalt. Trans.*, **2021**, *50*, 1142–1165.

61. Grabowski, S. J., New Type of Halogen Bond: Multivalent Halogen Interacting with π- and σ-Electrons, *Molecules*, **2017**, *22*.

62. Ivlev, S. I.; Gaul, K.; Chen, M.; Karttunen, A. J.; Berger, R. and Kraus, F., Synthesis and Characterization of $[Br_3][MF_6]$ (M=Sb, Ir), as well as Quantum Chemical Study of $[Br_3]^+$ Structure, Chemical Bonding, and Relativistic Effects Compared with $[XBr_2]^+$ (X=Br, I, At, Ts) and $[TsZ_2]^+$ (Z=F, Cl, Br, I, At, Ts), *Chem. Eur. J.*, **2019**, *25*, 5793–5802.

63. Cauliez, P.; Polo, V.; Roisnel, T.; Llusar, R. and Fourmigué, M., The thiocyanate anion as a polydentate halogen bond acceptor, *CrystEngComm*, **2010**, *12*, 558–566.

64. Xu, Z.; Yang, Z.; Liu, Y.; Lu, Y.; Chen, K. and Zhu, W., Halogen Bond: Its Role beyond Drug–Target Binding Affinity for Drug Discovery and Development, *J. Chem. Inf. Model.*, **2014**, *54*, 69–78.

65. Ho, P. S., Biomolecular Halogen Bonds. In: Metrangolo, P. and Resnati, G. (eds.), *Halogen Bonding I: Impact on Materials Chemistry and Life Sciences*, Springer International Publishing, Cham, 2015, vol. 358, p. a) 252-255.

66. Awwadi, F. F.; Willett, R. D.; Peterson, K. A. and Twamley, B., The Nature of Halogen···Halogen Synthons: Crystallographic and Theoretical Studies, *Chem. Eur. J.*, **2006**, *12*, 8952–8960.

67. Walter, S. M.; Jungbauer, S. H.; Kniep, F.; Schindler, S.; Herdtweck, E. and Huber, S. M., Polyfluorinated versus cationic multidentate halogen-bond donors: A direct comparison, *J. Fluor. Chem.*, **2013**, *150*, 14–20.

68. Kaasik, M.; Kaabel, S.; Kriis, K.; Järving, I.; Aav, R.; Rissanen, K. and Kanger, T., Synthesis and Characterisation of Chiral Triazole-Based Halogen-Bond Donors: Halogen Bonds in the Solid State and in Solution, *Chem. Eur. J.*, **2017**, *23*, 7337–7344.

69. Schulze, B.; Friebe, C.; Hager, M. D.; Günther, W.; Köhn, U.; Jahn, B. O.; Görls, H. and Schubert, U. S., Anion Complexation by Triazolium “Ligands”: Mono- and Bis-tridentate Complexes of Sulfate, *Org. Lett.*, **2010**, *12*, 2710–2713.

70. Lachman, A., A PROBABLE CAUSE OF THE DIFFERENT COLORS OF IODINE SOLUTIONS., *J. Am. Chem. Soc.*, **1903**, *25*, 50–55.

71. Barendt, T. A.; Docker, A.; Marques, I.; Félix, V. and Beer, P. D., Selective Nitrate Recognition by a Halogen-Bonding Four-Station [3]Rotaxane Molecular Shuttle, *Angew. Chem. Int. Ed.*, **2016**, *55*, 11069–11076.

72. Würthner, F., Aggregation-Induced Emission (AIE): A Historical Perspective, *Angew. Chem. Int. Ed.*, **2020**, *59*, 14192–14196.

73. Docker, A.; Shang, X.; Yuan, D.; Kuhn, H.; Zhang, Z.; Davis, J. J.; Beer, P. D. and Langton, M. J., Halogen Bonding Tetraphenylethene Anion Receptors: Anion-Induced Emissive Aggregates and Photoswitchable Recognition, *Angew. Chem. Int. Ed.*, **2021**, *60*, 19442–19450.

74. Hein, R.; Beer, P. D. and Davis, J. J., Electrochemical Anion Sensing: Supramolecular Approaches, *Chem. Rev.*, **2020**, *120*, 1888–1935.

75. Oliveira, R.; Groni, S.; Vacher, A.; Barrière, F.; Lorcy, D.; Fourmigué, M.; Maisonhaute, E.; Schöllhorn, B. and Fave, C., Electrochemical Activation of TTF-Based Halogen Bond Donors: A Powerful, Selective and Sensitive Analytical Tool for Probing a Weak Interaction in Complex Media, *ChemistrySelect*, **2018**, *3*, 8874–8880.

76. Patrick, S. C.; Hein, R.; Sharafeldin, M.; Li, X.; Beer, P. D. and Davis, J. J., Real-time Voltammetric Anion Sensing Under Flow**, *Chem. Eur. J.*, **2021**, *27*, 17700–17706.

77. Patrick, S. C.; Hein, R.; Beer, P. D. and Davis, J. J., Continuous and Polarization-Tuned Redox Capacitive Anion Sensing at Electroactive Interfaces, *J. Am. Chem. Soc.*, **2021**, *143*, 19199–19206.

78. Seah, G. E. K. K.; Tan, A. Y. X.; Neo, Z. H.; Lim, J. Y. C. and Goh, S. S., Halogen Bonding Ionophore for Potentiometric Iodide Sensing, *Anal. Chem.*, **2021**, *93*, 15543–15549.

79. Weis, J. G.; Ravnsbæk, J. B.; Mirica, K. A. and Swager, T. M., Employing Halogen Bonding Interactions in Chemiresistive Gas Sensors, *ACS Sensors*, **2016**, *1*, 115–119.

80. Jaini, A. K. A.; Hughes, L. B.; Kitimet, M. M.; Ulep, K. J.; Leopold, M. C. and Parish, C. A., Halogen Bonding Interactions for Aromatic and Nonaromatic Explosive Detection, *ACS Sensors*, **2019**, *4*, 389–397.

81. Liu, Z.-X.; Sun, Y.; Feng, Y.; Chen, H.; He, Y.-M. and Fan, Q.-H., Halogen-bonding for visual chloride ion sensing: a case study using supramolecular poly(aryl ether) dendritic organogel systems, *Chem. Commun.*, **2016**, *52*, 2269–2272.

82. Krause, M. R.; Goddard, R. and Kubik, S., Formation of a cyclic tetrapeptide mimic by thermal azide–alkyne 1,3-dipolar cycloaddition, *Chem. Commun.*, **2010**, *46*, 5307–5309.

83. Lim, J. Y. C.; Marques, I.; Thompson, A. L.; Christensen, K. E.; Félix, V. and Beer, P. D., Chalcogen Bonding Macrocycles and [2]Rotaxanes for Anion Recognition,

J. Am. Chem. Soc., **2017**, *139*, 3122–3133.

84. Picci, G.; Bazzicalupi, C.; Coles, S. J.; Gratteri, P.; Isaia, F.; Lippolis, V.; Montis, R.; Murgia, S.; Nocentini, A.; Orton, J. B. and Caltagirone, C., Halogenated isophthalamides and dipicolineamides: the role of the halogen substituents in the anion binding properties, *Dalt. Trans.*, **2020**, *49*, 9231–9238.

85. Zeiler, A.; Ziegler, M. J.; Rudolph, M.; Rominger, F. and Hashmi, A. S. K., Scope and Limitations of the Intermolecular Furan-Yne Cyclization, *Adv. Synth. Catal.*, **2015**, *357*, 1507–1514.

86. Hein, J. E. and Fokin, V. V, Copper-catalyzed azide–alkyne cycloaddition (CuAAC) and beyond: new reactivity of copper(i) acetylides, *Chem. Soc. Rev.*, **2010**, *39*, 1302–1315.

87. GRAHAM, J. D. P., Actions of sodium azide., *Br. J. Pharmacol.*, **1949**, *4*, 1–6.

APPENDICES

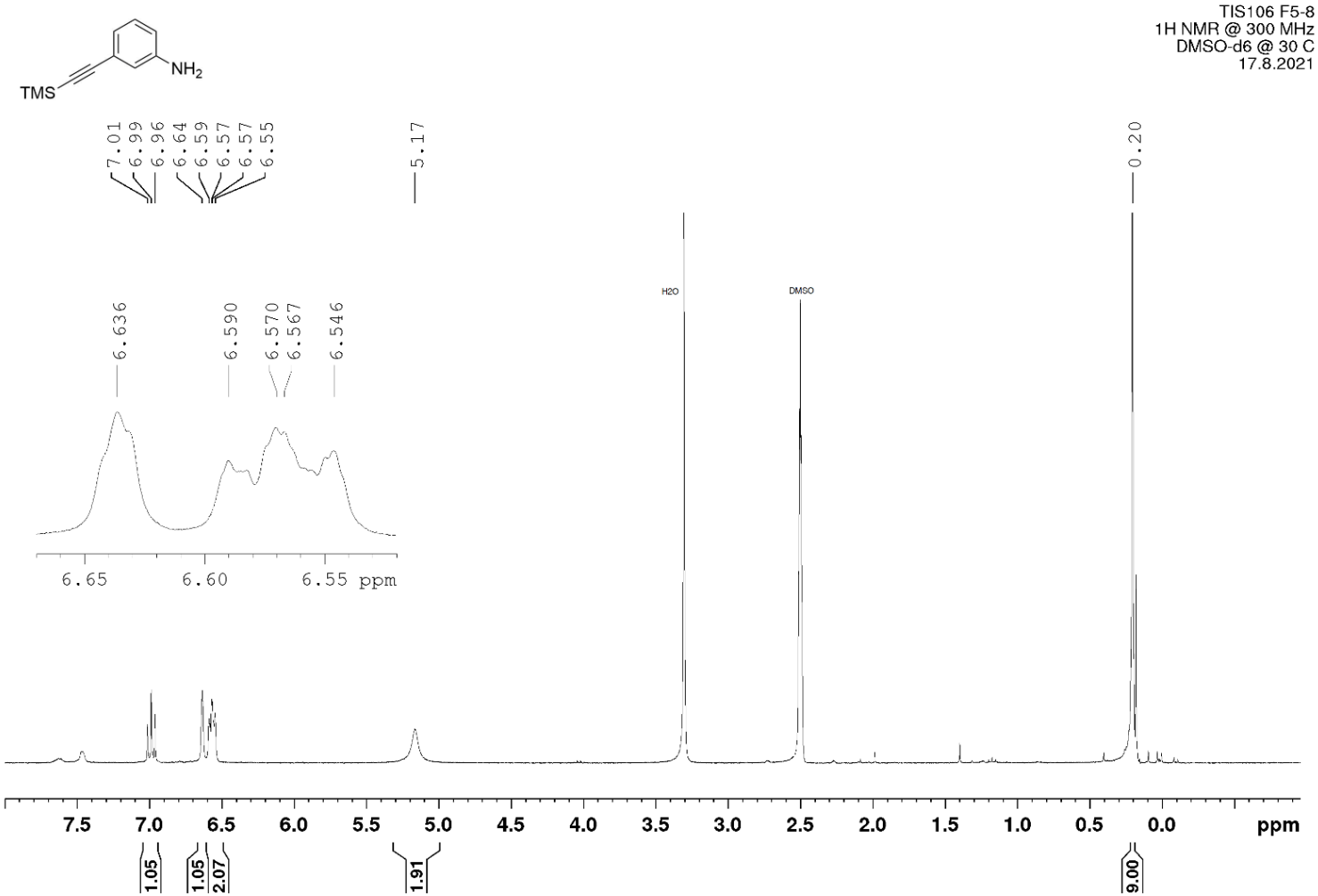

Appendix 1. ^{1}H NMR Spectrum of **1.**

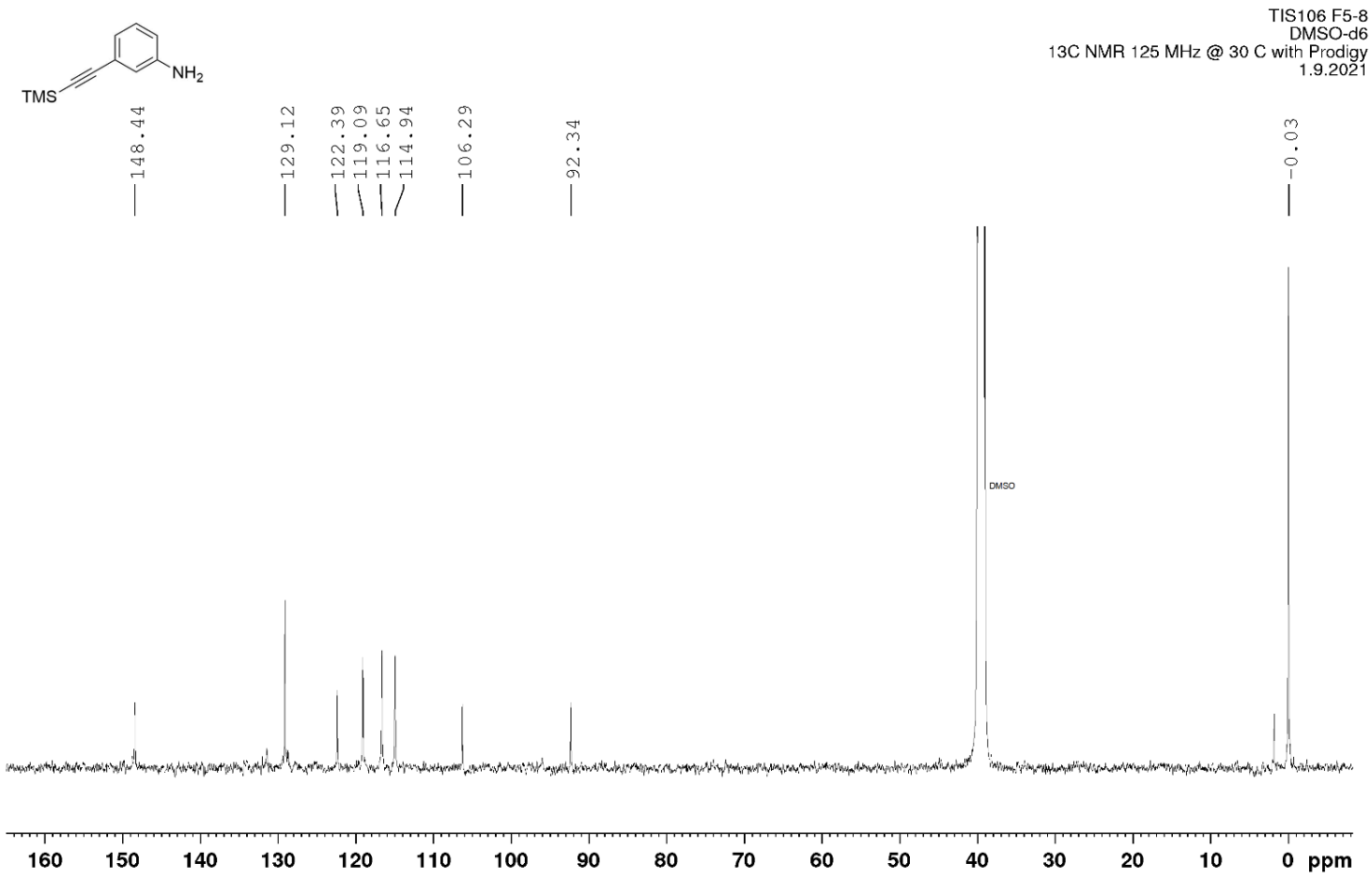

Appendix 2. ^{13}C NMR Spectrum of **1.**

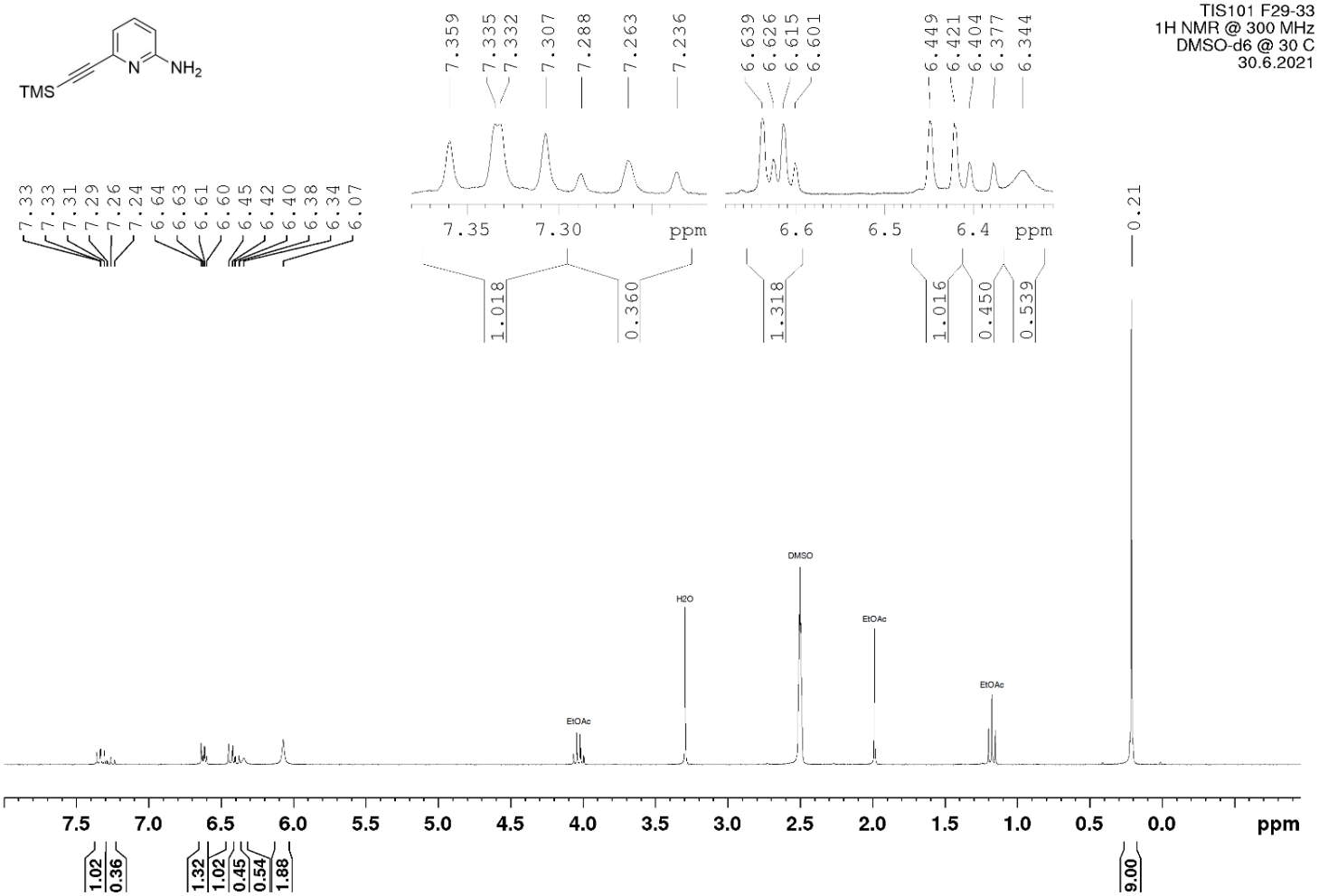

Appendix 3. ^{1}H NMR Spectrum of **2**.

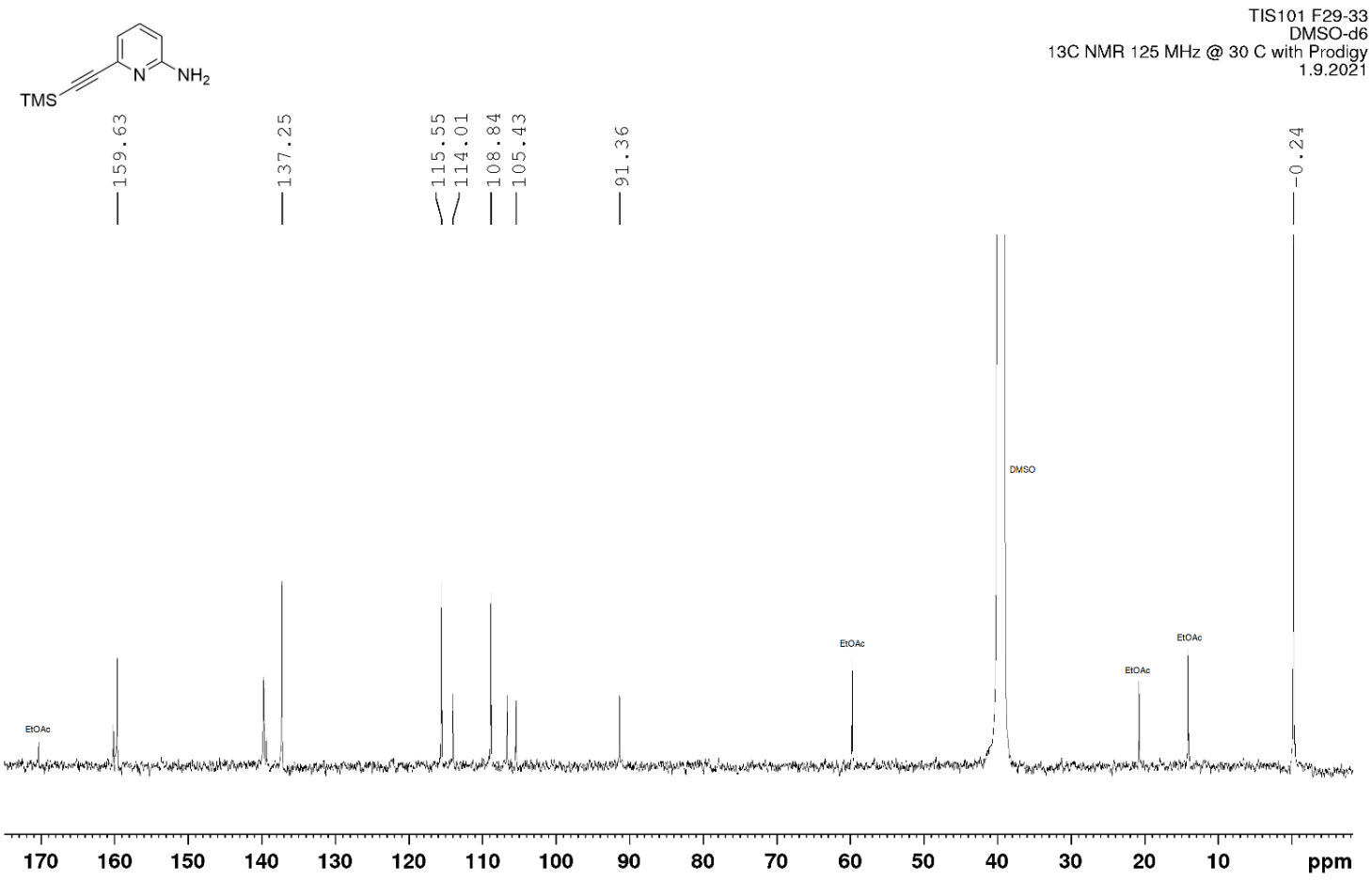

Appendix 4. ^{13}C NMR Spectrum of **2**.

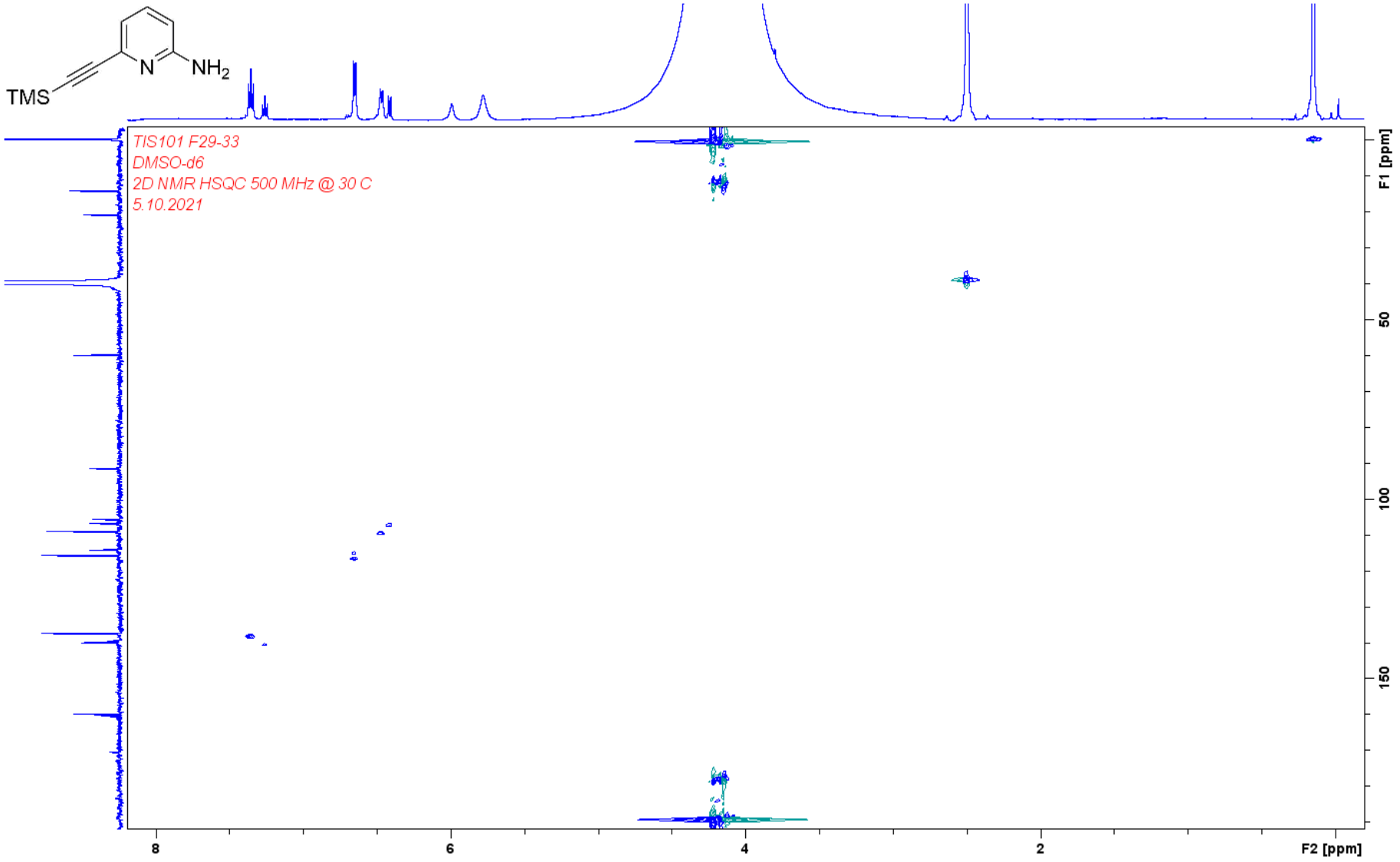

Appendix 5. ^{1}H–^{13}C HSQC Spectrum of **2**.

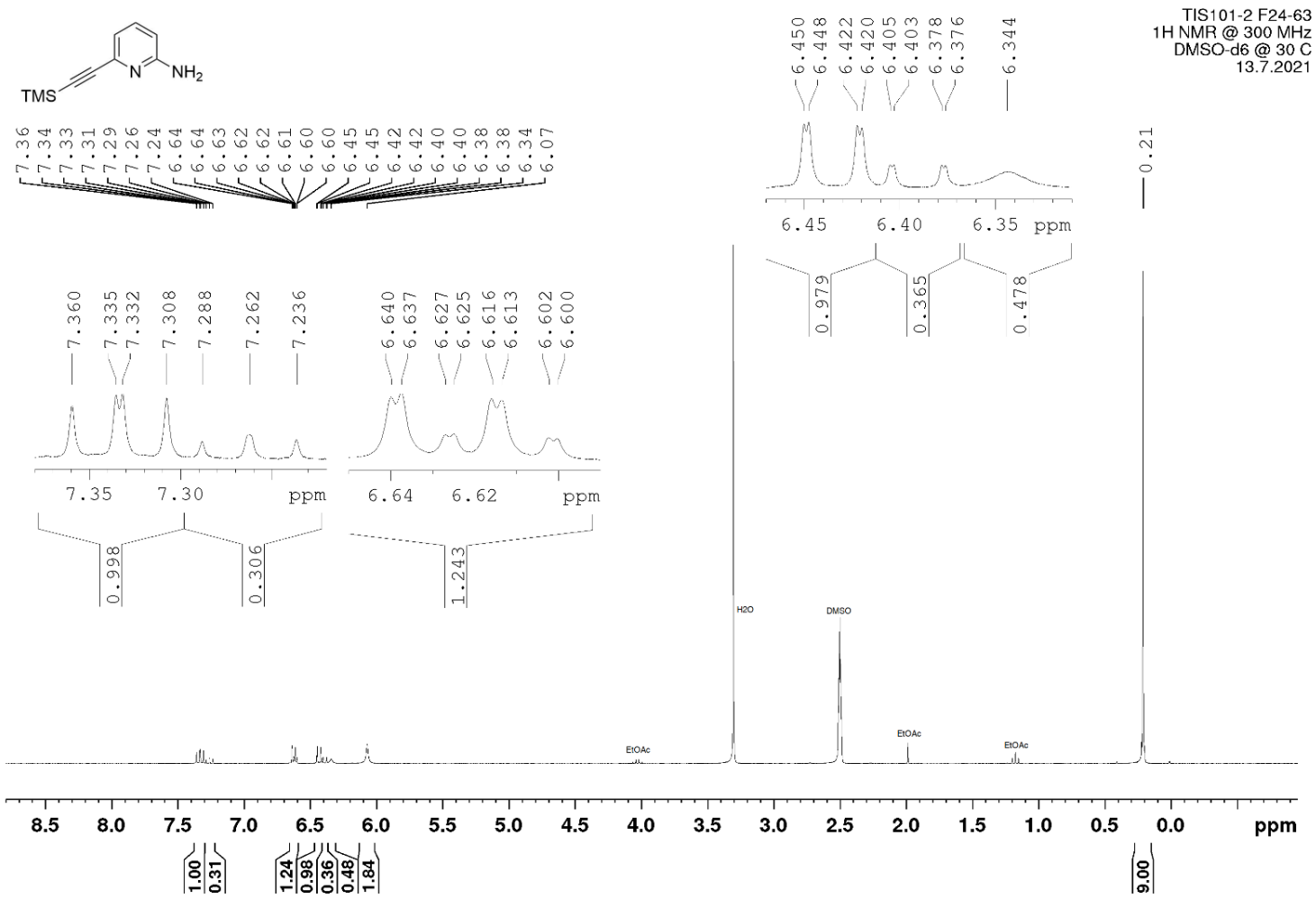

Appendix 6. ^{1}H NMR Spectrum of **2**-2.

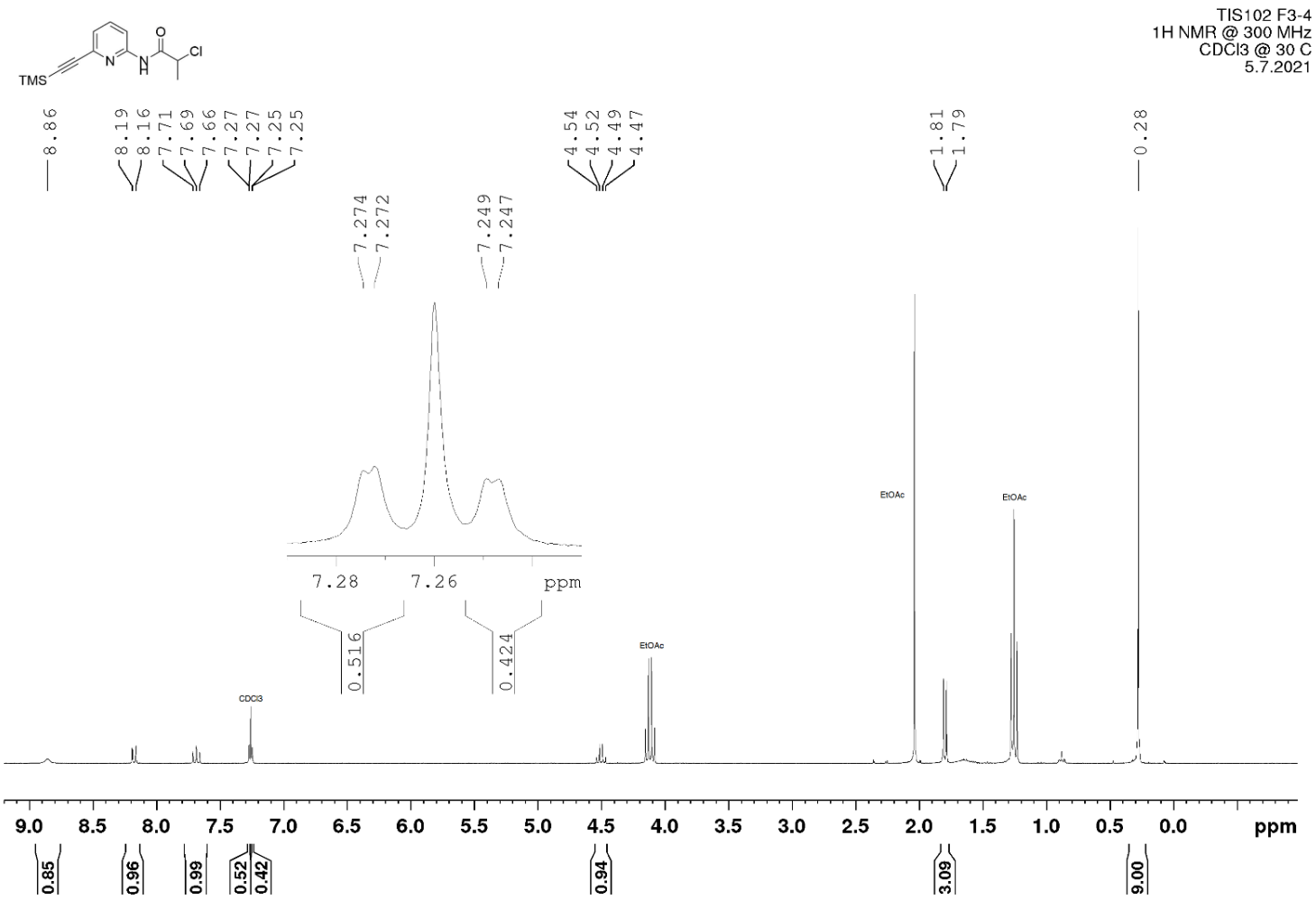

Appendix 7. ^{1}H NMR Spectrum of **3**.

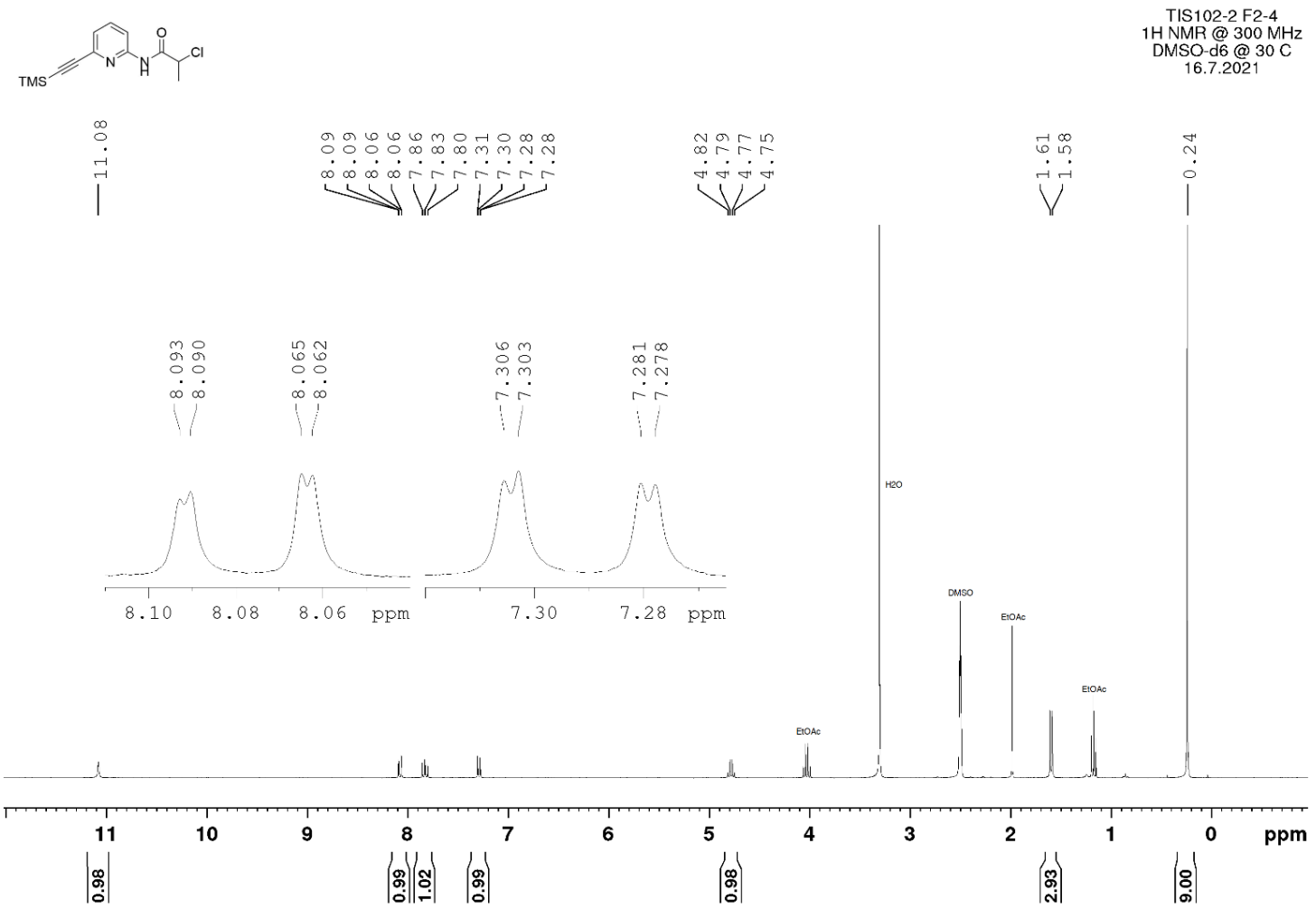

Appendix 8. ^{1}H NMR Spectrum of **3**-2.

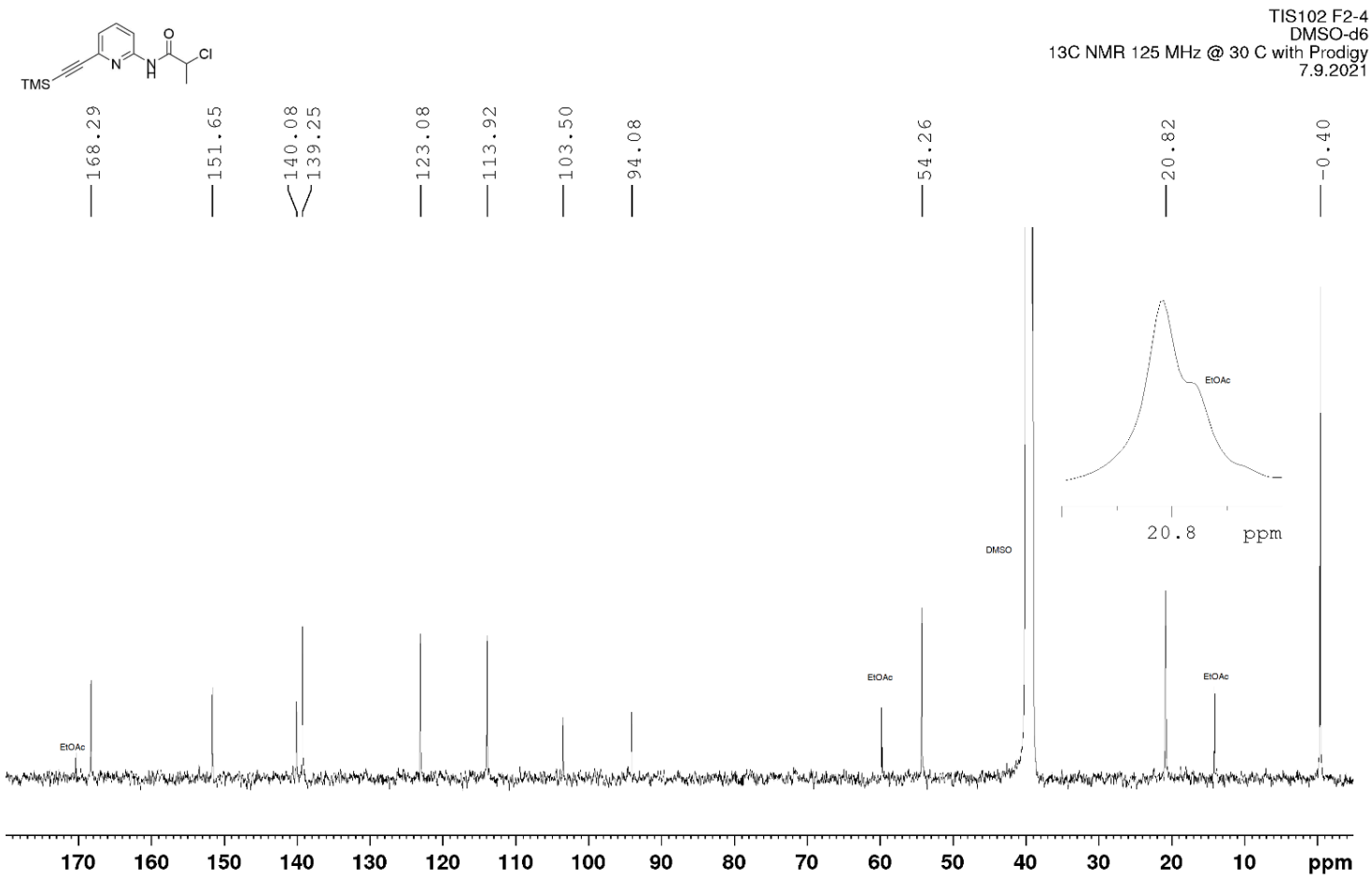

Appendix 9. ^{13}C NMR Spectrum of **3**-2.

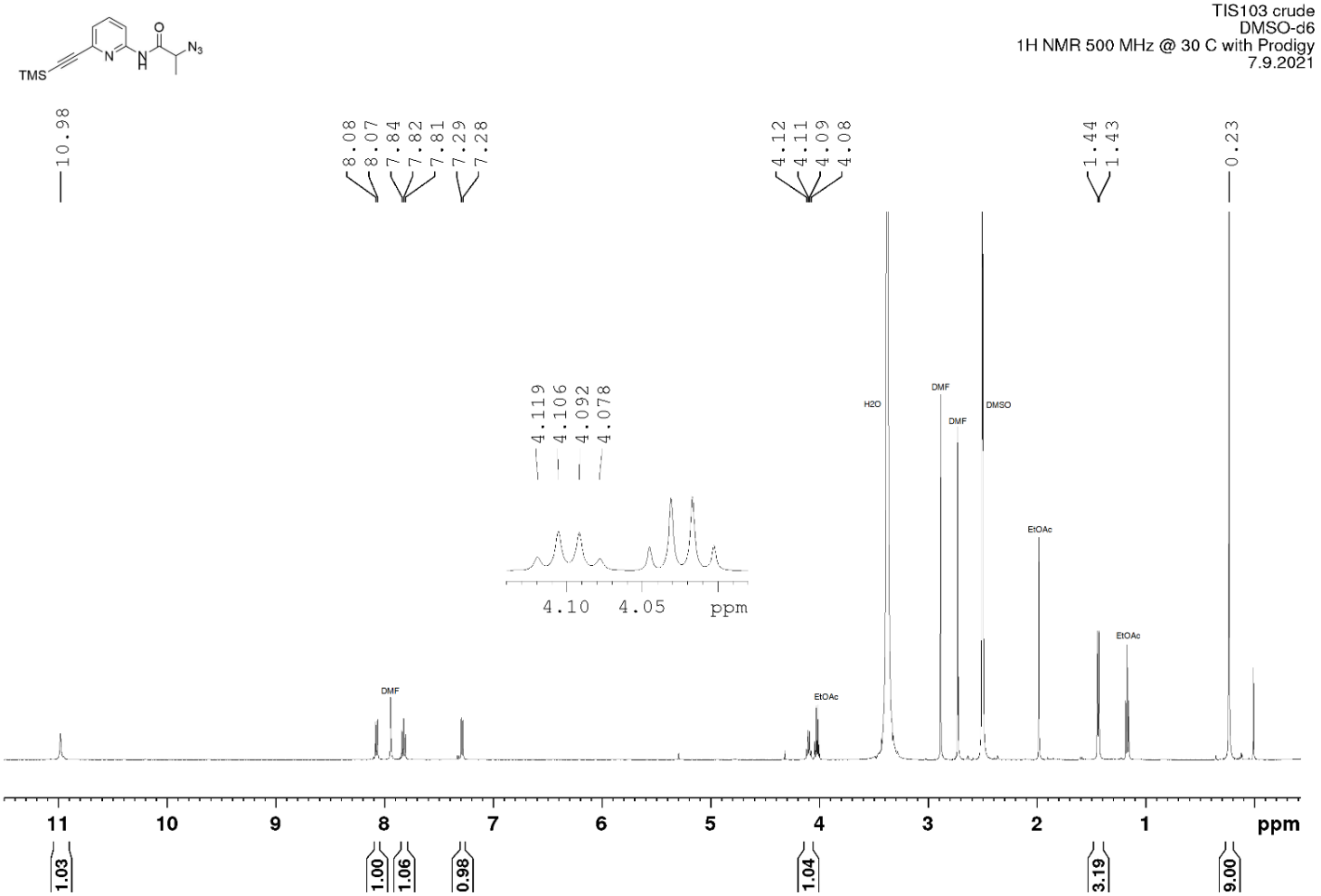

Appendix 10. ^{1}H NMR Spectrum of **4**.

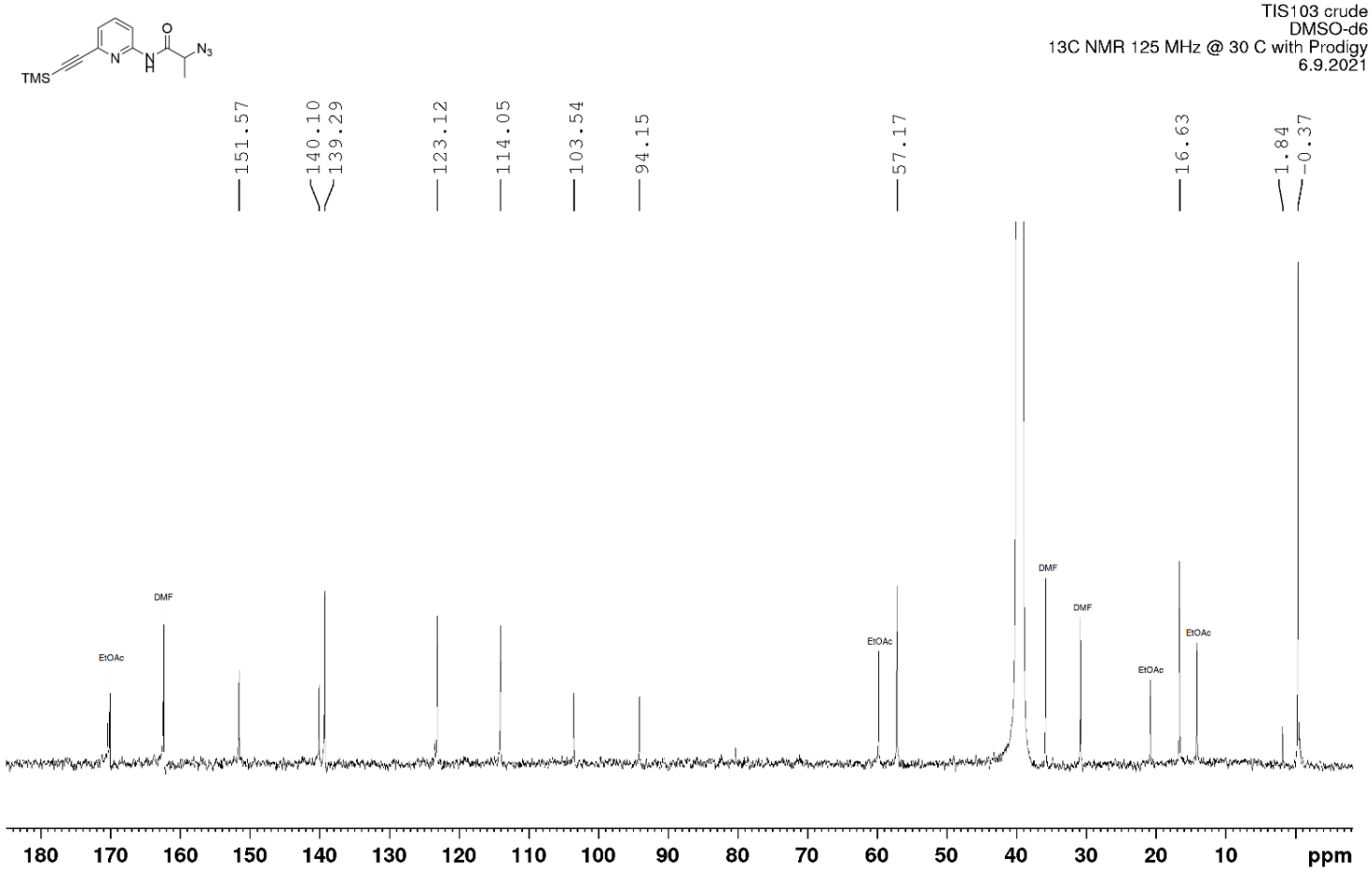

Appendix 11. ^{13}C NMR Spectrum of **4**.

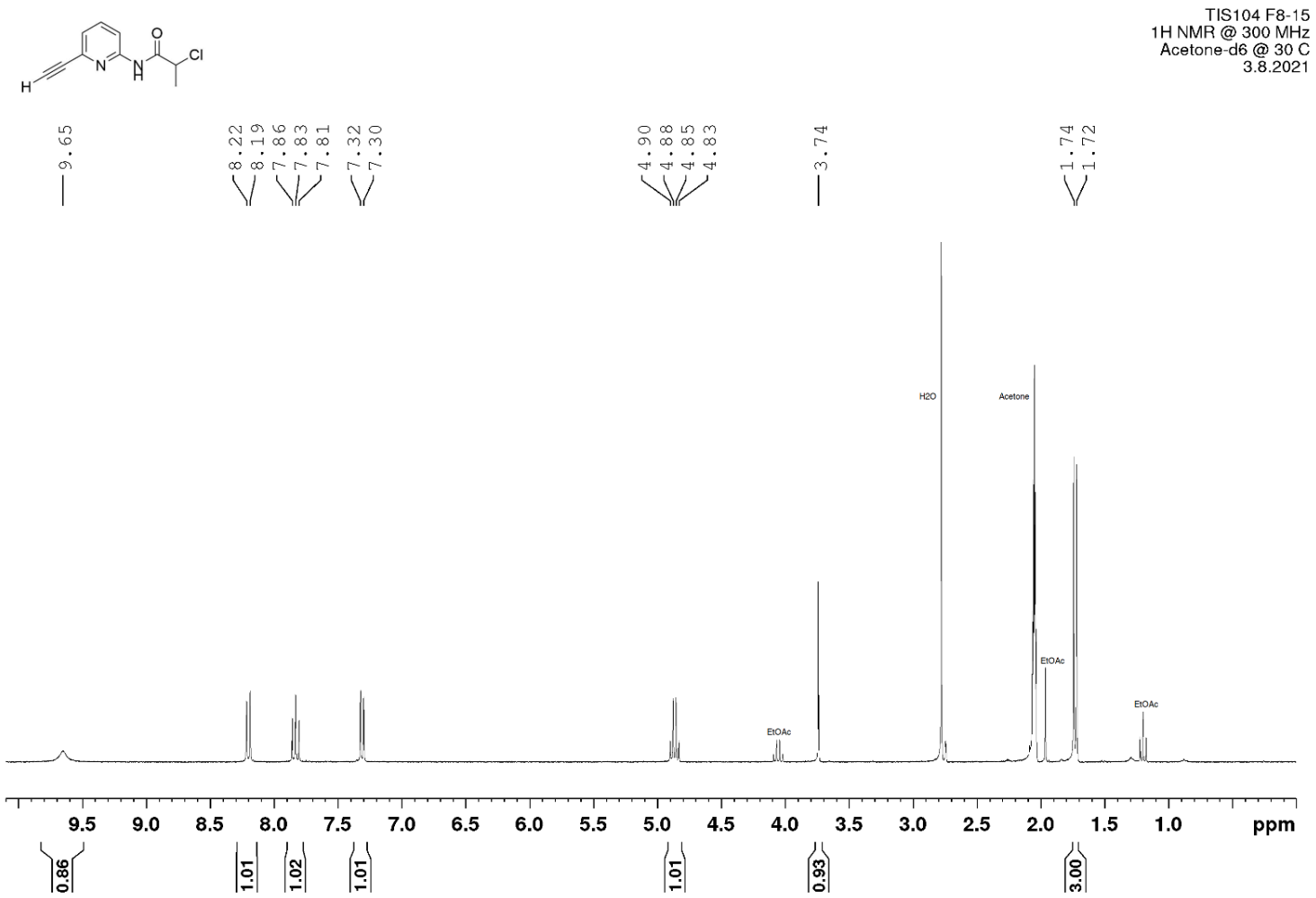

Appendix 12. ^{1}H NMR Spectrum of **5**.

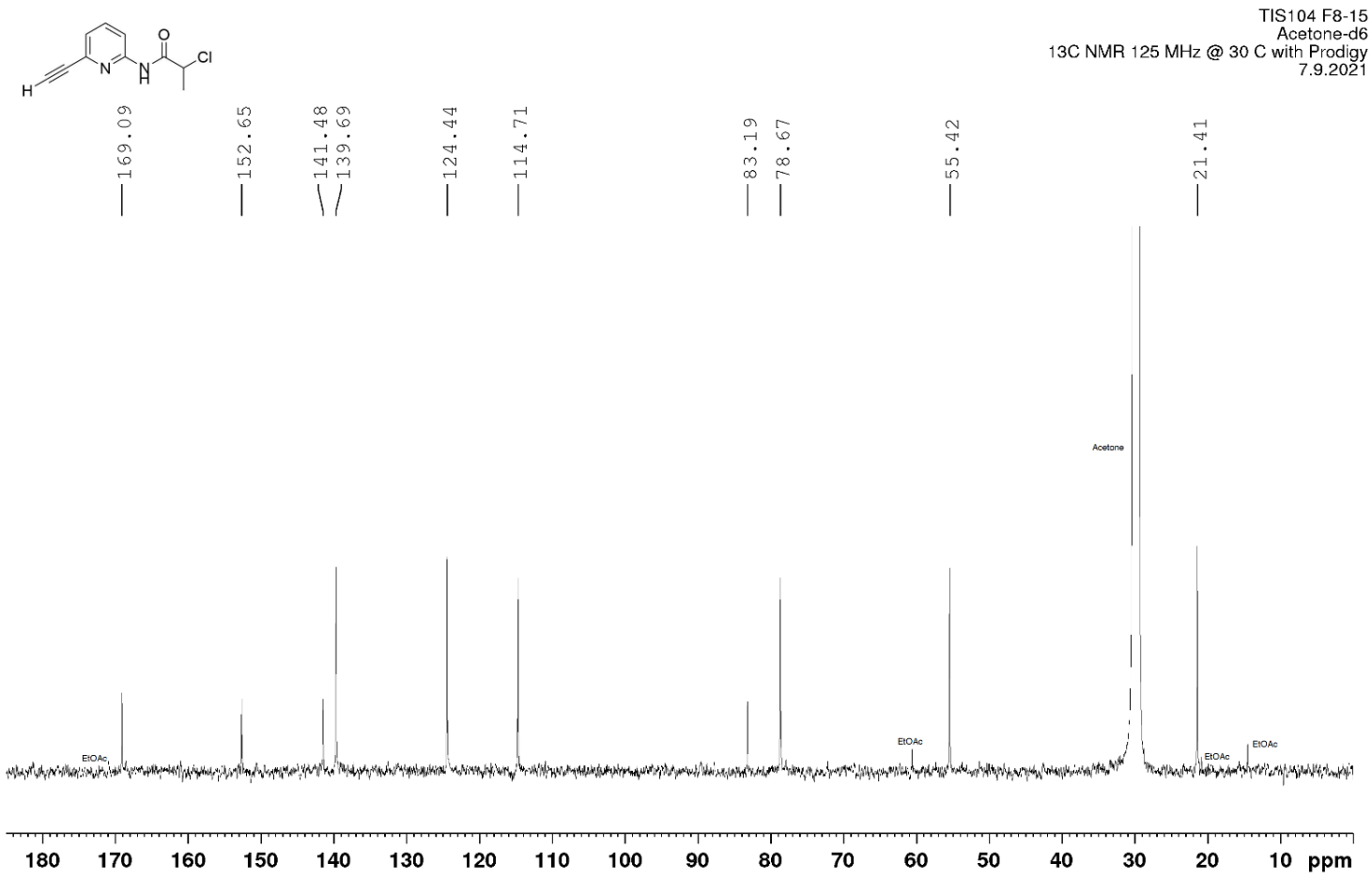

Appendix 13. ^{13}C NMR Spectrum of **5**.

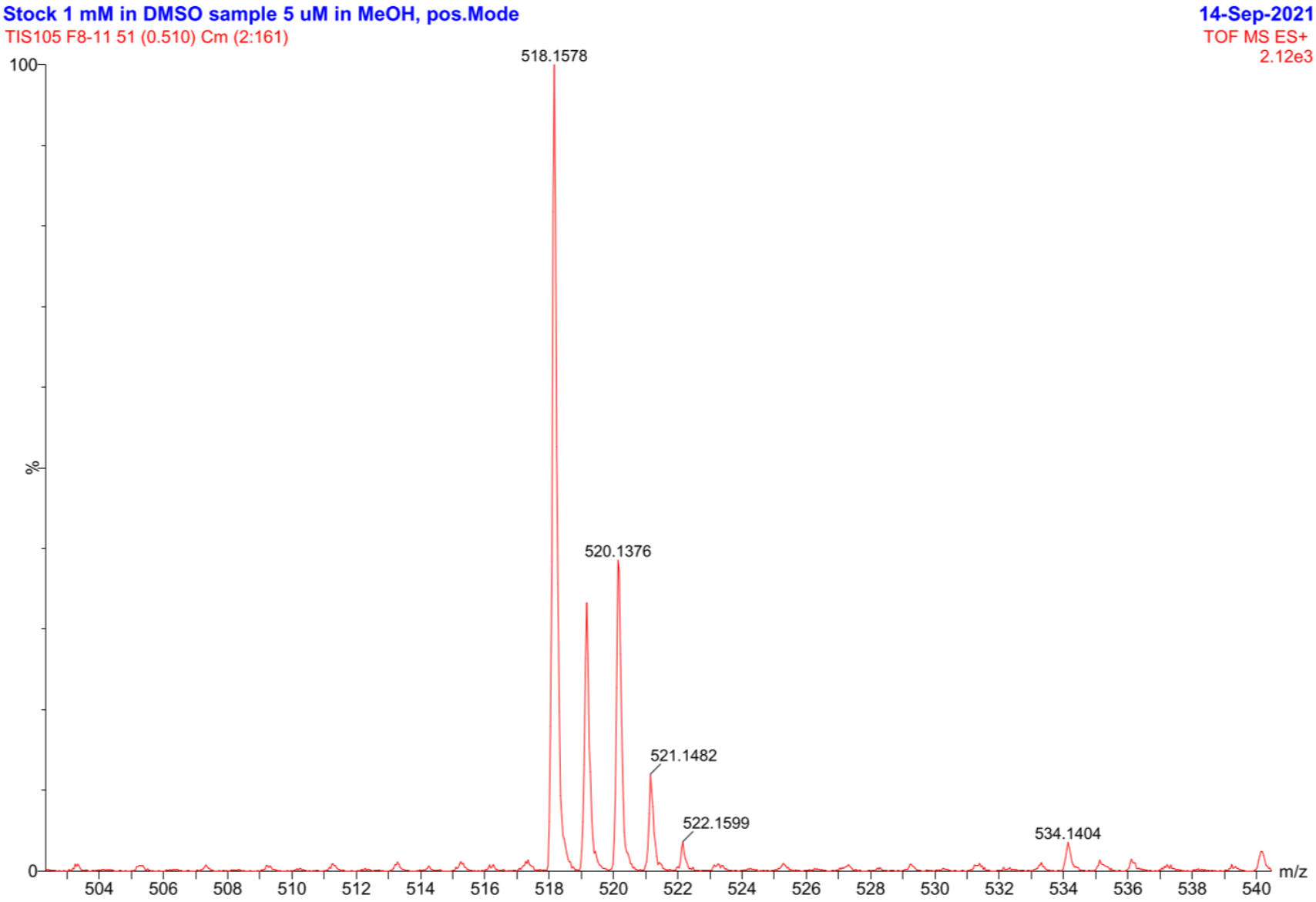
Stock 1 mM in DMSO sample 5 uM in MeOH, pos.Mode
TIS105 F8-11 51 (0.510) Cm (2:161)
14-Sep-2021
TOF MS ES+
2.12e3
518.1578
520.1376
521.1482
522.1599
534.1404
100
%
0
504
506
508
510
512
514
516
518
520
522
524
526
528
530
532
534
536
538
540
m/z

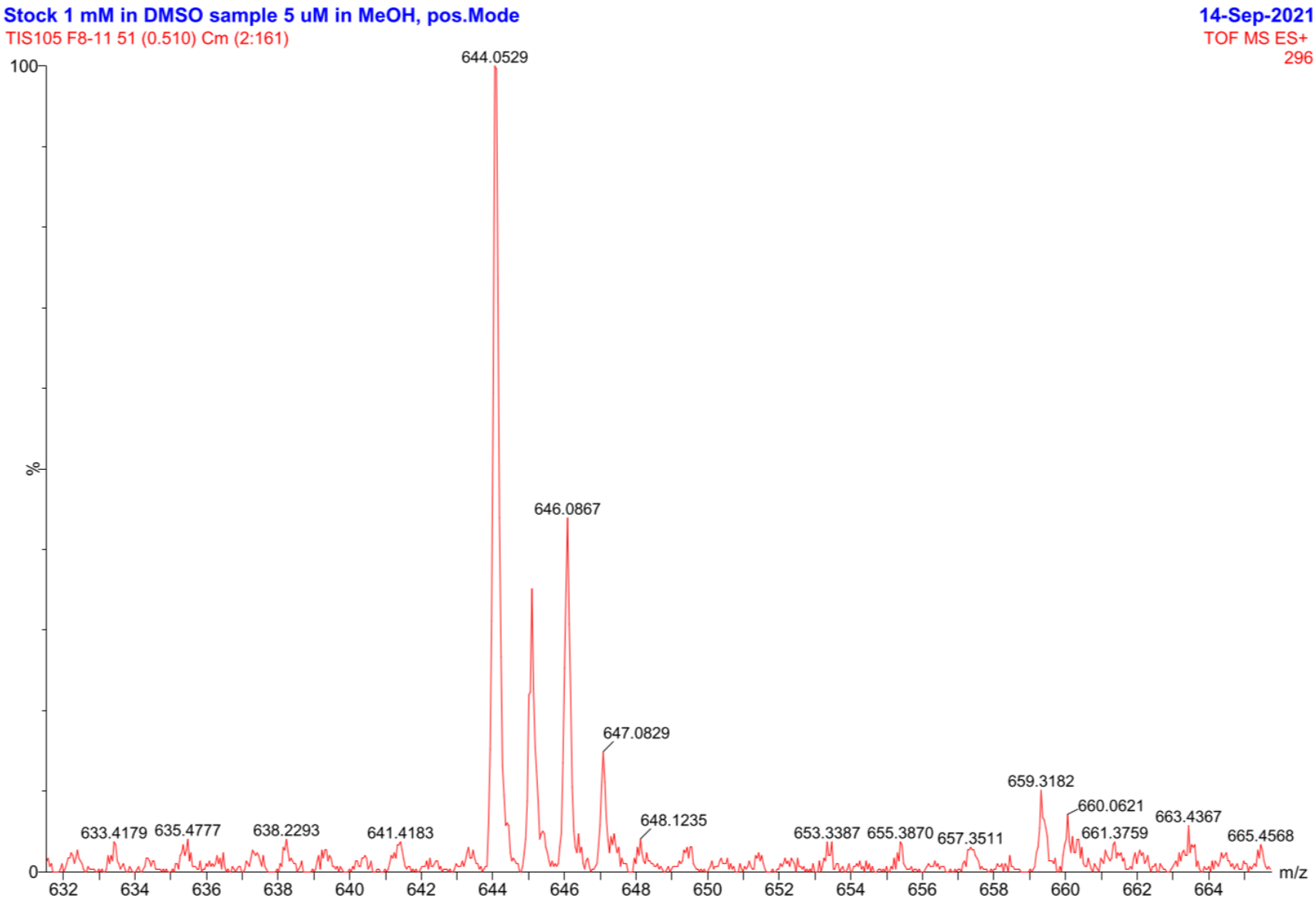
Stock 1 mM in DMSO sample 5 uM in MeOH, pos.Mode
TIS105 F8-11 51 (0.510) Cm (2:161)
14-Sep-2021
TOF MS ES+
296
100
%
0
644.0529
646.0867
647.0829
633.4179
635.4777
638.2293
641.4183
648.1235
653.3387
655.3870
657.3511
659.3182
660.0621
661.3759
663.4367
665.4568
632
634
636
638
640
642
644
646
648
650
652
654
656
658
660
662
664
m/z

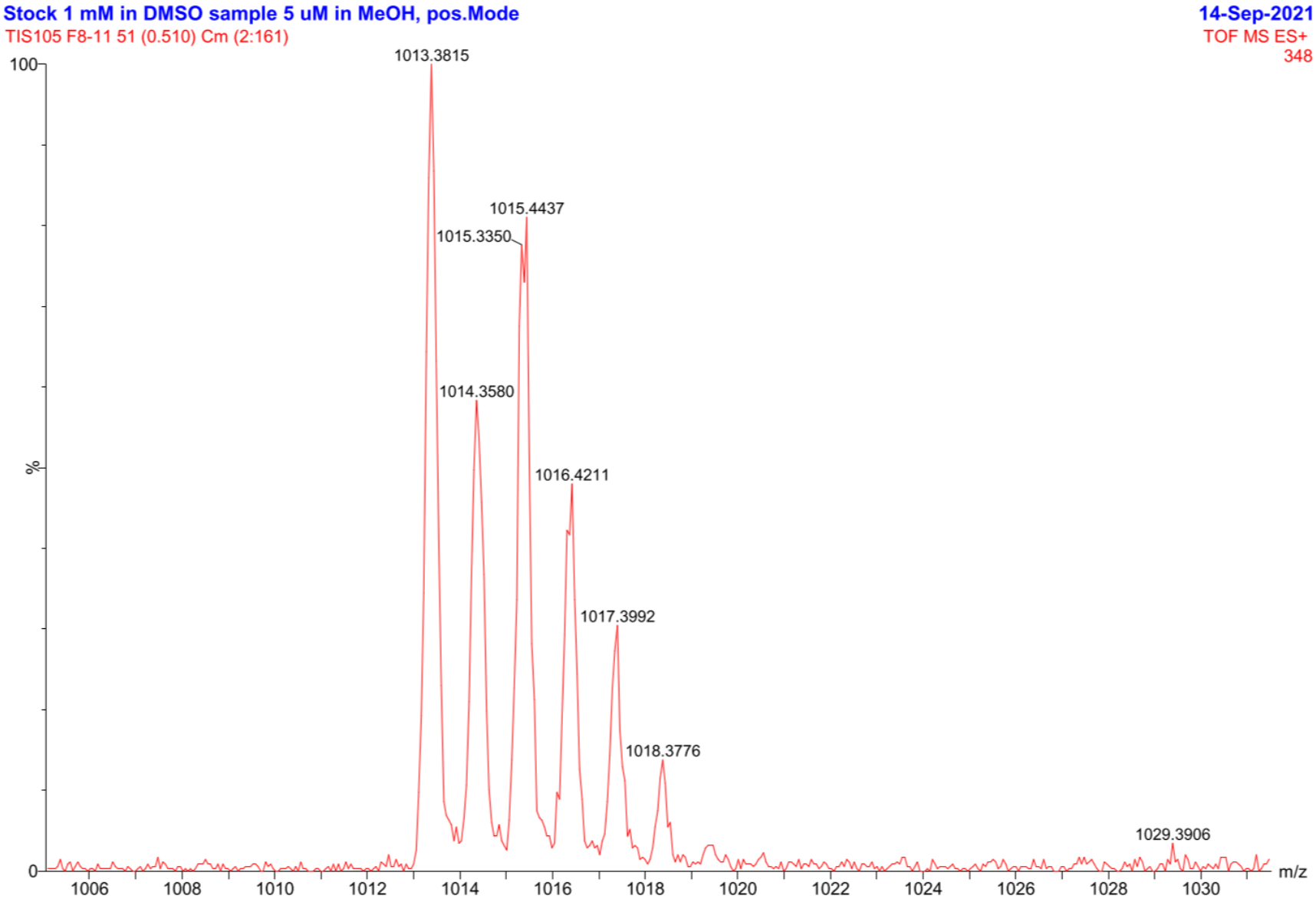
Stock 1 mM in DMSO sample 5 uM in MeOH, pos.Mode
TIS105 F8-11 51 (0.510) Cm (2:161)
14-Sep-2021
TOF MS ES+
348
100
%
0
1013.3815
1015.4437
1015.3350
1014.3580
1016.4211
1017.3992
1018.3776
1029.3906
1006
1008
1010
1012
1014
1016
1018
1020
1022
1024
1026
1028
1030
m/z

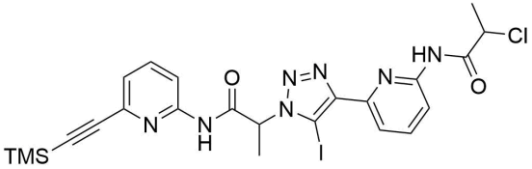

Compound **6**

Fragment	Formula	*m/z* calcd.	*m/z* exp.
$[(\mathbf{6} - I + H) + Na]^+$	$C_{23}H_{26}ClN_7O_2Si + Na^+$	518.1	518.2
$[\mathbf{6} + Na]^+$	$C_{23}H_{25}ClIN_7O_2Si + Na^+$	644.0	644.1
$[2 \cdot (\mathbf{6} - I + H) + Na]^+$	$C_{46}H_{52}Cl_2N_{14}O_4Si_2 + Na^+$	1013.3	1013.4

Appendix 14. The MS Spectrums and MS fragments of **6.**

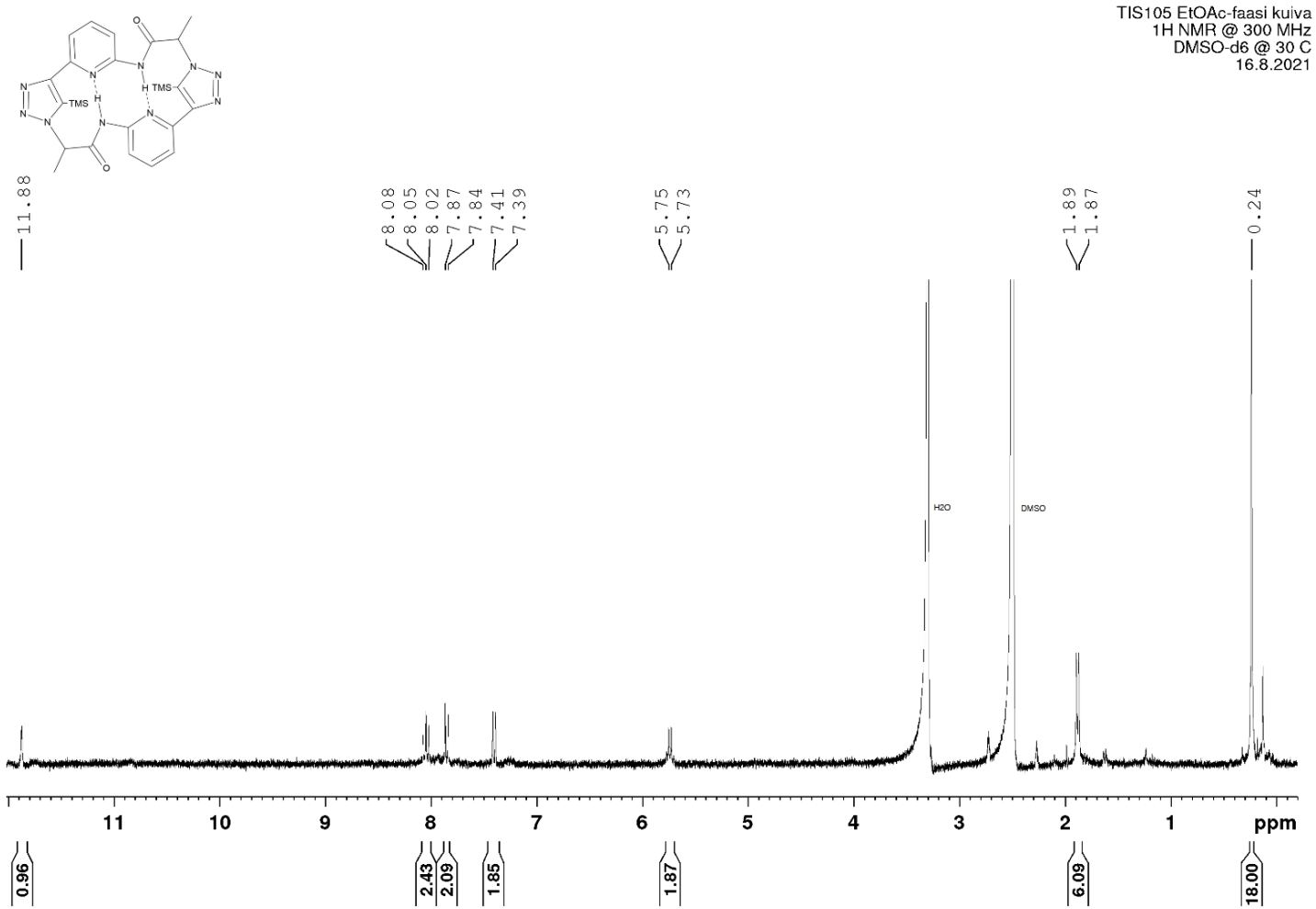

Appendix 15. ^{1}H NMR Spectrum of **7**.

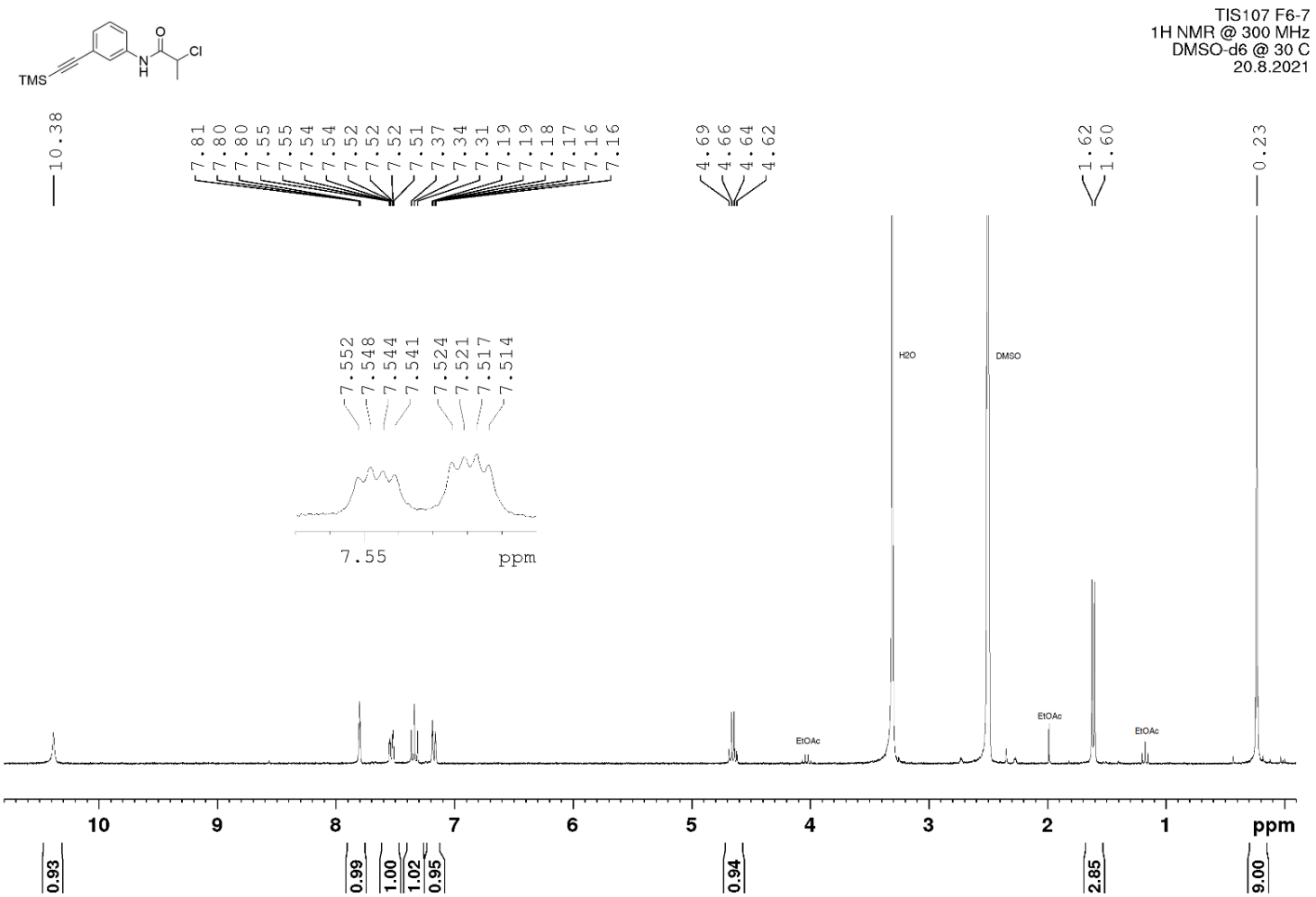

Appendix 16. 1H NMR Spectrum of **8.**

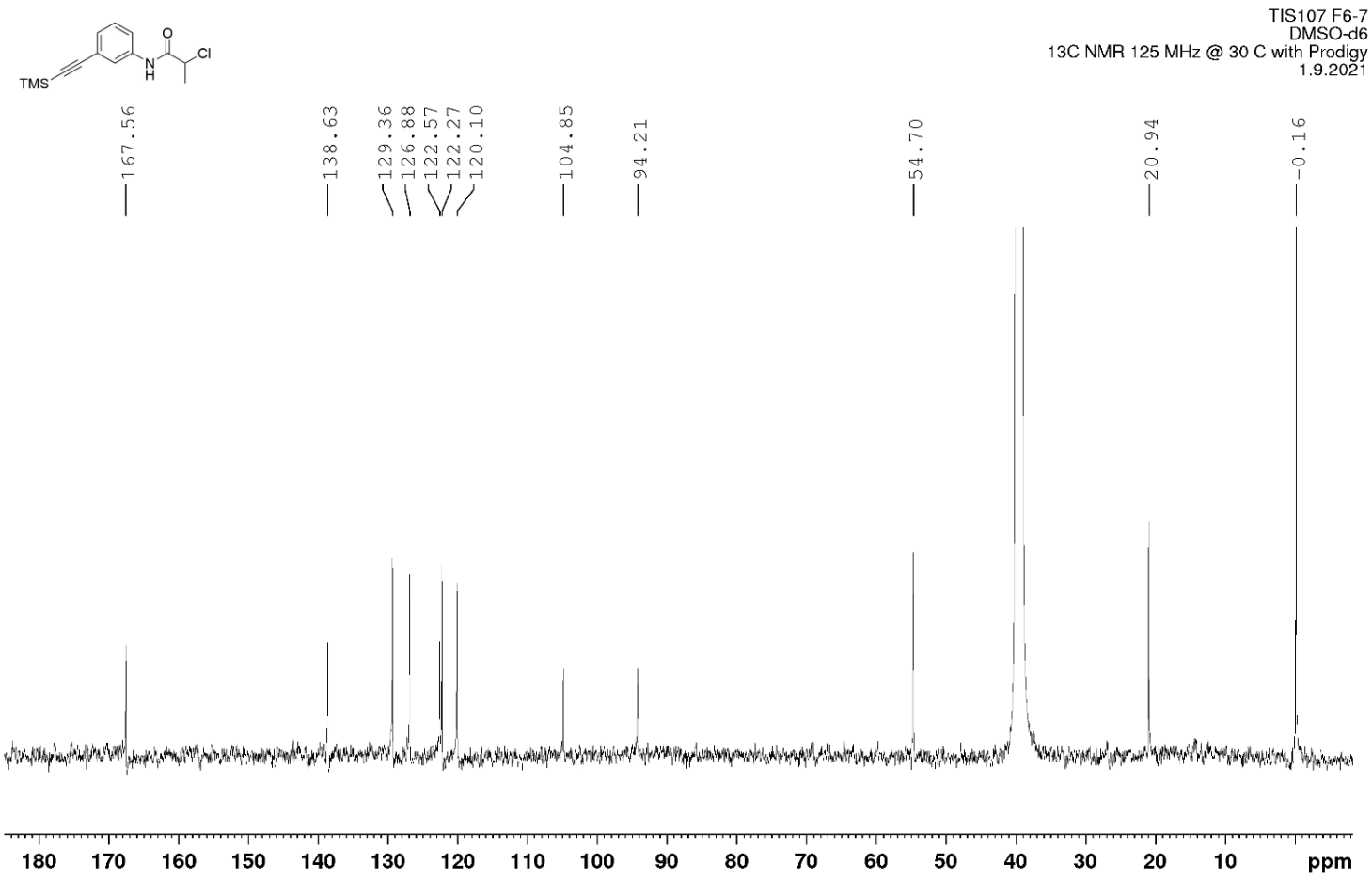

Appendix 17. ^{13}C NMR Spectrum of **8.**

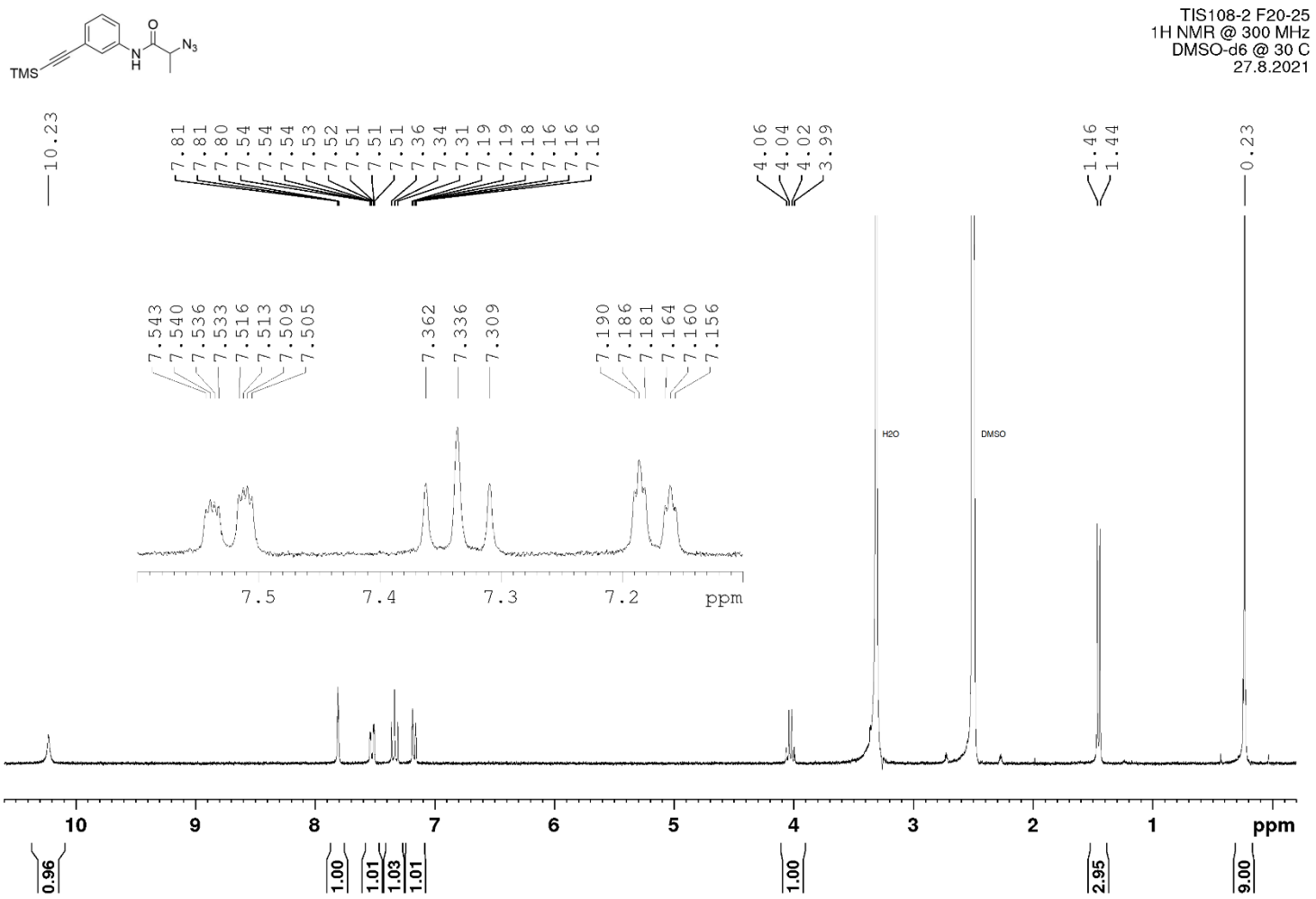

Appendix 18. ^{1}H NMR Spectrum of **9**-2.

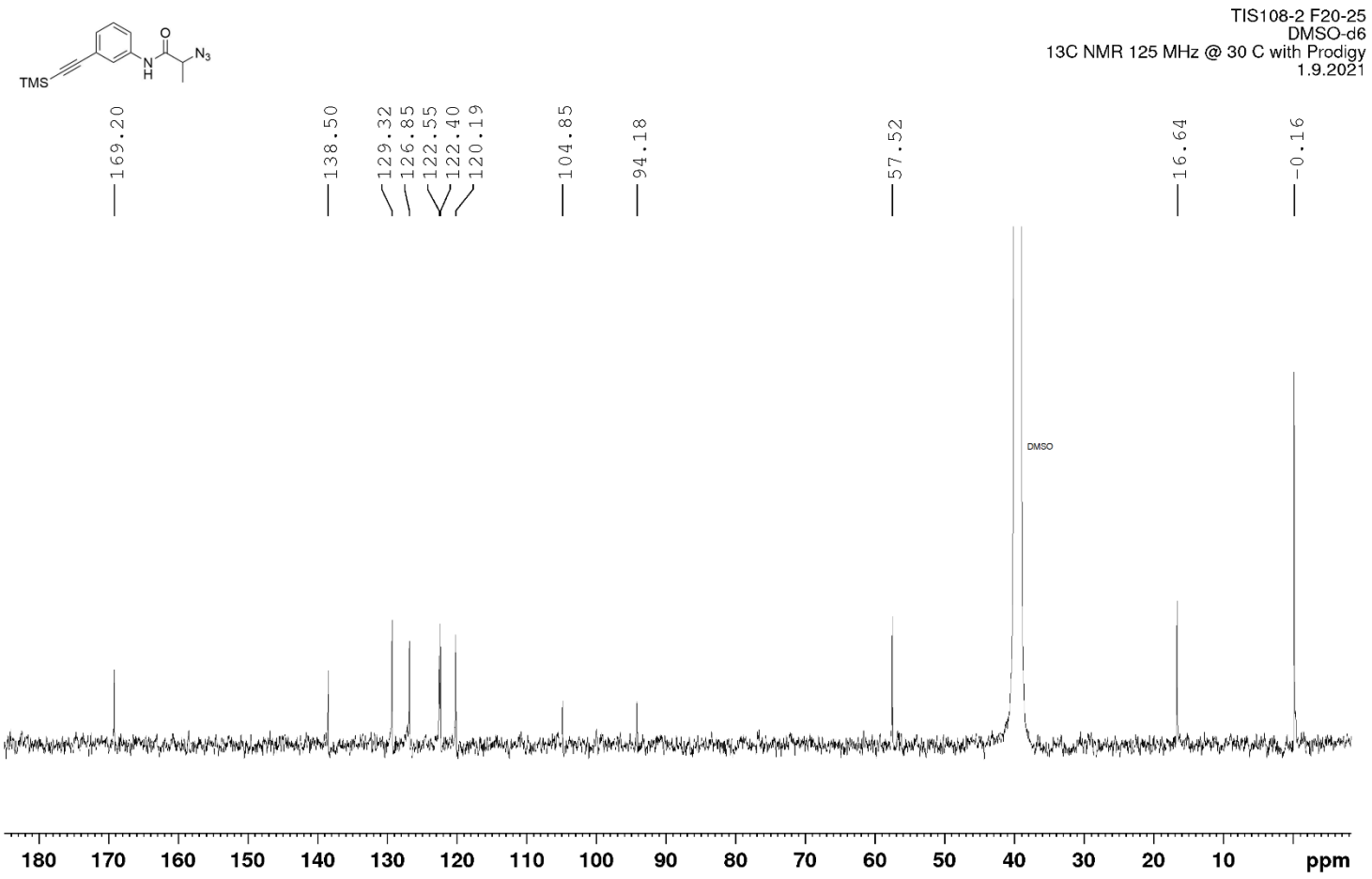

Appendix 19. ^{13}C NMR Spectrum of **9**-2.

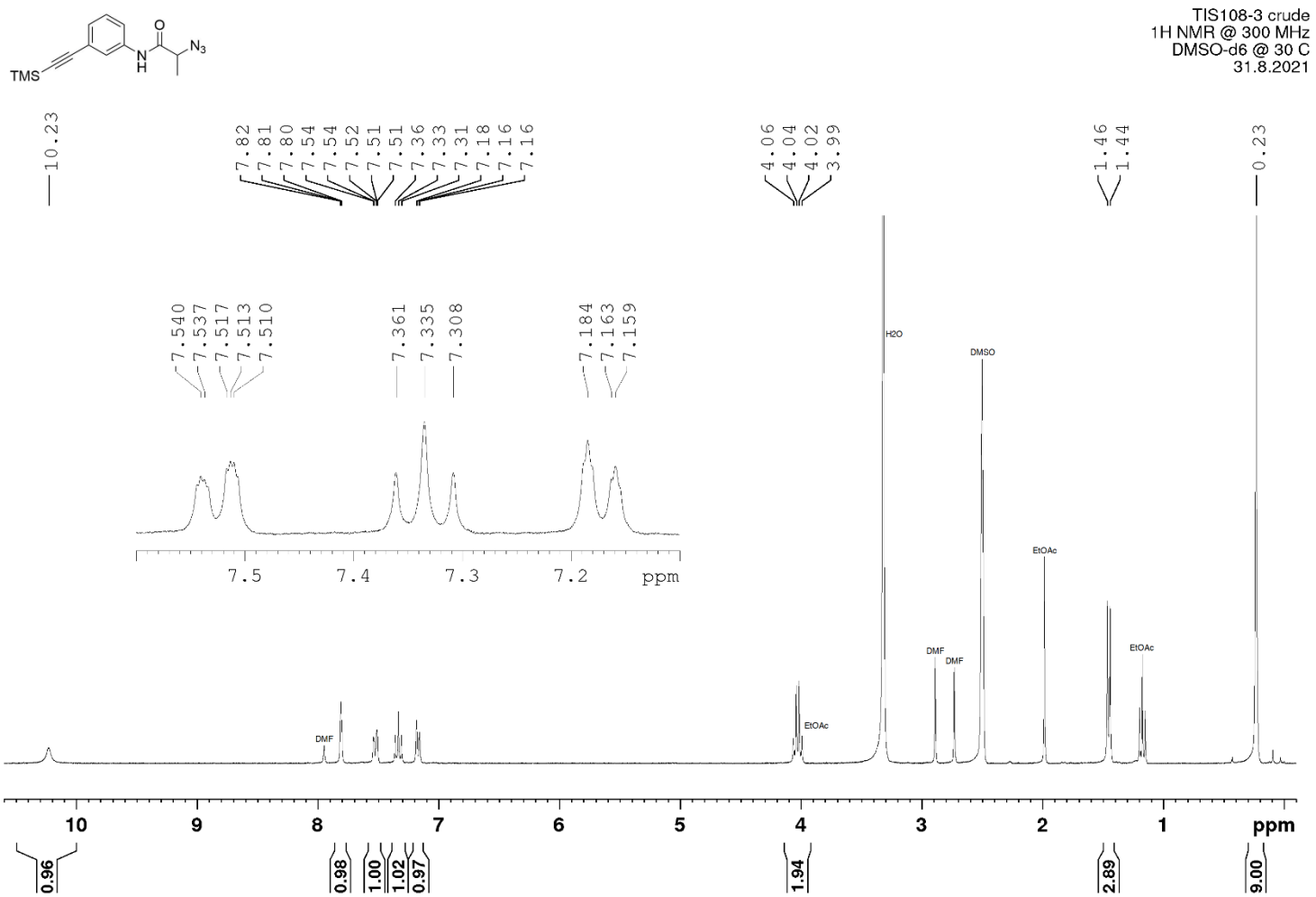

Appendix 20. ^{1}H NMR Spectrum of **9**-3.

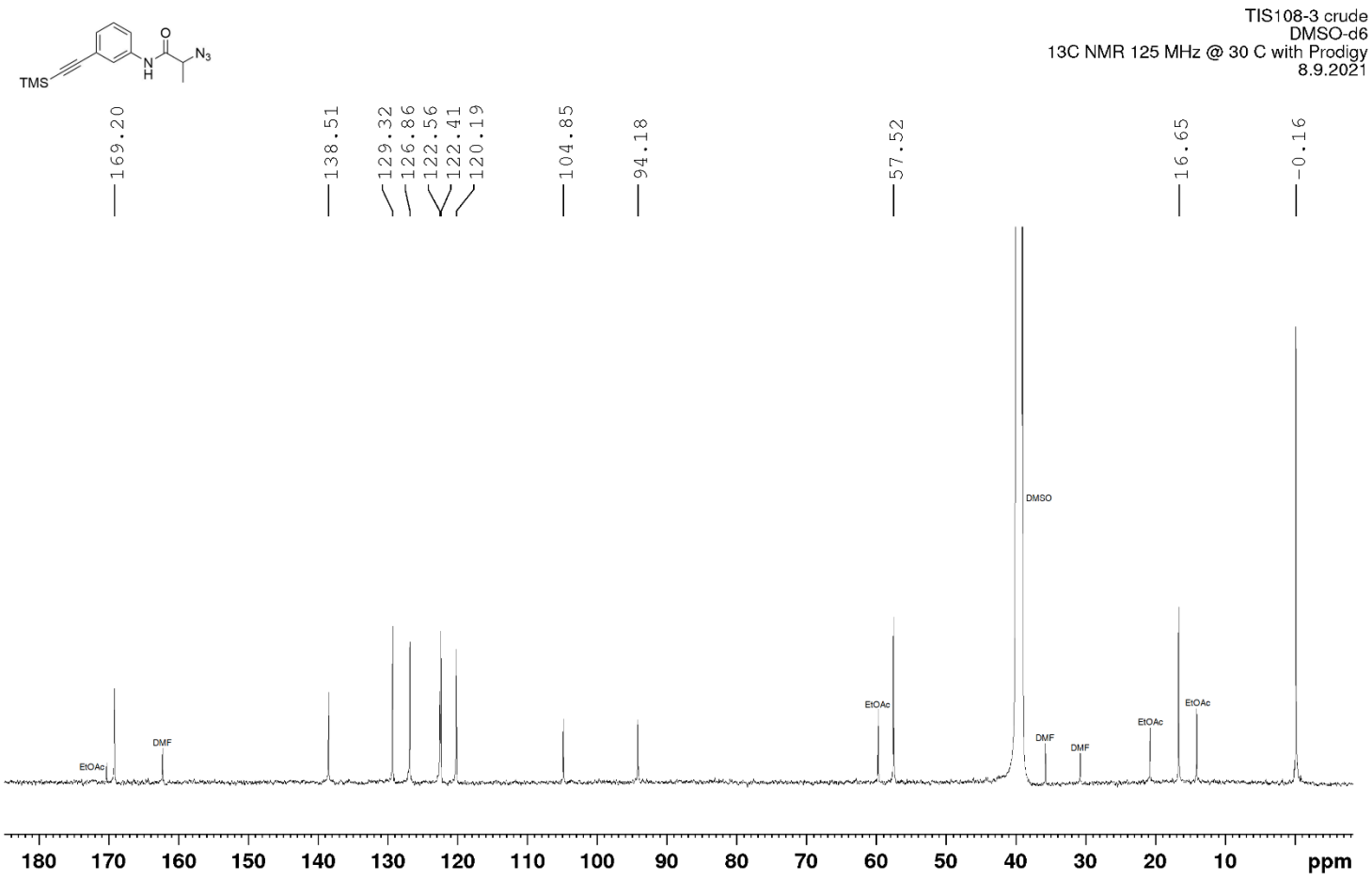

Appendix 21. ^{13}C NMR Spectrum of **9**-3.

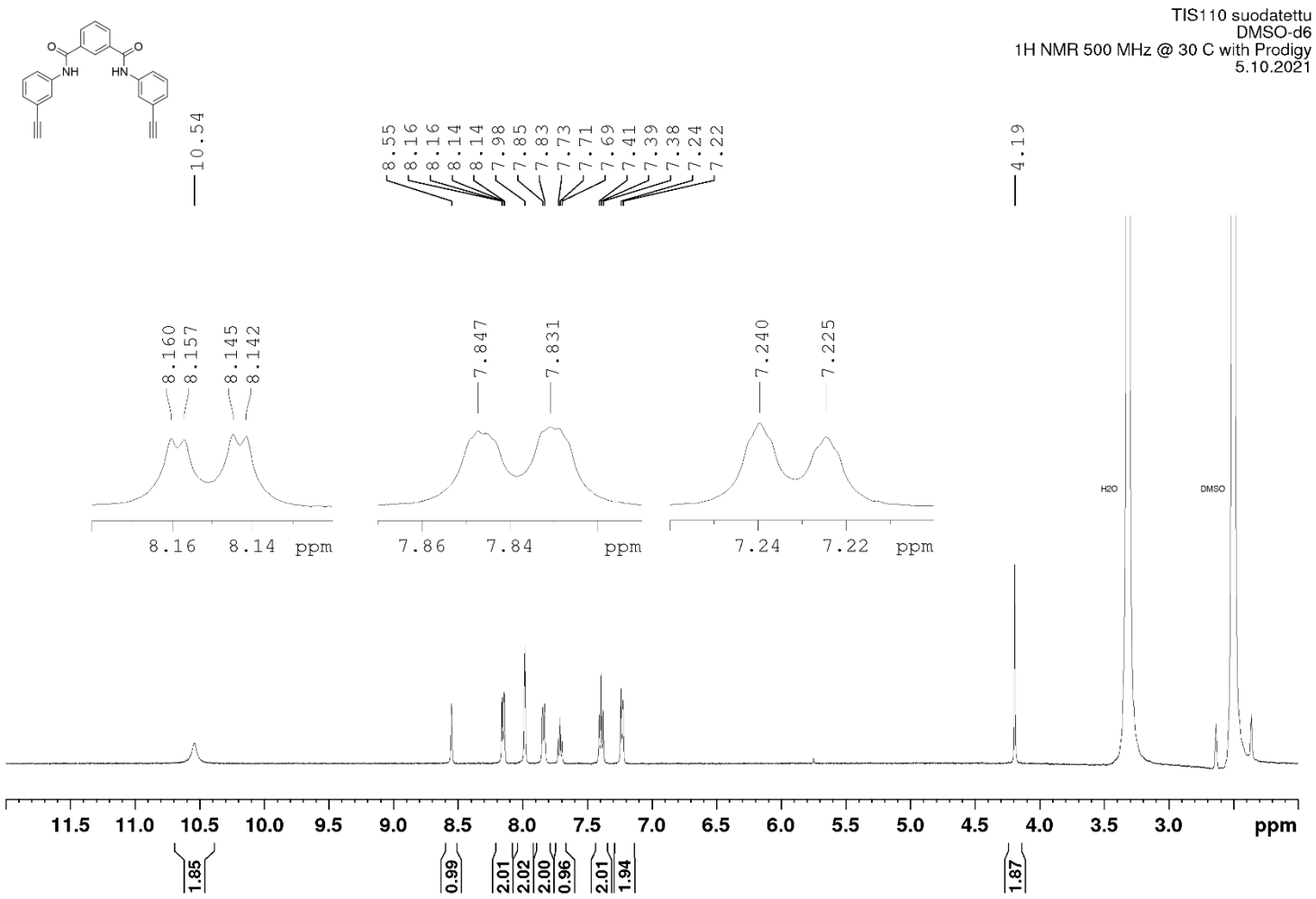

Appendix 22. ^{1}H NMR Spectrum of **11.**

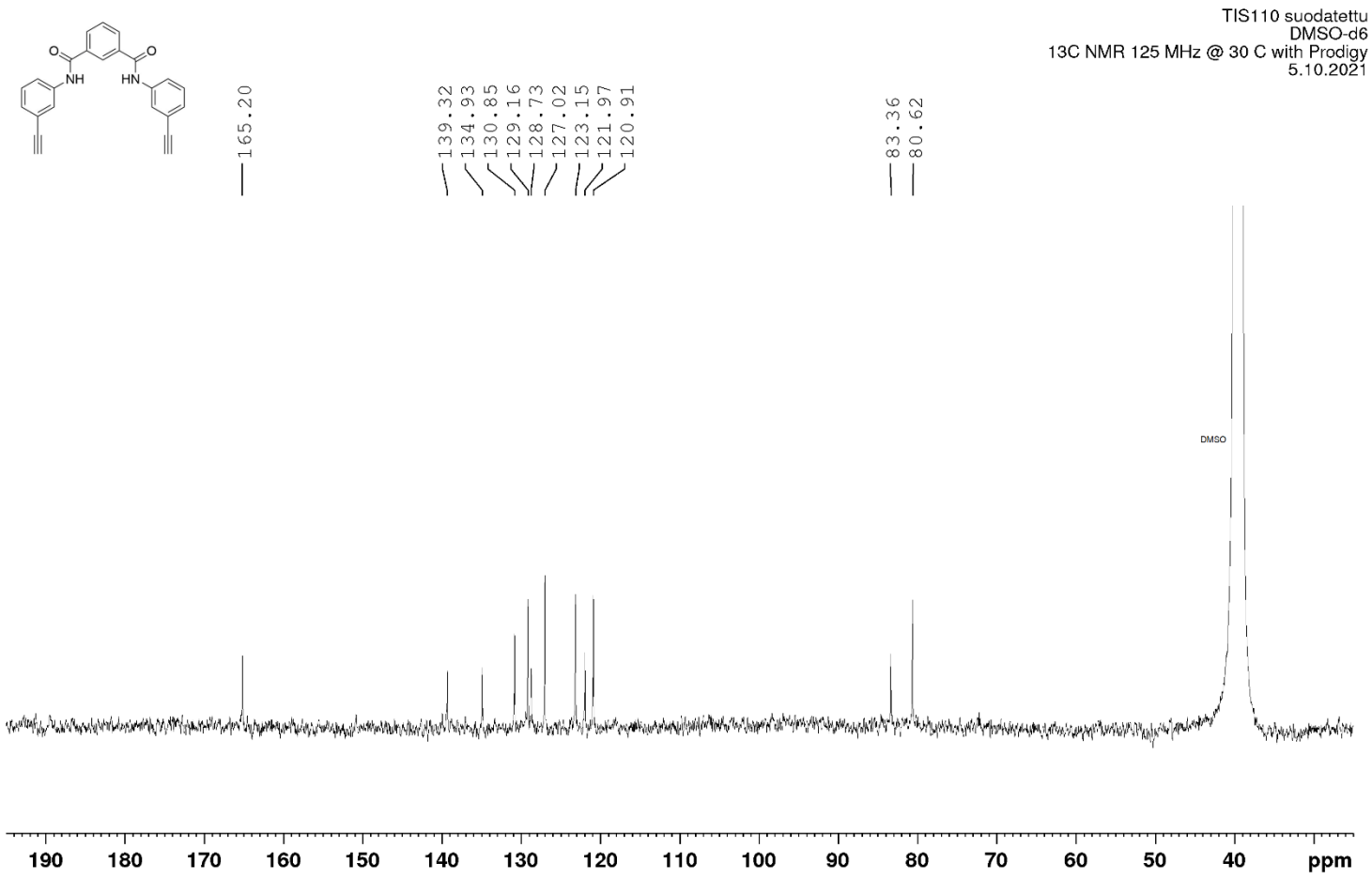

Appendix 23. ^{13}C NMR Spectrum of **11.**

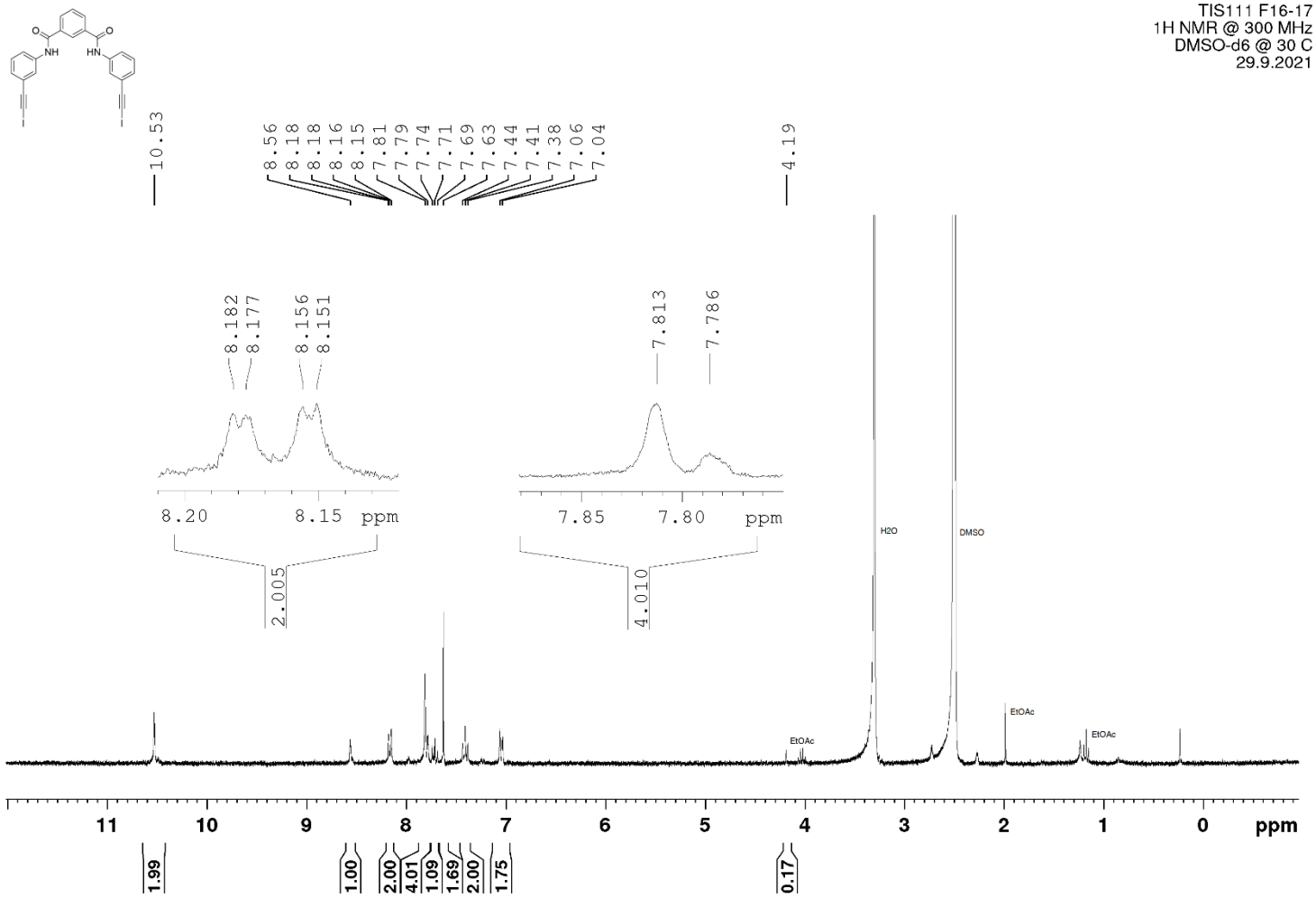

Appendix 24. ^{1}H NMR Spectrum of **12.**

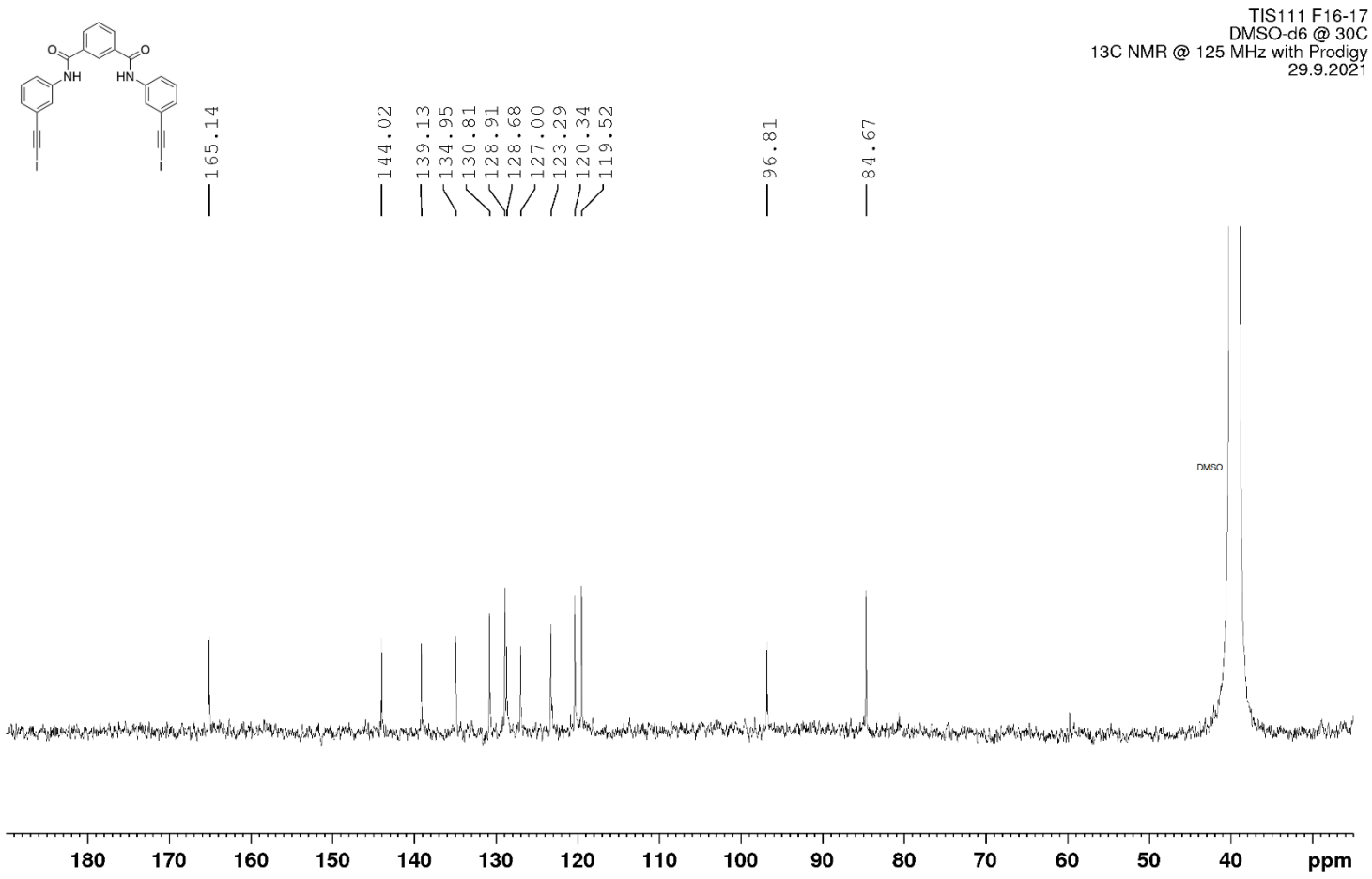

Appendix 25. ^{13}C NMR Spectrum of **12.**